To the Graduate Council:

I am submitting herewith a dissertation written by Christopher Patrick Leibman entitled "Secondary Ion Mass Spectrometry of Aromatic Compounds in Acidic Mixtures." I have examined the final copy of this dissertation for form and content and recommend that it be accepted in partial fulfillment of the requirements for the degree of Doctor of Philosophy, with a major in Chemistry.

Gleb Mamantov, Major Professor

We have read this dissertation
and recommend its acceptance:

Accepted for the Council:

Vice provost and
Dean of The Graduate School

SECONDARY ION MASS SPECTROMETRY OF AROMATIC COMPOUNDS IN ACIDIC MIXTURES

A Dissertation

Presented for the

Doctor of Philosophy

Degree

The University of Tennessee, Knoxville

Christopher Patrick Leibman

June 1988

DEDICATION

To my wife, Kim, for her constant support.

ACKNOWLEDGEMENT

The author is indebted to Peter J. Todd and Gleb Mamantov for their guidance and encouragement during the course of this investigation. Appreciation is also extended to the Analytical Spectroscopy Section of Oak Ridge National Laboratory for the use of their facilities and the assistance given by the staff. The author is grateful for the financial support received from the University of Tennessee, Oak Ridge National Laboratory, and the Department of Energy during his graduate studies. This publication is based on work performed in the Laboratory Graduate Participation Program under contract number DE-AC05-760R00033 between the U. S. Department of Energy and Oak Ridge Associated Universities.

ABSTRACT

Secondary ion mass spectrometry (SIMS) is an analytical method that can be used to obtain mass spectra of involatile/thermally labile compounds. The sensitivity of SIMS for organic compounds is enhanced if samples are first dissolved in an appropriate involatile liquid (or so-called matrix).

The use of acidic liquids and solids to improve the sensitivity of SIMS for aromatic compounds is investigated. SIMS spectra are obtained from substituted aromatic compounds dissolved in concentrated sulfuric acid (98 wt. %). Detection limits for some substituted aromatic compounds are estimated to be 10^{-12} moles. Simultaneously abundant molecular ions and protonated molecules characteristic of dissolved aromatics are observed for several aromatic compound classes including acids, aldehydes, ketones, nitriles, and nitrogen heterocycles. The molecular ion to protonated molecule intensity ratio observed in SIMS spectra of substituted aromatic/sulfuric acid solutions is characteristic of the dissolved analyte. Secondary ions observed from substituted aromatic/sulfuric acid solutions are consistent with known condensed phase chemistry of such solutions.

The utility of sulfuric acid as a SIMS matrix for detection of pterins, a group of biologically significant compounds, is demonstrated. Application of LSIMS using

sulfuric acid for detection of aromatics adsorbed on substrates is also investigated.

Use of acidic metal chlorides for enhanced secondary ion emission is also studied. Metal chlorides used as solid matrices or as additives to liquid matrices do not improve the sensitivity of SIMS for aromatic compounds significantly.

TABLE OF CONTENTS

CHAPTER		PAGE
I.	INTRODUCTION	1
	A. Occurrence of Aromatic Hydrocarbons and General Analytical Schemes	3
	B. Ionization Methods for Involatile Aromatic Compounds	5
	C. Experimental Aspects of Secondary Ion Production	7
	D. SIMS Nomenclature	9
	E. Aspects of Liquid Matrices	10
	F. Organic Secondary Ion Formation from Liquid Solutions	12
	G. Selection of LSIMS Matrices for Aromatic Compounds	16
	H. Chemistry of Aromatic/Sulfuric Acid Solutions	20
	I. Enhanced Molecular Radical Cation Emission	23
	J. Analytical Applications of Concentrated Sulfuric Acid as a LSIMS Matrix -- Comparison with Existing Methods	25
	K. Objectives of This Study	30
II.	EXPERIMENTAL	32
	A. Mass Spectrometer	32
	B. Concentrated Sulfuric Acid	33
	C. Metal Chlorides and Ambient Temperature Melts	37

CHAPTER PAGE

III. RESULTS AND DISCUSSION 45

A. LSIMS Spectrum of Sulfuric Acid 45

B. LSIMS Spectra of Substituted Aromatic/Sulfuric Acid Solutions 47

C. Chemical Noise in Aromatic/Sulfuric Acid Solutions 78

D. Effect of Current Density on Sensitivity . . . 81

E. Mechanistic Aspects 82

F. Effects of Matrix Modification on SIMS Spectra 101

G. Analytical Applications for Concentrated Sulfuric Acid 105

H. Metal Chlorides and Ambient Temperature Melts . 120

IV. SUMMARY AND CONCLUSIONS 139

LIST OF REFERENCES 142

APPENDICES 152

VITA 170

LIST OF TABLES

TABLE PAGE

1. Relative Intensities of Secondary Parent Ions from Sulfuric Acid Solutions 74
2. Comparison of [Molecular Ion]/[Protonated Molecule] Ratios of Substituted Aromatics to the Oxidation Potentials of the Unsubstituted Analog 76
3. Molecular Weights of the Pterins Investigated . . 107
4. Amounts of Acridine Deposited on Substrates and Concentrations of Extracts 118
5. Operating Temperatures for SIMS Spectra of Metal Chlorides 121
6. Low Vapor Pressure Solvents and Additives Used . . 138

LIST OF FIGURES

FIGURES PAGE

1. Schematic of secondary ion emission 2
2. Diagram of the primary and secondary ion sources used in SIMS 8
3. Diagram of drybox and secondary ion source interface 40
4. Schematic of volatile analyte introduction 44
5. Positive LSIMS spectrum of concentrated sulfuric acid. 46
6. Positive LSIMS spectrum of 9-oxodihydroanthracene/ sulfuric acid solution compared to electron impact ionization mass spectrum of 9-oxodihydroanthracene. 48
7. Positive LSIMS spectrum of 2-acetonaphthone/ sulfuric acid solution 53
8. Positive LSIMS spectrum of 9-phenanthrenecarbox- aldehyde/sulfuric acid solution 55
9. Positive LSIMS spectrum of 2-naphthoic acid/ sulfuric acid solution 57
10. Positive LSIMS spectrum of 9-phenanthrol/sulfuric acid solution 59
11. Positive LSIMS spectrum of 2-methoxynaphthalene/ sulfuric acid solution 61
12. Positive LSIMS spectrum of 2-t-butylanthracene/ sulfuric acid solution 63

FIGURE PAGE

13. Positive LSIMS spectrum of 9-anthracenecarbonitrile/ sulfuric acid solution 65
14. Positive LSIMS spectrum of acridine/sulfuric acid solution 68
15. Positive LSIMS spectrum of 9-aminophenanthrene/ sulfuric acid solution obtained 5 minutes after initiation of primary ion bombardment 69
16. Positive LSIMS spectrum of 9-aminophenanthrene/ sulfuric acid solution obtained 24 minutes after initiation of primary ion bombardment 70
17. Positive LSIMS spectrum of 1-nitronaphthalene/ sulfuric acid solution 72
18. Partial LSIMS spectrum of 10^{-4} M benzoic acid/ H_2SO_4 solution in the region of m/z 122-123 79
19. Log-log plots of various parameters which determine the sensitivity of LSIMS with sulfuric acid 80
20. Plot of the log of the fractional secondary ion current associated with anthraquinone $\{[(M+H)^+] + [(M+2H)^+]\}$ vs. the primary ion current density 83
21. Positive LSIMS spectra of 0.1 M anthraquinone/ sulfuric acid solutions at primary ion current densities of 2.4 $\mu A/cm^2$ and 0.08 $\mu A/cm^2$ 84

FIGURE PAGE

22. Kinetic energy distributions for the molecular ion of 9-anthracenecarbonitrile and protonated sulfuric acid 91

23. Partial LSIMS spectra of benzoic acid/H_2SO_4 solution obtained with primary ion current densities of 2.8 and 0.1 $\mu A/cm^2$ 93

24. Positive LSIMS spectra obtained from 9-phenanthrene/H_2SO_4 and 9-phenanthrene/NH_4HSO_4/H_2SO_4 solutions 106

25. Positive LSIMS spectrum of a 2 mole % pterin/sulfuric acid solution 108

26. Positive LSIMS spectrum of a 2 mole % lumazine/sulfuric acid solution 109

27. Positive LSIMS spectrum of a 2 mole % 6-methylpterin/sulfuric acid solution 110

28. Positive LSIMS spectrum of a 2 mole % xanthopterin/sulfuric acid solution 111

29. Positive LSIMS spectrum of a 2 mole % 6-formylpterin/sulfuric acid solution 112

30. Positive LSIMS spectrum of a 2 mole % leucopterin/sulfuric acid solution 113

31. Positive LSIMS spectrum of a 2 mole % pterin-6-carboxylic acid/sulfuric acid solution 114

32. Positive LSIMS spectrum of a 2 mole % 6-hydroxymethylpterin/sulfuric acid solution . . . 115

FIGURE PAGE

33. Positive SIMS spectrum of $AlCl_3$ 122

34. Positive SIMS spectrum of $SnCl_2$ 123

35. Positive SIMS spectrum of $ZnCl_2$ 124

36. Positive SIMS spectrum of $SbCl_3$ 125

37. Positive SIMS spectrum of benzene obtained using $AlCl_3$ matrix 129

38. Positive SIMS spectrum of aniline obtained using $AlCl_3$ matrix 130

39. Positive SIMS spectrum of anisole obtained using $AlCl_3$ matrix 131

40. Partial SIMS spectrum of a 2:1 (mole ratio) $AlCl_3$/BPC melt in the region of m/z 76 - 141 . . . 133

41. Positive SIMS spectrum of a 1.9/1 (mole ratio) $AlCl_3$/EMIC melt 134

42. Partial SIMS spectrum of naphthalene//2:1 $AlCl_3$/BPC melt (ca. 20 mole % naphthalene) in the region of m/z 120 - 141 135

43. Partial SIMS spectrum of pyrene//2:1 $AlCl_3$/BPC melt (ca. 20 mole % pyrene) in the region of m/z 130 -207 136

CHAPTER I

INTRODUCTION

Analysis of involatile/thermally labile organic samples is one of the most active areas of mass spectrometric research. One technique for production of gas phase ions directly from such samples is secondary ion mass spectrometry (SIMS). SIMS is based on mass analysis of charged atomic or molecular species formed from bombardment of solids or liquids by ions with keV energies. The essence of SIMS is shown in Figure 1. Bombardment of a sample with a beam of energetic (keV) heavy ions, focused into a primary ion beam, results in the sputtering into the gas phase of secondary ions (positive and negative), neutrals, and electrons which are characteristic of the sample (1). Secondary ions can be mass analyzed and their intensity measured to produce a secondary ion (SIMS) spectrum which is characteristic of the sample.

The analytical utility of SIMS is due largely to the discovery by Barber et al. that, by dissolving organic samples in involatile liquids, or so-called matrices, the intensity and duration of emission of sample-characteristic secondary ions are greatly enhanced (2). When analytes are dissolved in a liquid matrix the technique is termed liquid secondary ion mass spectrometry (LSIMS). LSIMS is still in its infancy and the number of compounds for which enhanced

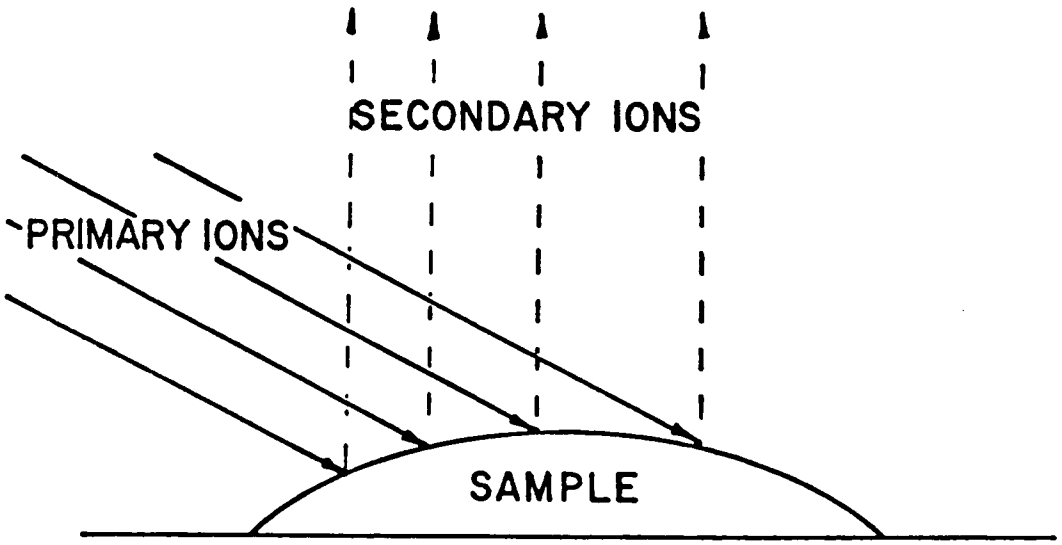


Figure 1. Schematic of secondary ion emission.

secondary ion emission has been observed is limited. Aromatic compounds represent a class of compounds which to date has not been found amenable to LSIMS analysis. Further, absence of a coherent theory for emission of secondary ions from liquid matrices hinders development of LSIMS as a routine analytical method.

The goal of the research presented in this dissertation is to expand the compound classes amenable to LSIMS analysis to include aromatic compounds and in the process gain insight into the mechanistic aspects of secondary ion emission from liquids. Identifying critical experimental parameters in LSIMS will facilitate its development for analyses of targeted compounds.

A. Occurrence of Aromatic Hydrocarbons and General Analytical Schemes

Aromatic compounds are widely dispersed throughout the environment arising from both natural and man-controlled processes. Pigments and cofactors in metabolic pathways are examples of common aromatic-containing natural products (3). Anthropogenic aromatic compounds are frequently associated with inefficient combustion. Many of the aromatics so derived are potentially carcinogenic and belong to a class of aromatic compounds known as polynuclear aromatic hydrocarbons (PAHs). They are released into the atmosphere during fossil fuel combustion (4-6). These airborne

aromatic pollutants are susceptible to chemical transformation which may form compounds more carcinogenic than the parent aromatic (7-13). The identity and the toxicity of many of these transformation products are not known. Developing methods for the detection and identification of aromatic compounds is important for investigating processes which are both beneficial and detrimental to life.

Involatile aromatic compounds often exist in real samples as trace components in complex mixtures. Extensive sample preparation is generally required before optical or mass spectral analysis is performed (3,4,6,14). This typically involves preconcentration and chromatographic separation of mixture components. Analysis of a complex mixture using these procedures may take weeks.

In principle, preconcentration and chromatographic separation could be eliminated or minimized were tandem mass spectrometry (MS/MS) employed (15). The need for preconcentration may be eliminated because the inherent sensitivity of mass spectrometry makes it well suited for trace analysis. It may be possible to eliminate chromatographic separation if mixture components are separated using mass spectrometry. In MS/MS, ions generated from mixture components are separated according to their mass-to-charge (m/z) ratios with a first mass spectrometer. The separated mass-selected ions then enter a reaction region or "collision

chamber" in which they undergo collision with a target gas (e.g. He) causing dissociation. Daughter ions formed in this reaction region are then analyzed with a second mass spectrometer. Ideally, each component targeted for analysis in the mixture is represented by a discrete ion. The sole criterion for MS/MS is that a persistent sample ion current be obtained (15). MS/MS is rapid, sensitive and selective. Application of MS/MS for analysis of involatile aromatics in complex samples requires application of a suitable ionization method.

B. Ionization Methods for Involatile Aromatic Compounds

Many pure aromatics and polar-substituted analogs are sufficiently volatile that electron ionization (EI) or chemical ionization (CI) mass spectra can be obtained. However, aromatics with multiple polar substituents or those which are strongly adsorbed on a substrate are not amenable to these ionization methods. EI and CI require the use of a gaseous sample with a partial pressure from 10^{-4} to 10^{-3} Pa (10^{-6} - 10^{-5} torr). This is generally accomplished by heating the sample, precluding analysis of thermally labile samples.

There are several desorption ionization methods designed to produce ions directly from involatile or thermally labile samples. In addition to SIMS, desorption ionization methods include plasma desorption and laser

desorption. In plasma desorption samples are bombarded with very energetic (MeV) ions produced from the spontaneous fission of a radionuclide (16). Sample-characteristic ions are emitted as a pulse associated with each decay event. In laser desorption, laser beams of various wavelengths can be used to desorb ions from either the front or back of a thin sample (17). The extent of fragmentation observed in laser desorption mass spectra is proportional to the power density of laser beam. In principle, changing the laser power density can provide either extensive fragmentation of organic molecules for structure analysis or minimal fragmentation for molecular weight determinations. Obtaining reproducible fragmentation patterns or determining absolute intensities is difficult with laser desorption mass spectrometry (LDMS) because of laser instability and variation in the absorbance of samples.

The distinct advantage of LSIMS compared to plasma or laser desorption is that intense sustained sample-characteristic ion currents can be routinely obtained. Such currents are required for MS/MS. Stable secondary ion currents are obtained in part because of the stability of the primary ion beam. Stable primary ion beams are routinely obtained since stable discharges, the basis of primary ion formation, are easily maintained.

Detection of involatile aromatic compounds by using SIMS requires first that the sensitivity be improved.

Application of SIMS to detection of trace quantities of aromatic compounds is difficult because secondary ionization of aromatics is inefficient (18). It is known that secondary ion emission is dramatically affected by changes in the chemical and physical environment of the condensed phase. The research presented in this dissertation has been directed toward improving the secondary ionization efficiency of aromatic compounds by manipulating the chemical and physical environment of aromatic analytes in the condensed phase. Since the most dramatic improvements in secondary ion emission are associated with sample dissolution, the emphasis of this work is on the use of liquid matrices for enhanced secondary ion emission.

C. Experimental Aspects of Secondary Ion Production

Production of secondary ions is conceptually simple. The ion source for SIMS shown in Figure 2 consists of a primary and secondary ion source (19). Typically, primary ions are formed via electron impact of a noble gas leaked into a discharge region of the primary ion source (labelled the boron nitride ion source in Figure 2). Primary ions thus formed are accelerated to typically 2-10 keV energies and focused. This primary ion beam can then be directed onto the sample in the secondary ion source. Alternatively, if the sample is a poor conductor, a beam of fast neutrals can be used for sample bombardment. Fast neutrals can be

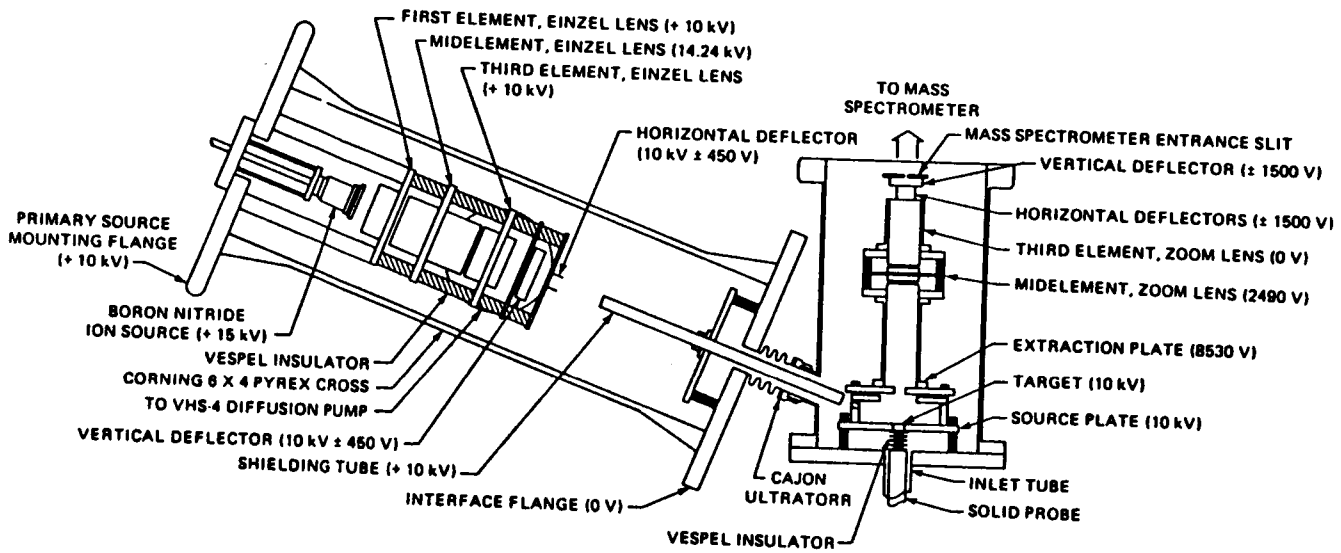


Figure 2. Diagram of the primary and secondary ion sources used in SIMS.

produced by passing the collimated primary ion beam through a collision chamber containing a high pressure, 10^{-1} - 10^{-2} Pa (10^{-3} - 10^{-4} torr), of the gas used for primary ion production (20). If fast neutrals are used the technique is termed fast atom bombardment (FAB). Secondary ions produced by particle bombardment are accelerated and focused in the secondary ion source prior to mass analysis.

D. SIMS Nomenclature

Benninghoven was the first to demonstrate that SIMS could be used to obtain useful mass spectra from organic samples deposited as monolayers on metal substrates (21). This method, "Static SIMS", uses a low primary ion current density (< 1 x 10^{-9} A/cm^2). By contrast, the method employed for inorganic samples, "Dynamic SIMS", employs a high primary ion current density (> 1 x 10^{-6} A/cm^2) (22,23). The high flux method is dynamic because the surface is eroded rapidly (>5 nm/min). Dynamic SIMS is not generally useful for organic analysis because the high flux results in a rapid decrease of the organic ion signal from thermal desorption and sample pyrolysis. The low primary ion currents used in static SIMS limit the secondary ion currents obtainable. Consequently, mass spectrometers with high transmission (eg. quadrupole and time of flight instruments) and pulse counting detection are required (1). Obtaining the high secondary ion currents generally

associated with dynamic SIMS from organic compounds would greatly expand the utility of SIMS.

E. Aspects of Liquid Matrices

Dissolution of organic analytes in involatile liquids appears to mitigate the effects of primary ion damage (2). Primary ion beam fluxes generally associated with dynamic SIMS can be used with liquid matrices without significant degradation of the resulting spectrum provided the liquid matrix does not completely evaporate. Sustained intense secondary ion currents are obtained (10^{-8} A) from liquid samples when high primary ion current densities are employed (24). Sample ion currents in LSIMS are comparable to those encountered using electron impact or chemical ionization. With LSIMS it is possible to scan large mass ranges with sector instruments, obtain high resolution, and MS/MS spectra (25-27). The technique is frequently known as fast atom bombardment or FAB since the authors who first used liquid matrices employed a primary beam of fast neutrals (2). However, the advantage is associated with the use of a liquid matrix rather than the use of a fast atom primary beam. Spectra obtained from liquids using fast atoms (FAB) or fast ions (LSIMS) are essentially the same (28) and are characterized by abundant pseudo-molecular ions, generally even electron molecular cations or anions (25,29). Commonly observed pseudo-molecular ions are

protonated molecules [$(M+H)^+$], deprotonated molecules [$(M-H)^-$], or molecular adducts with alkali metal cations [$(M+Na)^+$]. In general, radical cations ($M^{\cdot+}$) and other odd electron species are not abundant in FAB or SIMS spectra of liquid solutions (25,29).

Solvents used in LSIMS must have a low vapor pressure to be used easily. While spectra may be obtained from volatile matrices the spectra will be short lived and high pumping rates will be required to maintain the vacuum necessary for mass spectrometry.

Different matrices are employed for different analyte classes because subtle differences in chemical or physical properties have a pronounced effect on the enhancement of pseudo-molecular or molecular ion emission (30). The mechanism of secondary ion emission from liquid matrices is subject to much debate, with most of the attention focused on positive secondary ion emission (31).

It has been determined empirically that three criteria must be met for a particular matrix to enhance the positive secondary ion emission of a particular analyte: (a) the analyte must be soluble in the matrix (2,30,32), (b) the analyte must be basic (Bronsted definition) with respect to the matrix in the condensed phase (33), and (c) the gas phase proton affinity of the analyte must be greater than that of the matrix (34-36).

In addition to the above criteria for enhanced emission from matrices, other considerations are required for selection of matrices of analytical utility (25). Matrices should not react with the target compound except to promote specific ion formation reactions which increase the secondary ion yield. If reactive matrices are used, the reactions should be characterized if spectra are to be interpreted in a systematic fashion. Further, matrix-characteristic ions should not obscure analyte-characteristic ions represented in the SIMS spectrum if analytes present in trace quantities are to be detected. If primary ions are used, the sample must be conductive or sample charging can lead to instability in the secondary ion signal.

F. Organic Secondary Ion Formation from Liquid Solutions

Most reports of enhanced emission from liquid matrices are for compounds which exist to some extent as ions in solution. It has been proposed that solvated ions are precursors to the secondary parent ions observed in SIMS spectra (37). Alternatively, it is argued that gas phase ionization of ejected neutrals via proton transfer from protonated matrix species is the dominant process in enhanced secondary emission from liquid matrices (34-36). There is evidence which supports both models and it is possible that enhanced secondary ion emission may depend on

both processes. Regardless of the process responsible, any increase in the sensitivity of the method relies on increasing the secondary ion yields. Secondary ion yield is the ratio of secondary ions to primary ions.

1. Ion Formation in Solution

Producing solvated ions in the condensed phase has been shown to lead to an increase in the abundance of the corresponding gas phase species observed in LSIMS spectra. This "precursor model" (37) has led to development of a variety of methods for increasing the concentration of ions in the condensed phase. All of these methods promote formation of solvated ions in solution. These "promotion reactions" have been accomplished by 1) reactions of the analyte with the matrix (38,39), 2) reactions with additives (40,41), or 3) producing analyte-characteristic ions prior to addition to the matrix (salt formation) (42).

Acid-base reactions are the simplest promotion reactions. Increasing the acidity of a matrix has been shown to increase the positive secondary ion signal of analytes which can be protonated (38,39). Conversely, addition of base to matrices should increase the relative abundance of negative ions associated with proton loss (38).

Adduct formation between analytes and alkali metal or ammonium cations has been used to promote condensed phase

ion formation through addition of the appropriate salt (40,41).

As stated earlier, molecular radical cations ($M^{+\cdot}$), odd electron species, are not typically found in high abundance in SIMS spectra of solutions. When observed, they were generally associated with complexes of a solute with strong electron acceptors (43-45) or species produced by formal one electron oxidations (46,47) in the condensed phase. Depauw reported that formation of charge transfer complexes within a glycerol matrix enhanced the molecular ion ($M^{+\cdot}$) signal of the electron donor species (43). In these experiments the abundance of donor (tetramethyl-1,4-benzenediamine) molecular ions, $M^{+\cdot}$, relative to the abundance of protonated donor molecules, $(M+H)^+$, increased when electron accepting complexing agents (substituted p-benzoquinones) were added. It was suggested that formation of charge exchange complexes in solution led to an increase in the concentration of radical cations in the condensed phase. However, it is unlikely that dissociation of this complex to produce discretely charged species could occur without the perturbation caused by primary beam bombardment. Dissociation of charge transfer complexes requires absorption of photons, thus molecular ions detected were not radical cations in solution.

Enhanced aromatic molecular secondary ion emission has been observed from aromatic hydrocarbon/$SbCl_3$

mixtures (44). Since $SbCl_3$ is known not to oxidize the aromatics for which molecular ions were observed and is known to form complexes with such aromatic systems, it was suggested that the formation of analyte/$SbCl_3$ complex was related to the appearance of molecular ions in aromatic hydrocarbon/$SbCl_3$ mixtures. Cyano derivatives have also been employed as complexing agents to enhance production of radical cations which could not be detected without addition of the complexing agent (45).

2. Gas Phase Ion Formation

Sunner et al. have argued that ionization processes in secondary ion emission are dominated by gas phase ion-molecule reactions and they have proposed a gas phase collision model (GCM) (35). Work by these authors indicates that relative ion intensity parallels the gas phase proton affinity. The gas phase proton affinity (PA) is defined as the negative enthalpy change for reaction (1). Gas phase

$$A + H^+ \rightleftharpoons AH^+, \qquad -\Delta H^o = PA(A) \qquad (1)$$

proton affinity is fundamental to studies of gas phase ion-molecule reactions or chemical ionization; proton affinities determined via various thermodynamic cycles and kinetic studies have been tabulated (48). Sunner et al. observed that the percentage of the total ion current (analyte and matrix secondary ions) associated with the $(M+H)^+$ abundances

for analytes was greater for those analytes with the highest PA (35,36). However, gas phase proton affinity generally parallels solution basicity and it is not possible to determine which property is most significant in the secondary ion emission process. It is expected that particles sputtered from the condensed phase will undergo numerous collisions during expansion into the gas phase (49,50). Consequently, gas phase proton affinity will determine the "survivability" of molecules protonated in the condensed phase.

Formation of molecular radical cations in the gas phase through interaction of the primary beam with volatile samples has been demonstrated (51,52). It was proposed that radical cation formation takes place via a charge exchange process. In one of these investigations both solution and gas phase ionization were detected for some samples with the former yielding even molecular ions and the latter yielding radical cations (51).

G. Selection of LSIMS Matrices for Aromatic Compounds

Constraints imposed on matrix selection for enhanced aromatic secondary ion emission exclude matrices which are commonly used in LSIMS. Most aromatic compounds are insoluble in glycerol, the most commonly used liquid matrix in LSIMS. Two matrix properties required for enhanced secondary ion emission, analyte miscibility and matrix

involatility, are generally mutually exclusive when aromatic compounds are concerned. Solvents in which aromatic compounds readily dissolve tend to be volatile. Some have employed cooling to minimize matrix evaporation; however, freezing of the matrix effectively stops secondary ion emission (53). Meeting other criteria for enhanced aromatic secondary ion emission imposes additional limitations on matrix selection.

The majority of matrices studied to date have been organic compounds which act as weak acids in the condensed phase and usually have substantial gas phase proton affinities. Consequently, most investigations with LSIMS or FAB have been limited to compounds which are either basic or contain a basic moiety such as $-NH_2$. Aromatic compounds are weakly basic and their gas phase proton affinity is lower than the proton affinity of most involatile solvents. In only a limited number of investigations of aromatic secondary ion emission from liquids, the criteria of analyte miscibility and matrix involatility have been met. LSIMS spectra have been obtained for a few small aromatic compounds which were dissolved in glycerol (54). In another investigation, a technical grade hydrocarbon fraction (boiling range 620-810 K) has been used as a liquid matrix to obtain FAB spectra of a few aromatic hydrocarbons (55). An obvious problem in using a hydrocarbon matrix in LSIMS or

FAB to detect hydrocarbons is that matrix-characteristic ions can obscure analyte-characteristic ions.

LSIMS spectra contain peaks characteristic of analyte and matrix, as well as peaks which reflect sample damage caused by the primary beam (56). These latter peaks, which arise from non-specific fragmentation of analyte and matrix molecules as well as their clusters, are frequently small, but found at nearly every mass, and provide no analytical information about either analyte or matrix. Because such peaks raise limits of detection by their interference with analyte-characteristic peaks, they are referred to as "chemical noise". This chemical noise can severely limit detection of species present at low concentrations. Thus, the ideal matrix should not contribute significantly to the mass spectrum in region of interest. Matrices which are structurally simple produce relatively few fragments, improving detection limits. Use of a matrix which lacks a hydrocarbon backbone, such as polyphosphoric acid (32,57), reduces chemical noise attributable to the matrix, because its elemental composition will not yield ions at every integral mass.

The criteria for enhanced secondary ion emission suggest that strong acids such as H_2SO_4 may extend the range of compound classes which are amenable to study by LSIMS. Many organic compounds are basic with respect to H_2SO_4 in both gas and condensed phases and are soluble in it.

As the gas phase proton affinity of H_2SO_4 (711 kJ/mole) (58) is lower than that of any arene used in this investigation (e.g. the proton affinity of hexafluorobenzene is (755 kJ/mole) (59), gas phase proton transfer should favor arene protonation in all cases. The criterion of analyte basicity for enhanced secondary ion emission is met by substituted aromatics dissolved in concentrated sulfuric acid. Many aromatics are extensively protonated in concentrated sulfuric acid (60-63).

The physical properties of H_2SO_4 are compatible with use in the mass spectrometer. The vapor pressure of concentrated sulfuric acid at 23°C is 5.3×10^{-3} Pa (4×10^{-5} torr) (64), substantially less than that of glycerol (65) at the same temperature. This low volatility makes concentrated sulfuric acid amenable to the vacuum of the ion source and, at the same time limits contamination and corrosion of the mass spectrometer. Corrosion of components likely to contact liquid sulfuric acid can be avoided by constructing them from stainless steel as it is not attacked by concentrated sulfuric acid at temperatures below 100 °C (66). Even though concentrated sulfuric acid is hygroscopic, maintaining a high vacuum will prevent formation of dilute sulfuric acid which can attack stainless steel.

Sulfuric acid is structurally simple and the SIMS spectrum of the neat matrix cannot yield peaks at every integral mass. Additionally, with a matrix such as sulfuric

acid, ions containing sulfur are distinguishable from sulfur-free analyte ions because of the substantial mass defect of sulfur (M.W. S^{32} - 31.97207) compared to carbon (M.W. C^{12} - 12.000).

Concentrated sulfuric acid has a high dielectric constant (ϵ = 100) (67) which promotes condensed phase ionization (68), and is itself relatively ionic ($K_{diss} \sim 5 \times 10^{-6}$) (69). Thus sulfuric acid is relatively conductive; primary ion bombardment should not lead to sample charging.

It is worth noting that SIMS spectra of a number of arenes have been reported in the literature (54,55,70-73) as has the use of mineral acids to enhance secondary ion emission (57,74). In this work the emphasis has been placed on the investigation of the secondary ion mass spectral behavior of a number of substituted arene/H_2SO_4 solutions to evaluate the general applicability of the technique for identification and detection of various arene compound classes. Also, investigation of the relationship between such secondary ion mass spectra and the chemistry of these solutions may provide additional information about the mechanism of secondary ion emission from liquids.

H. Chemistry of Aromatic/Sulfuric Acid Solutions

The chemistry of aromatic/H_2SO_4 solutions has been studied extensively by using cryoscopy (62,75), UV

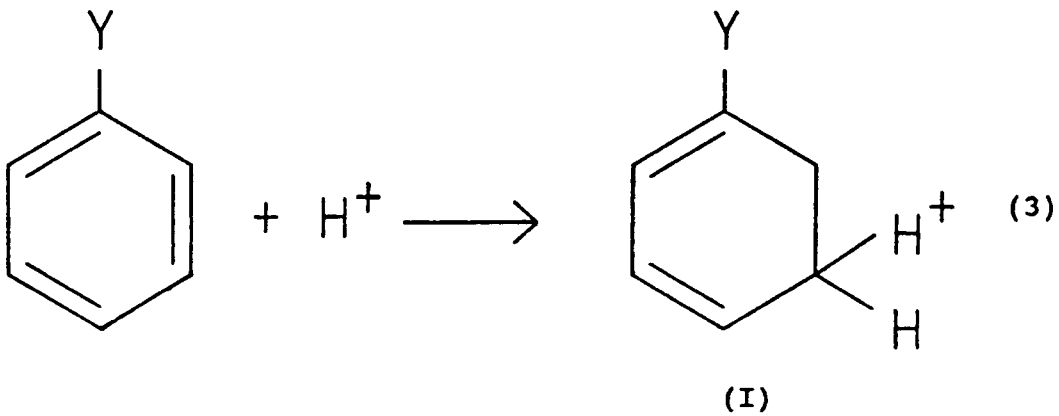
spectroscopy (76-79), nuclear magnetic resonance (NMR) (80-82), and electron spin resonance (ESR) (78,83-85). Of particular interest here is reaction (2) where ArY

$$ArY + H_2SO_4 \rightleftharpoons ArYH^+ + HSO_4^- \qquad (2)$$

represents a substituted arene. Even weak bases such as 3-nitrobenzoic acid are more than 50% protonated in concentrated H_2SO_4 (86,87). It is reasonable to expect, then, that stronger bases, which would include virtually any substituted arene, would give rise to a significant concentration of their conjugate acids in 98% H_2SO_4 solution. If there is any credence to the notion that secondary ions arise from condensed phase ionic precursors, arene/H_2SO_4 solutions should yield intense arene-characteristic secondary ion currents.

Sulfuric acid is a reactive medium. Aromatic compounds which possess electron-donating groups such as $-OCH_3$ and $-CH_3$ are subject to rapid mono-, di- and trisulfonation (61,88,89). On the other hand, sulfonation of aromatic compounds lacking such activating groups proceeds to completion at an appreciable rate in sulfuric acid only at elevated temperature and/or in the presence of excess SO_3 (i.e., oleum) (89), conditions which are easily avoided.

Furthermore, aromatic sulfonation is an extensively studied reaction, and within some limitations, the speciation of aromatic compounds dissolved in sulfuric acid, as protonated species and as complexes, is better characterized than in most other media. This feature makes substituted aromatic/sulfuric acid solutions ideal for investigating the mechanism of secondary ion emission from liquids. As stated earlier, substituted aromatic compounds are basic with respect to sulfuric acid in the gas phase, so that exothermic gas phase proton transfer always favors protonation of the aromatic. In sulfuric acid solution the only question is which site of a substituted aromatic compound is protonated. In other words, protonation of the substituent site is competitive with protonation of sites on the aromatic ring(s). In the latter case, the protonated species is a particular case of what is known as a σ-complex (90). Protonation of the aromatic ring of a substituted aromatic compound forming the σ-complex (I) is shown in reaction (3).



(3)

(I)

Formation of σ-complexes (and charge-transfer or π-complexes) has been associated with enhanced emission of analyte molecular ions, $M^{+\cdot}$, from $SbCl_3$ (44), and from glycerol solutions (43). Molecular ions cannot be formed by gas phase proton transfer. Consequently, comparison of the relative intensities of aromatic molecular ions and protonated aromatic molecules observed in the LSIMS spectra of various aromatic/sulfuric acid solutions can provide some information about the importance of gas phase chemistry, as opposed to solution phase chemistry, in secondary ion emission from liquids.

I. Enhanced Molecular Radical Cation Emission

If condensed phase ionization leads to enhanced secondary ion emission, it is reasonable to investigate reactions which form molecular radical cations in solution. In aromatic/CH_2Cl_2/$AlCl_3$ solutions, electron spin resonance and optical spectroscopic methods indicate the presence of solvated aromatic cations, $M^{+\cdot}$, formed as products of reaction (4) at room temperature if the ionization energy (IE) of the aromatic is about 8 eV of less (91).

$$M \overset{AlCl_3}{\rightleftharpoons} M^{+\cdot} \qquad (4)$$

Clearly CH_2Cl_2 is too volatile to use as a component of an LSIMS matrix. By substitution of an involatile liquid for CH_2Cl_2, it may be possible to increase the molecular radical cation abundance in LSIMS by addition of the appropriate reagent. This is dependent on the selection of an involatile liquid in which the analyte(s) and additive are soluble.

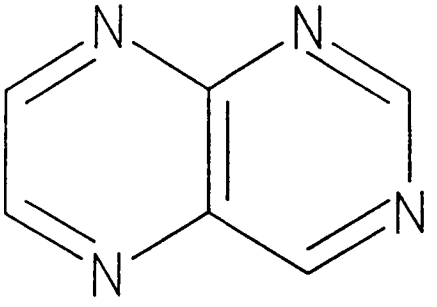
Organic salt melts may be useful as LSIMS matrices for dissolution of aromatic compounds and metal chlorides. Mixtures of appropriate amounts of the organic salts N-(1-butyl)pyridinium chloride (BPC) or 1-ethyl-3-methylimidazolium chloride (EMIC) with $AlCl_3$ are liquids at room temperature (92,93). These ionic liquids are involatile and some aromatic compounds are soluble in these melts (94). Further, Robinson and Osteryoung reported that certain aromatic hydrocarbons are spontaneously oxidized to their radical cations in a 2:1 (mole ratio) solution of $AlCl_3$ and butyl pyridinium chloride, respectively (92). These room temperature melts are potential LSIMS matrices for enhanced arene secondary molecular ion emission. SIMS spectra have been reported from $AlCl_3$/BPC melts containing 45 to 67 mole % $AlCl_3$ (95).

J. Analytical Applications of Concentrated Sulfuric Acid as a LSIMS Matrix -- Comparison with Existing Methods

Concentrated sulfuric acid should be a very good matrix for LSIMS analysis of involatile aromatics containing multiple polar substituents. Further, concentrated sulfuric acid may be a useful LSIMS matrix for in situ analysis of substituted aromatics adsorbed on substrates. Examples of these types of analyses, which are subjects of investigations conducted in this doctoral research, are described below.

1. Biological Applications: Pterins

Pterins are involatile multiply substituted aromatic compounds which contain the heterocyclic ring pyrimido [4,5-b]-pyrazine (II) (3). They are encountered



(II)

frequently as trace components in a variety of naturally occurring sources and are found throughout the animal kingdom. They are often cofactors in various metabolic pathways and are of interest in biochemistry and

medicine (3,14). Analysis of pterins is difficult since they are generally isolated in trace quantities and chromatographic methods do not always provide the selectivity required for identification of unknown compounds (96). Mass spectrometry is well suited for such problems. However, the low volatility of free pterins makes direct analysis by mass spectrometry using electron impact or chemical ionization difficult at best (14,96-98). Formation of trimethylsilyl derivatives is generally required for mass spectral analysis (96-98). Mass spectra of these derivatives are not very suitable for structure elucidation because of poor and non-specific fragmentation (96). Derivatization could be eliminated by using LSIMS.

The analysis of pterins by secondary ion mass spectrometry using a liquid matrix (LSIMS) has been limited by the absence of a suitable matrix; pterins are poorly soluble in water and most organic solvents (14). Finding an appropriate LSIMS matrix for pterins would enable the use of MS/MS for analysis of pterins in complex biological samples.

2. Environmental Applications: Detection and Identification of Transformation Products of Polynuclear Aromatic Hydrocarbons

As stated earlier, polynuclear aromatic hydrocarbons (PAHs) are commonly derived from use of wood, petroleum, and

coal. Major sources of PAHs include emissions from motor vehicles, heat and power generation, industrial processes, and refuse burning (4,6). PAHs are pollutants which are widely dispersed throughout our environment; they are present in the air, soil, and water. Further, the relationship between PAHs and cancer is well established from epidemiological (99,100) and experimental studies (4-6,99,100). Determining the fate of PAHs released into the environment is critical for evaluating the occupational and environmental health impact of these compounds.

Fossil fuel combustion is the largest technological source of PAHs (4,6). PAHs formed from combustion frequently condense on particulate matter as cooling occurs (101). PAHs from coal combustion are commonly associated with coal derived particulates or fly ash. The highest concentrations of adsorbed PAHs tend to be associated with respirable particles of less than 3 μm aerodynamic diameter (4,6,102,103). Particulates of this size can remain in the atmosphere for several days (104).

PAHs are known to undergo photochemical oxidation as neat solids (105) or adsorbed on substrates such as alumina (106), silica gel (106), glass (107), soot (108) and coal fly ash (109). The products formed in these transformations are not always known; however, ketones, aldehydes, and phenols have been observed (110). In addition, non-photochemical attack of adsorbed PAHs by

atmospheric co-pollutants such as ozone, sulfur trioxide and nitric acid, has been demonstrated under controlled conditions (110).

The extent to which transformation products are formed on airborne particulates, their identity and consequently their mutagenic and carcinogenic potential are not known. The wide dispersion of PAHs on respirable particulates and the possibility that they may transform to mutagenic compounds in the atmosphere warrant surveillance of particulates containing PAHs.

Identifying PAHs on fly ash is difficult for several reasons. Fly ash has a high affinity for PAHs; adsorbed PAHs are strongly retained (111). Further, PAHs may exist only as trace constituents of fly ash (< 200 ng PAH/g fly ash) (4). Transformation products may exist at even lower concentrations. Fly ash is likely to contain a multitude of aromatics which are strongly adsorbed onto a complex matrix. Such complex samples are difficult to characterize with any analytical technique. These facts have complicated investigations of the fate of fly ash-borne PAHs.

A number of analytical methods have been developed for isolation, detection, and identification of PAHs adsorbed onto fly ash. These methods generally include extraction, chromatographic separation and optical or mass spectral identification (4,6). A method for in situ

detection of PAHs and their derivatives would be desirable to avoid the time consuming and inefficient extraction techniques currently employed. Optical methods, such as UV absorption or fluorescence spectroscopies, are well suited for quantitation of PAHs extracted from fly ash (4,6). Nevertheless, in situ detection of PAHs adsorbed on fly ash by UV absorption or fluorescence spectroscopies has not been demonstrated, largely because the optical absorbance of fly ash is large compared to the absorbance of the trace quantities of PAHs present on the fly ash.

Mass spectrometry is an inherently sensitive and selective analytical technique which may be useful for in situ detection of PAHs (or their derivatives) adsorbed on fly ash. Adsorption of PAHs on fly ash substantially reduces their vapor pressure. Consequently, high temperatures are required to desorb sufficient quantities of PAHs from fly ash for gas phase ionization. High temperatures, the presence of a variety of adsorbed compounds, and the possible catalytic activity of fly ash could result in chemical transformation of PAHs during the volatilization. This suggests that desorption mass spectrometric methods would be the best methods for in situ characterization of fly ash. Desorption ionization methods are capable of producing ions from the condensed phase as opposed to gas phase ionization. Laser desorption mass spectrometry (LDMS) has been used for qualitative

characterization of coal and oil particulate matter (112). In that investigation many of the elements present in fly ash were identified when high laser fluence was used. At low laser fluence, possible assignments for organic species detected were based on compounds which were known to exist on coal fly ash.

Absolute identification of organic components on airborne particulates could be accomplished in principle if sample ion currents suitable for MS/MS were obtained. LSIMS would be the best candidate for such analysis. Implementation of LSIMS for analysis of adsorbed aromatics is dependent on effectively removing aromatics from the substrate and enhancing secondary ion emission. Sulfuric acid may effectively extract substituted aromatics from substrates and enhance secondary ion emission as well.

K. Objectives of This Study

The objectives of this study are 1) to develop methods for analysis of substituted aromatic compounds using LSIMS and 2) provide additional insight into secondary ion emission from liquids. The focus of this dissertation concerns use of concentrated sulfuric acid as a LSIMS matrix.

The method for improving the sensitivity of LSIMS for aromatic compounds outlined in this dissertation is a general one. First, LSIMS spectra of singly substituted

aromatics dissolved in concentrated sulfuric acid were characterized. Employing such test compounds makes it easier to evaluate the effectiveness of SIMS matrices for individual compound classes and permits some insight into the mechanistic aspects of secondary ion emission from matrices. The chemistry of aromatic/sulfuric acid solutions is well characterized; correlations between known solution phase behavior and the secondary ion emission from such solutions are presented in this dissertation.

Subsequent to investigations of model compounds, the analytical utility of H_2SO_4 as a LSIMS matrix is demonstrated for aromatics containing multiple polar substituents. Abundant and persistent secondary ion currents were obtained from involatile aromatics, namely pterins. In addition the efficacy of methods developed herein for the detection of aromatics adsorbed on fly ash is investigated.

CHAPTER II

EXPERIMENTAL

This chapter is divided into three sections. Section A is devoted to discussion of the secondary ion mass spectrometer and the experimental parameters associated with its use for investigations presented in this dissertation. Section B concerns use of concentrated sulfuric acid as a liquid matrix for the enhanced emission of substituted aromatic compounds. Section C is devoted to experimental aspects of use of metal chlorides and room temperature melts as matrices.

A. Mass Spectrometer

The primary and secondary ion sources employed, shown in Figure 2 (p. 8), have been described previously (19,113). The primary 5 keV Ar^+ beam was focused and aligned so that the entire 0.9 cm diameter surface of the targets was irradiated. The extent of the target irradiation was indicated by light emitted from a target loaded with NaI. Sodium iodide fluoresces when irradiated by the energetic primary ion beam. The current density of the primary beam could be varied from 10 to 0.05 $\mu A/cm^2$ by adjusting the potentials on the lens elements of the primary source. The current density was measured using a Faraday cup mounted on the end of a specially fitted probe. The secondary ion

accelerating voltage was 8.0 keV. Potentials applied to the lens elements of the secondary ion source were swept for investigations of the kinetic energy spread of the emitted secondary ions. The mass analyzer, a Nier-Johnson (EB) mass spectrometer, is described elsewhere (114). The electrodes in the electrostatic sector were gold plated to prevent attack by the metal chlorides investigated. Secondary ions were detected by using a continuous dynode electron multiplier operated at potentials from -900V to -2300V.

B. Concentrated Sulfuric Acid

1. Materials

Reference compounds and reagents used in these investigations are given in Appendix A.

2. Targets

Targets must be conductive when using a beam of fast ions to mitigate against secondary ion beam instability associated with sample charging. Targets for the sample support were constructed from a stainless steel plug, 6.35 x 9.5 mm diameter. Platinum filter cloth (10% rhodium, mesh size: 120x400, Unique Wire Weaving Co.) was spot-welded to the center of the stainless steel plug. The mesh, combined with the viscosity of H_2SO_4, limits the flow of sample down the face of the target and minimizes source contamination and corrosion (115). After use, targets were

cleaned by repeated submersion in ultrasonic baths of water and subsequently, trichloroethylene. Despite repeated use, no macroscopic evidence of target corrosion was observed.

3. Sample Preparation

Approximately 100 μg of analyte was transferred to the center of a target via the clean glass tip of a disposable transfer pipette. The analyte was dissolved in 2 mg H_2SO_4 by depositing the sulfuric acid onto the analyte-loaded target. This method produces a solution ca. 2 mole % PAH. Primary ion beam irradiation of the sample commenced ca. 6 minutes after sample preparation. Mass spectra were obtained approximately one minute later.

Samples were generally prepared in a drybox (to be described in Section C) attached directly to the secondary ion mass spectrometer. Absolute containment of hazardous reference compounds is essential. It was repeatedly observed that when a sample vial is opened a small amount of the sample is dispersed into the still drybox atmosphere. Inhalation of these compounds is particularly hazardous. For less toxic compounds, or for samples where the analyte is strongly adsorbed onto some secured substrate, such precautions may not be necessary. SIMS spectra were identical whether the sample was prepared in the drybox or not. Pterins used in this investigation were handled under red light to prevent photo-induced decomposition.

For measurements of aromatic secondary ion intensity *versus* analyte concentration, sulfuric acid solutions were prepared using recrystallized benzoic acid, which had been titrated with 0.0100 N NaOH to assure dryness. Concentrations of the prepared solutions were 1.0×10^{-4} - 0.5 M benzoic acid. One μL of each solution was loaded as described above. Secondary ion currents of both m/z 99 ($H_3SO_4^+$) and m/z 123 ($C_7H_7O_2^+$) emitted from each solution were recorded manually from the amplified detector output. Complete and partial mass spectra of each solution were also recorded. Signal averaging was accomplished by using a Nicolet Model 1170 Signal Averager.

4. Superacid Preparation

One of the strongest acids known to exist in H_2SO_4, based on its ability to protonate nitroaromatic compounds, is tetra(hydrogen sulfato) boric acid [$HB(HSO_4)_4$] (116,117). The reaction of oleum (fuming sulfuric acid) and boric acid to form this superacid is shown in reaction (5).

$$H_3BO_3 + 3H_2S_2O_7 \rightleftharpoons H_3SO_4^+ + B(HSO_4)_4^- + H_2SO_4 \quad (5)$$

Tetra(hydrogen sulfato) boric acid dissociates in solution and results in the protonation of sulfuric acid, as indicated in the above reaction. This superacid was produced by mixing one mole boric acid for every three moles

of free SO_3. The density of the oleum was measured to determine the concentration of free SO_3.

5. Adsorbed Aromatics

a. Deposition Methodology

Substrates investigated include alumina, silica gel, filter paper, and Texas and Kaneb fly ash. Acridine was loaded onto all the substrates investigated except the filter paper using a vapor deposition apparatus described elsewhere (118). Acridine was deposited onto substrates by passing acridine vapors in a nitrogen carrier gas through the substrate.

A known quantity of a substrate (ca. 20 mg) was added to a cell for vapor deposition of acridine. The amount of acridine deposited on the substrate was the difference between how much acridine passed through the deposition apparatus with and without the substrate present for the given period. During acridine deposition, the effluent from the deposition apparatus was collected in a cold trap for the entire deposition period. The flow rate of acridine without substrate present was constant and was determined by collecting the effluent from the deposition apparatus for a known period of time. The collected acridine was removed from the cold trap by washing with 50 mL of methanol. The concentrations of the resulting acridine/methanol solutions were determined using ultraviolet absorption spectroscopy.

Analyses were performed using a Varian DMS 70 UV/Visible Spectrophotometer. The absorption band of acridine centered at 249.5 nm was used for quantification. Standard solutions were prepared by placing an appropriate amount of acridine into a 100 mL volumetric flask and then making the appropriate dilutions to obtain the desired concentrations. During acridine deposition, the effluent from the deposition apparatus was collected for the entire deposition period.

Filter paper (42 cm, ashless) was loaded with acridine by placing the filter in a 0.09 M acridine/methanol solution. The paper was then removed from the solution and dried in an oven.

b. Sample Preparation for SIMS Analysis

The samples were prepared for SIMS assay by mixing 10 - 25 mg of the substrate with 10 μl of concentrated H_2SO_4. One set of extractions was carried at room temperature, the other at 90 ^{o}C in an oven. After approximately 12 hours the mixtures were placed in a centrifuge. The supernatant was then removed with a transfer pipette and loaded onto a target.

C. Metal Chlorides and Ambient Temperature Melts

1. Materials

For experiments employing metal chlorides, both high purity and reagent grade compounds were used. High purity

reagents and their method of purification are discussed below. Other compounds used in this investigation and their suppliers are given in Appendix A.

High purity $AlCl_3$ was obtained from Brisco Harward (University of Tennessee, Knoxville). It was obtained from Fluka AG and purified in a drybox by digesting the molten $AlCl_3$ with a small quantity of NaCl. $AlCl_3$ and $AlCl_3$/NaCl phases resulted with more noble metal impurities being extracted into the $AlCl_3$/NaCl phase. The pure $AlCl_3$ layer was then sublimed under reduced pressure three times to remove oxychlorides (92).

High purity $SbCl_3$ was obtained from S. P. Zingg (Oak Ridge National Laboratory). It had been purified by first digesting the $SbCl_3$ with antimony metal and Sb_2O_3. The $SbCl_3$ phase was then sublimed twice under reduced pressure and then zone refined (24 passes, 7 zones).

1-ethyl-3-methylimidazolium chloride (EMIC) (93) was obtained from G.P. Smith (Oak Ridge National Laboratory). N-(1-butyl)pyridinium chloride (BPC) (119) was obtained from Timothy Laher (University of Tennessee, Knoxville).

2. Drybox

A drybox (90 cm x 87 cm x 65 cm) was used for all experiments involving air sensitive metal chlorides. The drybox with antechamber was interfaced directly to the secondary ion source via a 7 mm thick neoprene diaphragm

fitted with hardware for coupling to the mass spectrometer insertion lock as shown in Figure 3. The drybox was mounted on wheels and could be removed from the spectrometer as necessary. High purity (typically 99.997%) argon was used as filler gas. Water and oxygen were continually removed from the drybox atmosphere by recirculating the argon through an attached manifold containing deoxygenation catalyst and molecular sieve. This manifold, which could be isolated from the drybox, was also fitted with a cold trap to remove organic vapors from the drybox atmosphere. The moisture level of the drybox, typically <10 ppm, was monitored using an Ondyne Model 1400 hygrometer. The oxygen level, typically <10 ppm, was monitored using a Teledyne Model 310 oxygen meter. The slightly positive pressure of the drybox was regulated using a Dwyer Instruments Photohelic Pressure Switch/Gauge in conjunction with solenoid valves controlling argon introduction and venting.

3. Melt Preparation

$AlCl_3$-BPC and $AlCl_3$/EMIC ambient temperature melts were prepared by addition of $AlCl_3$ to the corresponding organic chloride salt (93,119). The reaction is exothermic and the $AlCl_3$ must be added slowly since overheating results in decomposition of the organic salt. Melts equimolar in $AlCl_3$ and organic salts were colorless. Melts 66 mole %

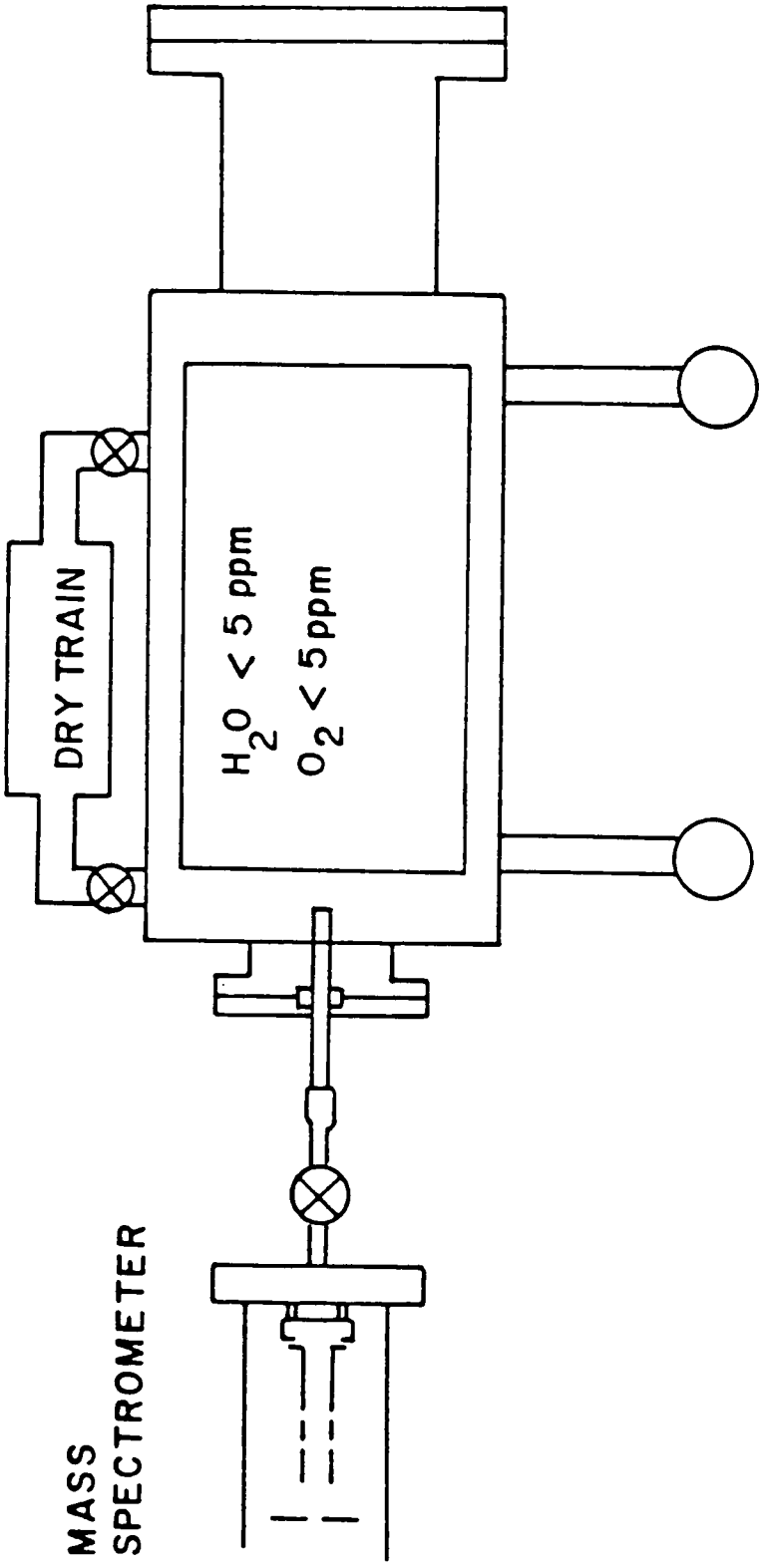


Figure 3. Diagram of drybox and secondary ion source interface.

$AlCl_3$ were slightly tan. Dark melts were indicative of decomposition of the organic salt.

4. Targets

Gold targets were fabricated since they are resistant to attack by corrosive salts and are good conductors. These targets were produced by melting gold in a 10 mm hole which had been bored into a graphite block. A 5-40 threaded hole with a set screw inserted in it was centered in the base of this mold. The set screw was used to attach the target to the probe. The gold button with set screw was then machined to the appropriate dimensions. Targets were cleaned with water and acetone after they had been removed from the drybox.

5. Furnace

The metal chlorides had to be attached to the targets because of the vertical sample orientation in the secondary ion source. Solid metal chlorides were either melted or sublimed onto the gold targets using a small furnace. The furnace consisted of two concentric quartz tubes approximately 5 cm long. The internal diameter of the inner tube was approximately 10 mm. The outer tube had six 3 mm notches cut into both ends. A single nichrome ribbon was wrapped longitudinally, secured by the notches. The inner tube was inserted into this wrapped outer tube. Ends of the

nichrome ribbon were attached to a variable voltage transformer which was adjusted to control the temperature of the furnace. This entire assembly was supported on a 10 mm post centered on an aluminum base.

Samples were prepared by placing the gold target, loaded with approximately 20 mg of metal chloride, on the post. The furnace was then placed on the post and heated gently until the sample melted. For those salts which sublimed, such as $AlCl_3$, vapors condensed onto another gold target held above the furnace.

6. Sample Preparation for Volatile Metal Chlorides

Salts with vapor pressures at ambient temperature incompatible with the vacuum requirements of the secondary ion source were cooled prior to insertion into the mass spectrometer. Samples could be cooled to -60°C within the drybox by placing the salt loaded target on a cooling block. The cooling block consisted of a cylinder of aluminum (5 cm dia. x 8 cm) with 6 mm copper tubing coiled around it. The ends of the copper tubing passed through the walls of the drybox via bulkhead swaged fittings. The block was cooled by forcing liquid nitrogen through the tubing.

Since the target ultimately made contact with the source flange in the secondary ion source, the source flange had to be cooled. This was accomplished by contacting a liquid nitrogen cooled probe, or cold finger, to the source

flange. The cold finger passed through a 25.4 cm bulkhead mounted "O" ring fitting (Cajon) into the secondary ion source. It had to be retracted prior to application of the accelerating potential to the source flange. The source temperature was monitored using a chromel/alumel thermocouple.

7. Volatile Sample Introduction

Volatile analytes were introduced onto the matrix in the secondary ion source via molecular leak and heated introduction tube as shown in Figure 4. Analytes entered the source approximately 3 cm from the target. Secondary ions, $M^{\cdot+}$, were then sputtered into the gas phase by the Ar^+ ion beam and subsequently mass analyzed. The all glass heated inlet system (R.J. Brunfeldt Co., Bartlesville, Oklahoma) temperature was approximately 200 ^{o}C.

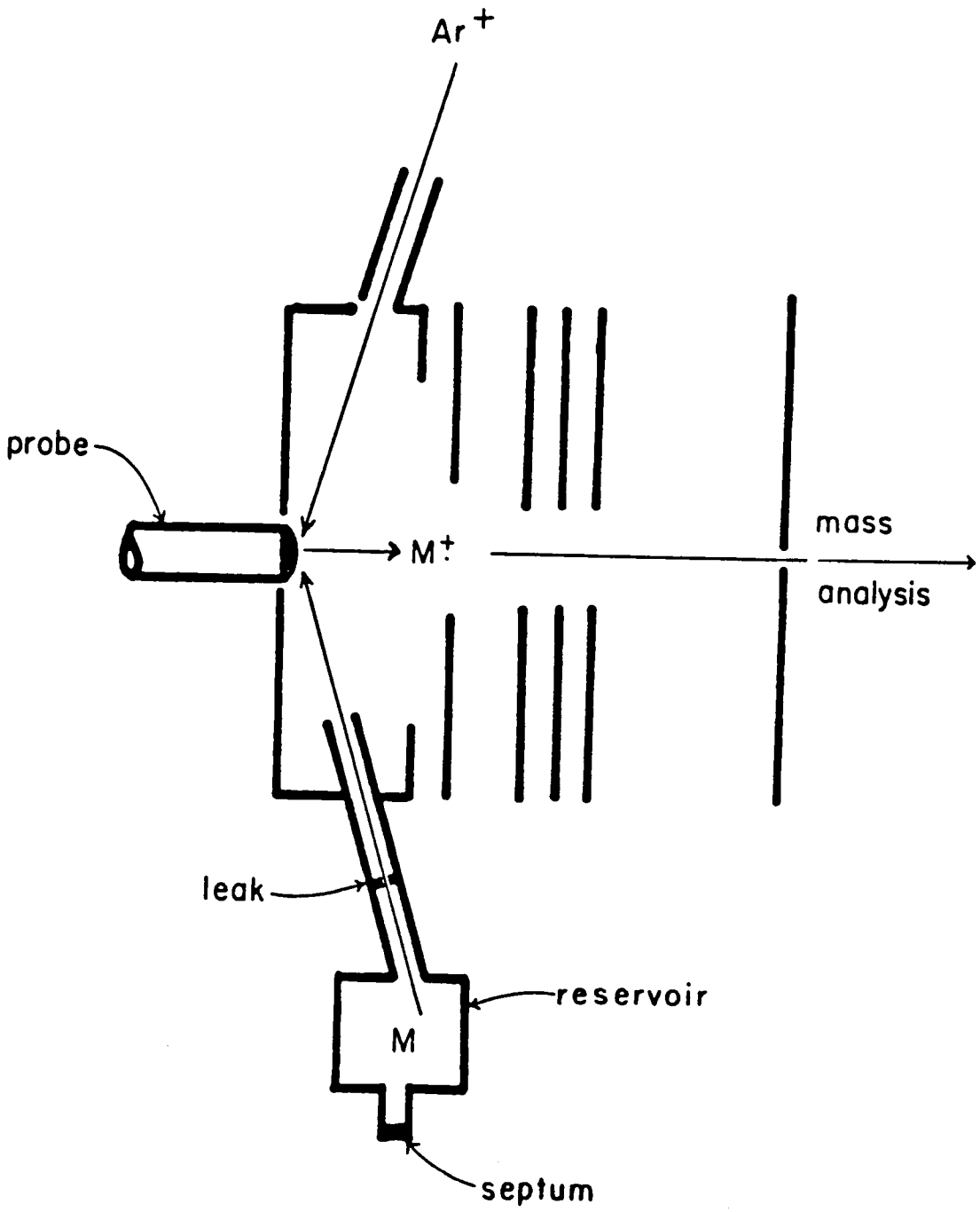


Figure 4. Schematic of volatile analyte introduction.

CHAPTER III

RESULTS AND DISCUSSION

A. LSIMS Spectrum of Sulfuric Acid

The positive LSIMS spectrum of concentrated sulfuric acid is shown in Figure 5. It is characterized by peaks corresponding to the even electron ions $H_3SO_4^+$, $H_3SO_3^+$, HSO_3^+, HSO_2^+, SO^+, $(H_2SO_4)_nH^+$ and $(H_2SO_4)_nH_3O^+$, where $1 < n < 6$ for spectra reported here. The intensity of secondary ($H_3SO_4^+$) ions from 98% sulfuric acid is approximately 10 times that of secondary (glycerol + H)$^+$ ions emitted from neat glycerol under identical ion source conditions. The total secondary ion current emitted from concentrated sulfuric acid is comparable to that generally encountered in LSIMS. Further, the vapor pressure of concentrated sulfuric acid is sufficiently low that mass spectra could be obtained continuously for over an hour from a 2 mg (ca. 1μL) sample. Sulfuric acid is sufficiently conductive (120) that fluctuations in secondary ion intensity attributable to sample charging are not observed. Secondary ion emission from concentrated sulfuric acid is persistent, stable and intense. Despite the corrosive nature of sulfuric acid, no corrosion of the mass spectrometer or associated pumping components has been observed in the three years sulfuric acid has been used as a LSIMS matrix.

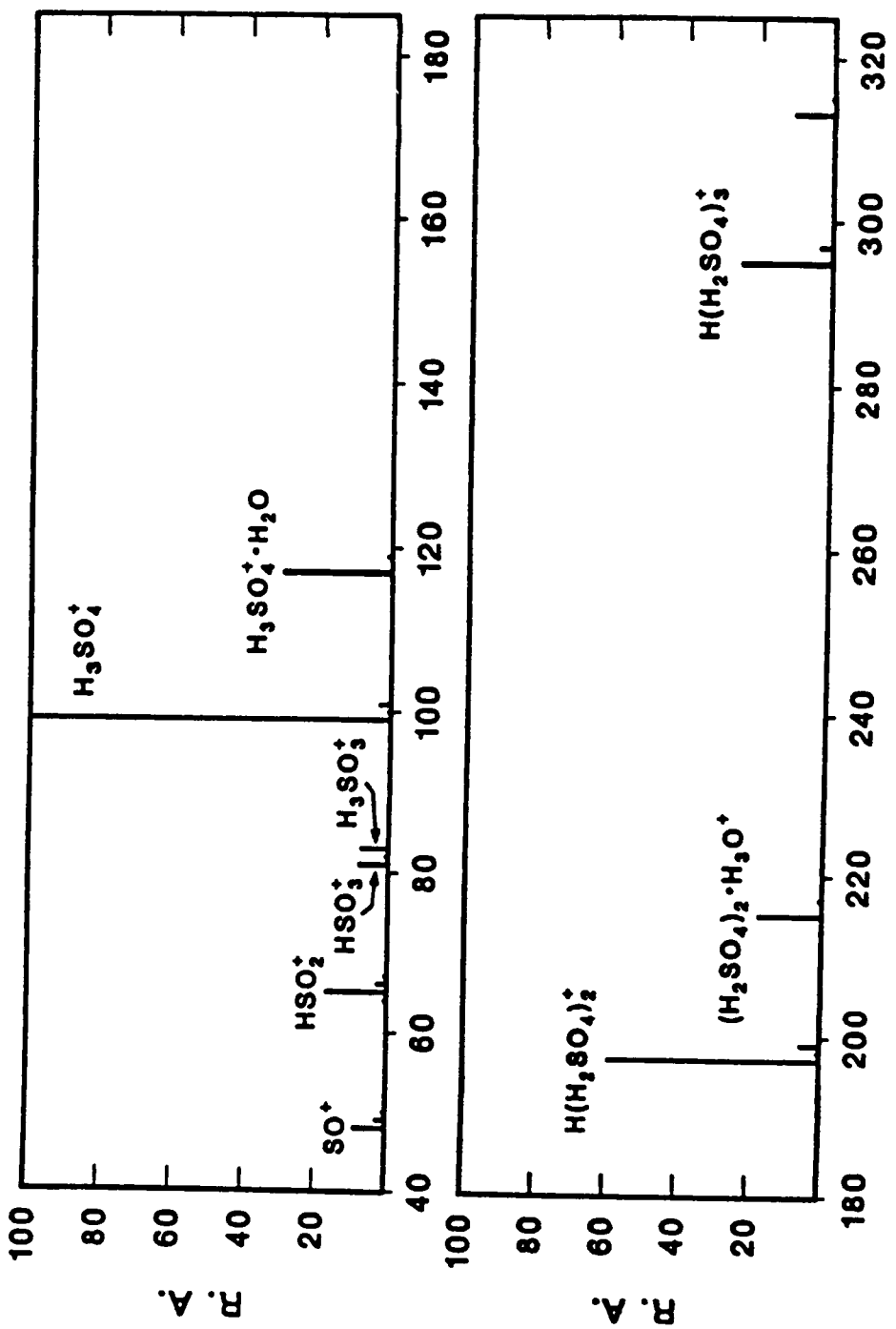


Figure 5. Positive LSIMS spectrum of concentrated sulfuric acid.

B. LSIMS Spectra of Substituted Aromatic/Sulfuric Acid Solutions

Secondary ion mass spectra of all the singly substituted aromatic/sulfuric acid solutions investigated in this dissertation and their respective molecular weights are presented in Appendix B (p. 157-169); contributions from sulfuric acid are subtracted from those LSIMS spectra. LSIMS spectra presented below reflect secondary ions characteristic of the substituted aromatics and sulfuric acid. All spectra obtained for aromatic compounds containing a single substituent were from sulfuric acid solutions approximately 1 mole % aromatic. The effectiveness of concentrated sulfuric acid as an LSIMS matrix for individual compound classes can be evaluated by comparing the aromatic secondary ion abundance relative to the base sulfuric acid-characteristic ion, $H_3SO_4^+$. Organic solutes at these concentrations do not affect the secondary ion abundances of sulfuric acid-characteristic ions.

Aromatic Ketones.

Very good secondary ion yields are obtained from aromatic ketones dissolved in concentrated sulfuric acid. Figure 6 shows the LSIMS spectrum obtained from a 1 mole % solution of 9-oxodihydroanthracene (anthrone) dissolved in H_2SO_4 compared to the electron impact mass spectrum of anthrone. In the LSIMS spectrum the protonated molecule

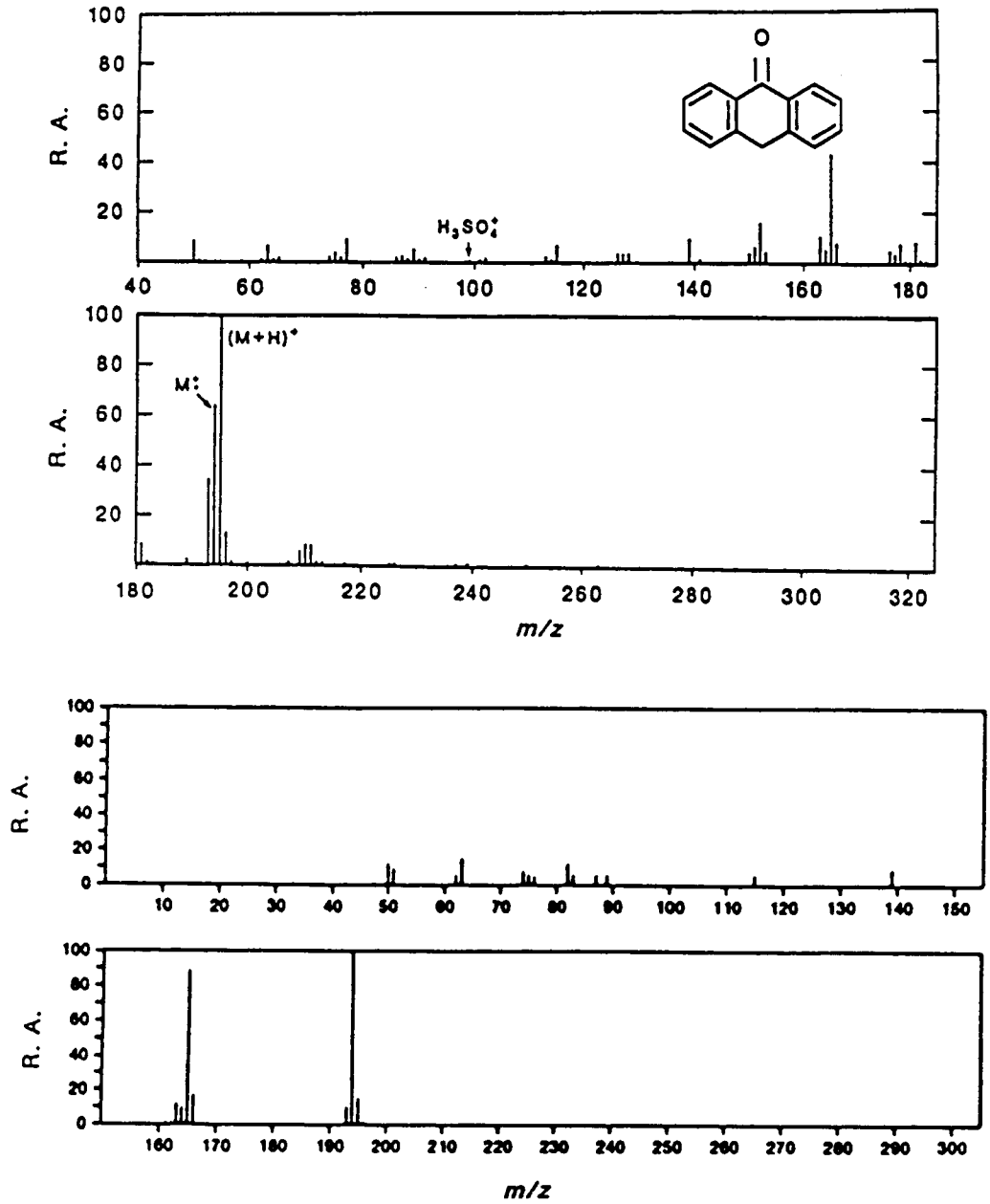


Figure 6. Positive LSIMS spectrum of 9-oxodihydroanthracene/sulfuric acid solution (top) compared to electron impact ionization mass spectrum of 9-oxodihydroanthracene (bottom).

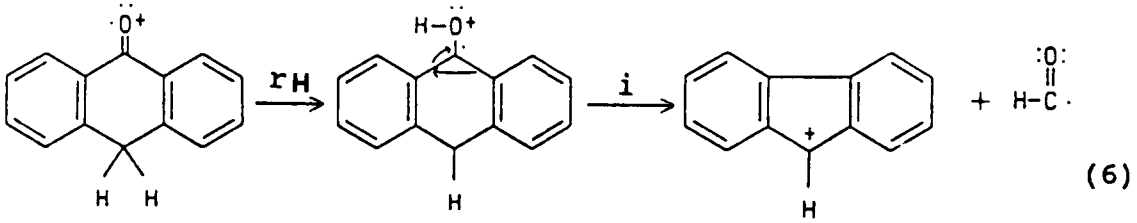
(m/z 195) is nearly two orders of magnitude more abundant than the base $H_3SO_4^+$ peak (m/z 99). Carbonyl compounds are, in general, fully protonated in concentrated H_2SO_4 (60,61). Consistent with this, the base peak in LSIMS spectra of the ketones studied corresponds to the protonated molecule. However, abundant molecular ions ($M^{+\cdot}$) are observed in all LSIMS spectra of aromatic ketone/sulfuric acid solutions as well. For the anthrone/sulfuric acid solution the molecular ion ($M^{+\cdot}$) is approximately 60% the abundance of the protonated anthrone molecule.

Fragment ions observed in LSIMS spectra of a particular aromatic/sulfuric acid solution generally correspond to fragment ions observed in EI and CI mass spectra where such spectra are available for comparison. This suggests that fragment ions evident in LSIMS spectra arise from unimolecular (gas phase) decomposition of the molecular ion or protonated molecule. Because both the molecular ion and protonated molecule are observed in LSIMS spectra of aromatic/sulfuric acid solutions it is difficult to determine the parent of the fragment ion reflected in the spectrum.

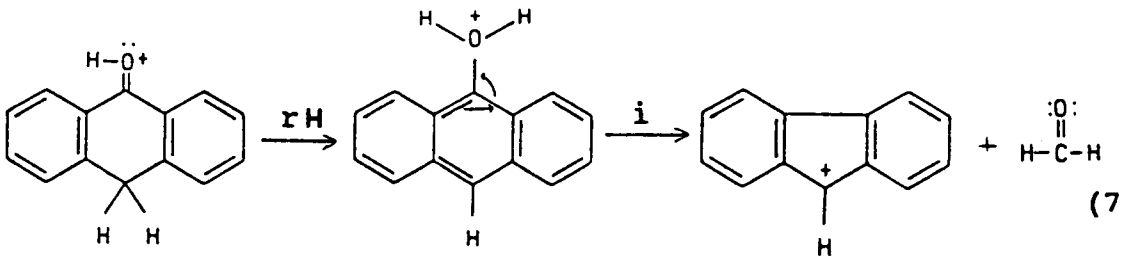
Anthrone-characteristic ions indicated at m/z 181, 178, 165, 163 and 152 in the LSIMS spectrum of anthrone (Figure 6) correspond to $(M-CH)^+$, $(M-O)^+$, $(M-COH)^+$, $(M-COH_3)^+$, and $(M-COCH_2)^+$, respectively. The spectrum of

1,9-benzanthr-7-one (Appendix B, p. 159) reveals fragment ions at m/z 202, 201, 200, and 189, corresponding to $(M-CO)^+$, $(M-COH)^+$, $(M-COH_2)^+$ and $(M-CHCO)^+$, respectively.

The fragment ion at m/z 165 in the LSIMS spectrum of anthrone dissolved in sulfuric acid could arise from loss of -COH from the molecular ion and/or loss of $-COH_2$ from the protonated molecule. Fragmentation reactions for the anthrone molecular ion and protonated anthrone which yield the fragment ion observed at m/z 165 are shown in reactions 6 and 7, respectively. Both reactions lead to loss of the functional group and ring contraction. This behavior is commonly exhibited in LSIMS spectra of the aromatic/ sulfuric acid solutions investigated.



(III) (IV) (V) (6)



(VI) (VII) (V) (7)

The first step in the decomposition of the anthrone molecular ion (III), shown in reaction 6, involves hydrogen transfer (rH) resulting in the formation of the tautomeric anthracene-9-ol molecular ion (IV). Rearrangement reactions are common in unimolecular decompositions (121). Following rearrangement the positive charge on the phenolic oxygen initiates a cleavage reaction by attracting an electron pair from an adjacent bond. The positive charge migrates from the functional group to the ring. Inductive cleavage (i) results in the formation of the fluorenyl cation (V) which corresponds to the peak observed at m/z 165 in the LSIMS spectrum of anthrone.

Alternatively, (V) could arise from the unimolecular decomposition of the protonated molecule (VI) as shown in Reaction 7. Protonation of the carbonyl oxygen is followed by hydrogen rearrangement to give protonated anthracene-9-ol (VII). This is followed by inductive cleavage of CH_2O to produce (V). CH_2O is a common leaving group from even electron ions such as protonated molecules.

It is important to recognize that reactions 6 and 7 do not occur at thermal energies encountered in the condensed phase where the internal energy distribution of molecules is less than one eV. Since the fluorenyl cation observed at m/z 165 (V) has the cyclopentadienyl cationic structure, it is unreasonable to expect this ion to exist in the condensed phase. However, under the superthermal

conditions of keV particle-induced ionization, the internal energy distribution of secondary ions may be sufficient for reactions such as 6 and 7 to occur.

The LSIMS spectrum of 2-acetonaphthone, shown in Figure 7, displays fragment ions different from its cyclic counterparts. Fragment ions observed at m/z 155, 128, 127, and 115 correspond to $(M-CH_3)^+$, $(M-CH_2O)^+$, $(M-C_2H_3O)^+$ and $(M-C_3H_3O)^+$, respectively. The fragmentation pattern revealed in the LSIMS spectrum of 2-acetonaphthone is indicative of another common unimolecular decomposition reaction, alpha cleavage. Alpha cleavage is the fission of a bond to an atom adjacent to the one bearing the charge. This cleavage reaction is initiated from the strong tendency for electron pairing and thus is a common mode of dissociation for odd electron ions such as the molecular ion. The odd electron can be donated to form a new bond to an adjacent atom (α atom). The other electron required for bond formation comes from another bond to the α atom which is subsequently cleaved. In 2-acetonaphthone there are two bonds susceptible to alpha cleavage. These reactions are reflected in the appearance of fragment ions corresponding to $(M-CH_3)^+$ and $(M-C_2H_3O)^+$ in EI mass spectra of acetonaphthone. These losses are illustrated in Reactions 8 and 9. In either reaction the odd electron is donated from the carbonyl oxygen. In Reaction 8 an electron is donated from the carbonyl-methyl bond which then cleaves producing a

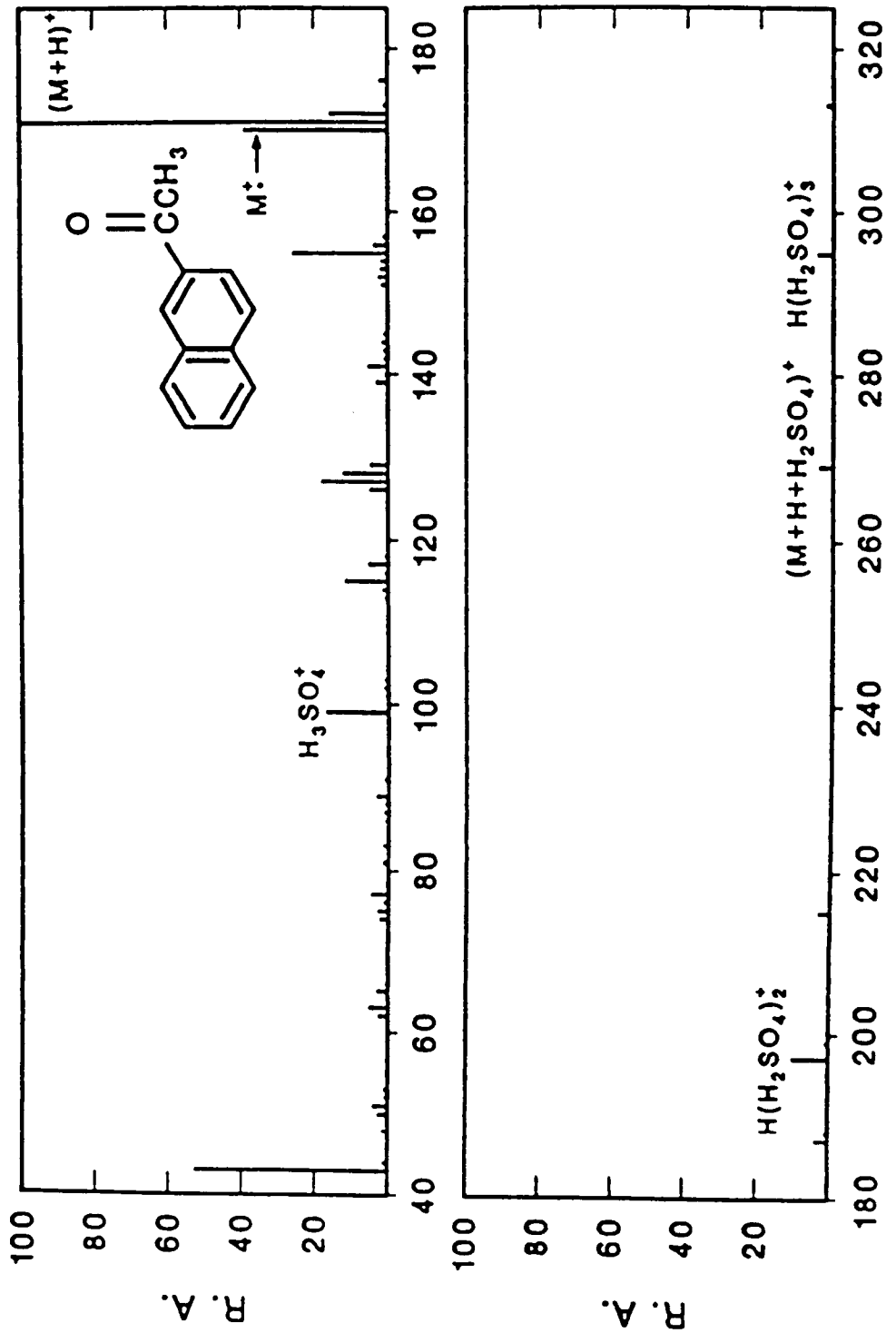
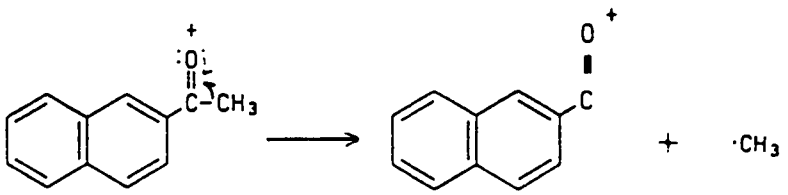
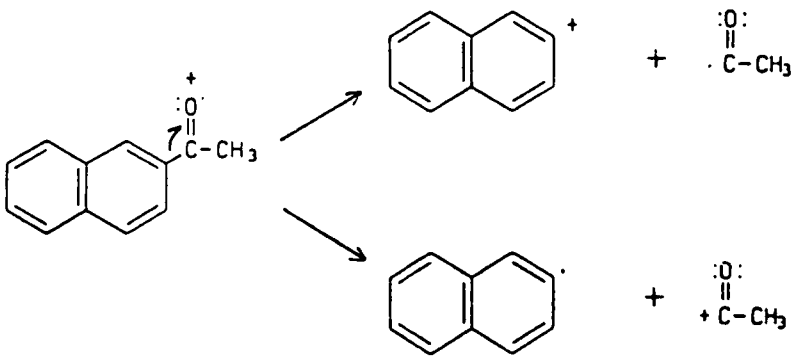


Figure 7. Positive LSIMS spectrum of 2-acetonaphthone/sulfuric acid solution.

methyl radical and the ion observed at m/z 155 (VIII). In Reaction 9 two ionic products are derived from alpha cleavage of the carbonyl-aromatic carbon bond. The two products, corresponding to $(M-C_2H_3O)^+$ and $(C_2H_3O)^+$, are reflected in Figure 7 at m/z 127 and 43, respectively.



(VIII) (8)



(9)

The fragmentation reflected in LSIMS spectra of aromatic/sulfuric acid solutions is generally consistent with analyte structure and gas phase unimolecular decompositions.

Aromatic Aldehydes.

The LSIMS spectrum of 9-phenanthrenecarboxaldehyde dissolved in H_2SO_4 is shown in Figure 8. This spectrum is

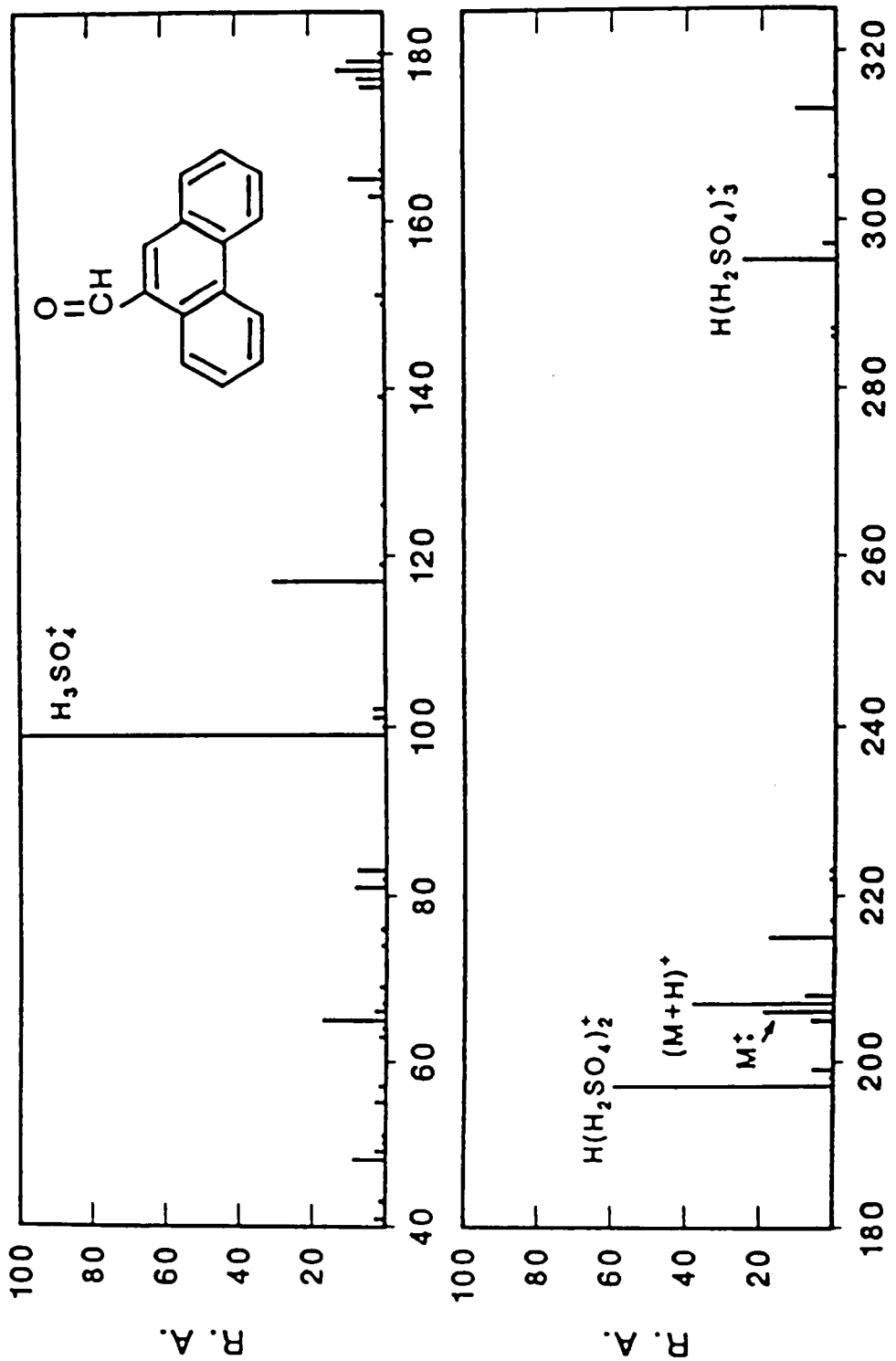


Figure 8. Positive LSIMS spectrum of 9-phenanthrenecarboxaldehyde/sulfuric acid solution.

fairly representative of the aldehydes investigated. Intense molecular ions, $(M^{+\cdot})$, and protonated molecules, $(M+H)^+$, are observed at m/z 206 and 207, respectively. Characteristic ions observed at m/z 179, 178, 177, and 165 correspond to fragment ions $(M+H-CO)^+$, $(M-CO)^+$, $(M-CHO)^+$ and $(M-C_2HO)^+$, respectively, fragments which can be rationalized by gas-phase decomposition. Proton-bound dimers of the analyte and H_2SO_4 were observed in spectra of 2-naphthaldehyde, 9-anthracenecarboxaldehyde, and 9-phenanthrenecarboxaldehyde (Appendix B, p. 160). These ions, $(M+H+H_2SO_4)^+$, were observed in the LSIMS spectra of 9-anthracenecarboxaldehyde and 9-phenanthrenecarboxaldehyde at m/z 305.

Aromatic Carboxylic Acids.

Abundant molecular ions and protonated molecules were observed in the LSIMS spectra of the aromatic carboxylic acids investigated. The intensity ratio $[(M^{+\cdot})/(M+H)^+]$ increases for the series benzoic, naphthoic, and anthracene carboxylic acids (Appendix B, p. 161). The $[(M^{+\cdot})/(M+H)^+]$ ratio for 2-naphthoic acid, reflected in its LSIMS spectrum presented in Figure 9, is near unity. Fragment ions observed at m/z 155 and 127 in the LSIMS spectrum of a 2-naphthoic acid/sulfuric acid solution correspond to loss of $\cdot OH$ and $\cdot CO_2H$, respectively, from the molecular ion. These neutral losses are typically observed in LSIMS spectra of aromatic acid/sulfuric acid solutions.

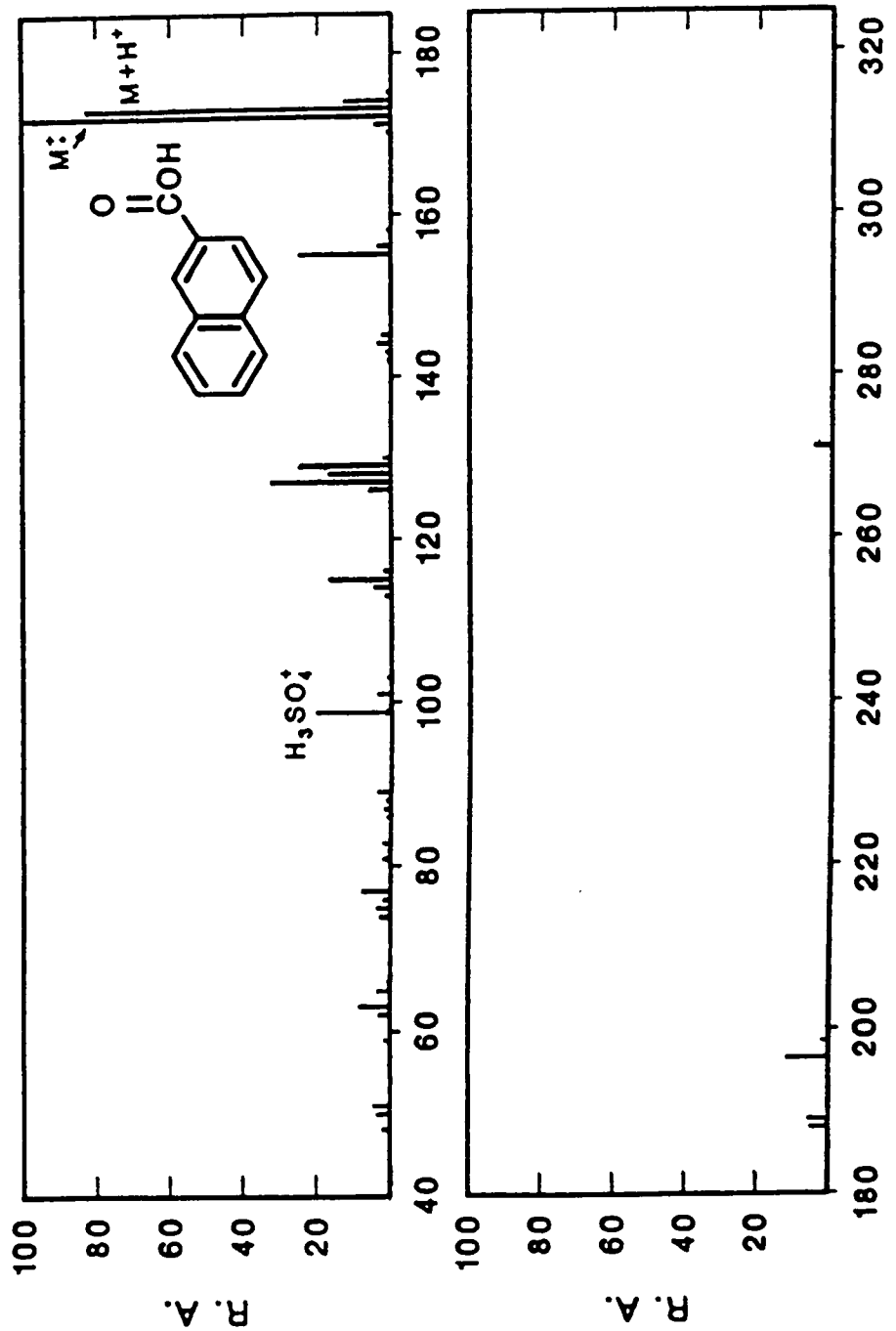


Figure 9. Positive LSIMS spectrum of 2-naphthoic acid/sulfuric acid solution.

The base peak in the spectrum of 9-anthracene carboxylic acid observed at m/z 302, corresponds to the sulfonate of the aromatic acid. It is not known whether this species represents the sulfonic acid produced from sulfonation of 9-anthracene carboxylic acid or the sigma complex intermediate. In subsequent discussions the ions observed at (M+80) and (M+81) in LSIMS spectra will be referred to as the sulfonic acid radical cation and the protonated sulfonic acid, respectively.

Phenols.

The base analyte-characteristic peak in SIMS spectra of the fused-ring phenol/H_2SO_4 solutions investigated (Appendix B, p. 162) corresponds to the protonated molecule, except for benzo(a)-pyrene-6-ol where the base peak corresponds to $(M-H)^+$. The spectrum of 9-phenanthrol shown in Figure 10 is fairly representative of the fragmentations observed for the phenols studied. Ions observed at m/z 181, 165, and 152, corresponding to $(M-CH)^+$, $(M-COH)^+$, and $(M-CHCOH)^+$, respectively, can be rationalized as resulting from gas phase decomposition of the parent.

Aromatic Ethers.

Aryl ethers are generally only sparingly soluble in H_2SO_4 (88) and the abundance of analyte-characteristic secondary ions obtained from arylether/H_2SO_4 mixtures is very low. 2-Methoxynaphthalene does dissolve in H_2SO_4 and a

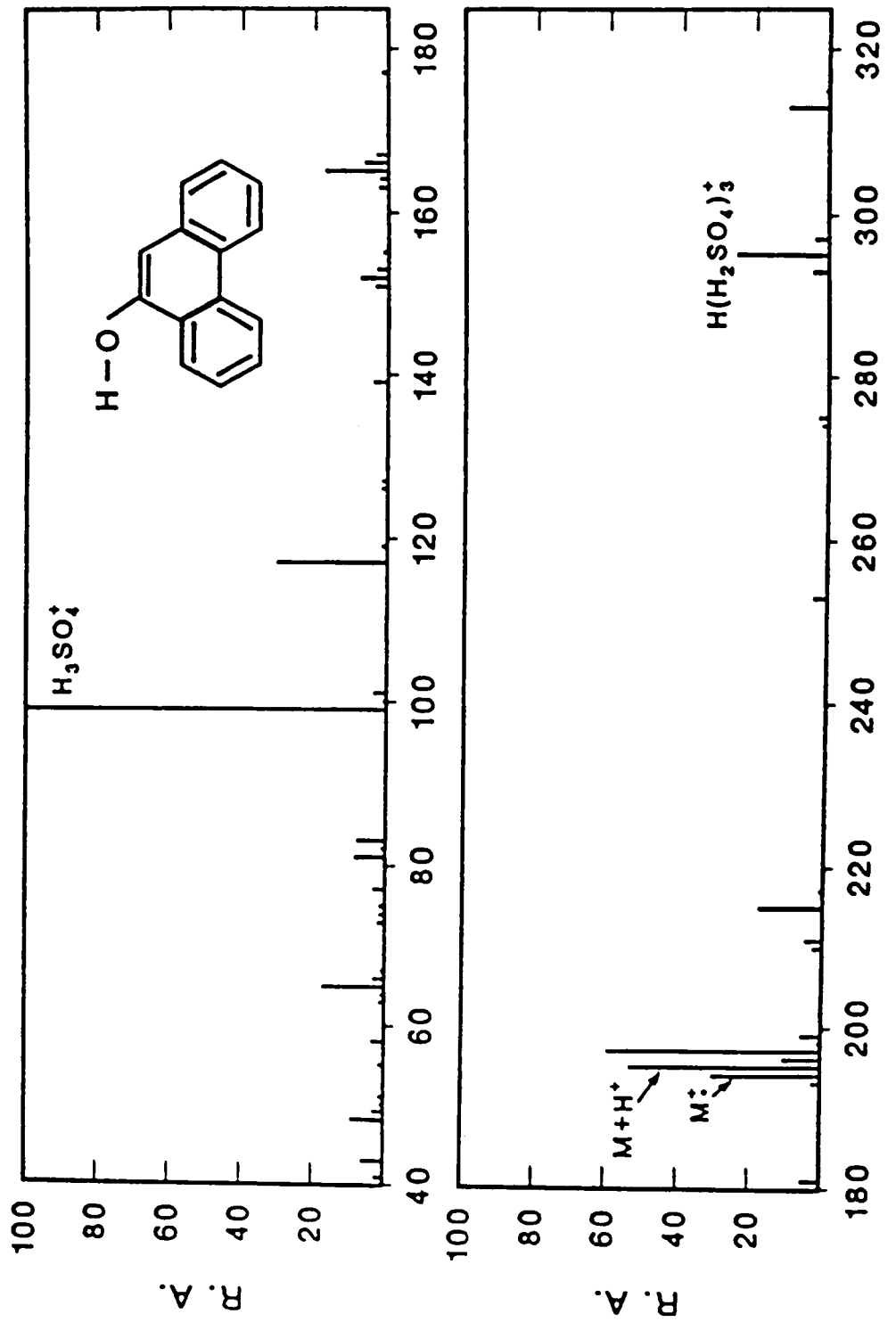


Figure 10. Positive LSIMS spectrum of 9-phenanthrol/sulfuric acid solution.

moderately intense peak due to the protonated aromatic molecule is observed at m/z 159, with a slightly less intense molecular ion at m/z 158 as shown in Figure 11. Fragment ions observed in the spectrum at m/z 145, 144, 143, 128, 127, and 102 correspond to $(M-CH)^+$, $(M-CH_2)^+$, $(M-CH_3)^+$, $(M-OCH_2)^+$, $(M-OCH_3)^+$ and $(M-COCH_3)^+$, respectively. The most abundant ether-characteristic ion in the SIMS spectrum is the sulfonated molecular ion $(M+SO_3)$. Disulfonation is also evident from the peak at m/z 318.

Alkyl and Aryl Substituted Aromatics.

Dramatic variations are observed in the intensity of secondary ions characteristic of this compound class. For example, the abundance of M^+ and $(M+H)^+$ relative to the $H_3SO_4^+$ ion abundance, varies from 15% (1-methylpyrene) to 150% (9-phenylanthracene) (Appendix B, p. 163-164). This variation may be attributable to analyte-matrix miscibility, as many of these compounds do not readily dissolve in H_2SO_4.

Fragment ions for the aromatic hydrocarbon/sulfuric acid solution investigated generally are attributable to loss of the functional group or portions thereof. In the SIMS spectrum of dihydroanthracene dissolved in H_2SO_4 (Appendix B, p. 163), the base analyte-characteristic peak corresponds to the fragment ion $(M-2H)^+$. It is reasonable to believe that dihydroanthracene is oxidized to anthracene prior to sputtering (122), and this species is the precursor to the $(M-2H)^+$ ion detected. Product ions indicating

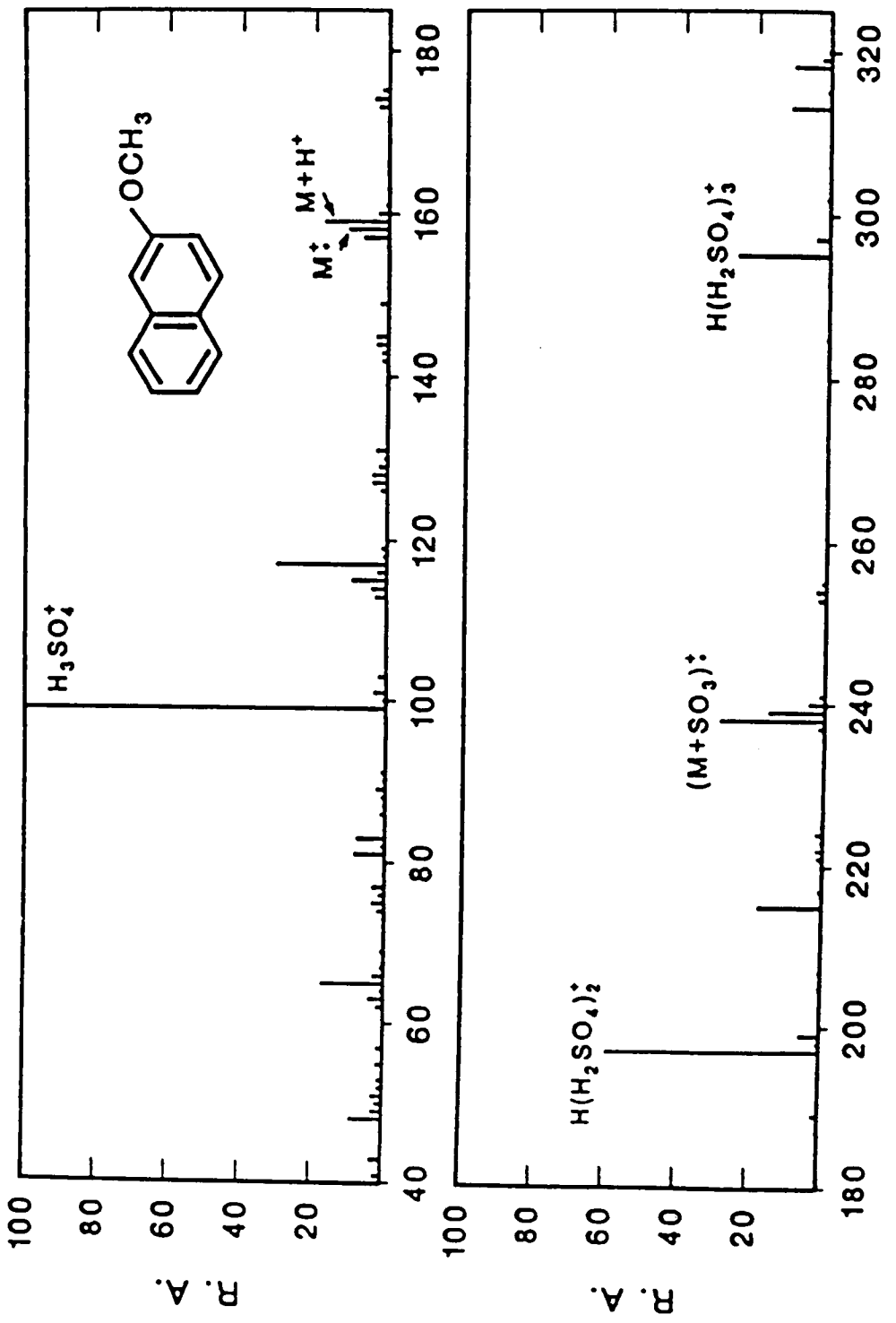


Figure 11. Positive LSIMS spectrum of 2-methoxynaphthalene/sulfuric acid solution.

disulfonation of analytes are observed in SIMS spectra of all the aromatic hydrocarbons investigated.

The SIMS spectrum of 2-t-butylanthracene, shown in Figure 12, is interesting because it reflects a broad range of reactions. The base peak at m/z 57 corresponds to the t-butyl ion. While this ion could arise from an alpha cleavage of the molecular ion (m/z 234) in the gas phase, the peak at m/z 291 which corresponds to $[M+C(CH_3)_3]^+$ suggests that a portion of the m/z 57 arises from direct sputtering of t-butyl cations in solution. Condensed phase dealkylation of 2-t-butylanthracene is also indicated by the appearance of a peak at m/z 337 which corresponds to the disulfonic acid of anthracene. Free t-butyl ions presumably exist in solutions of t-butyl-substituted aromatic/H_2SO_4 solutions, as the unsubstituted arene has been isolated from such solutions (123). The products formed from the condensed phase reaction of 2-t-butylanthracene in H_2SO_4 discussed above are represented in Scheme I.

Aromatic Nitriles.

In SIMS spectra of aromatic nitrile/H_2SO_4 solutions, molecular ion ($M^{\cdot+}$) intensities are greater than those of the protonated aromatic nitrile (Appendix B, p. 164-165). The SIMS spectrum of 9-anthracenecarbonitrile presented in Figure 13 is fairly typical of the aromatic nitriles investigated. Abundant $M^{\cdot+}$ and $(M+H)^+$ are observed at m/z 203 and 204, respectively.

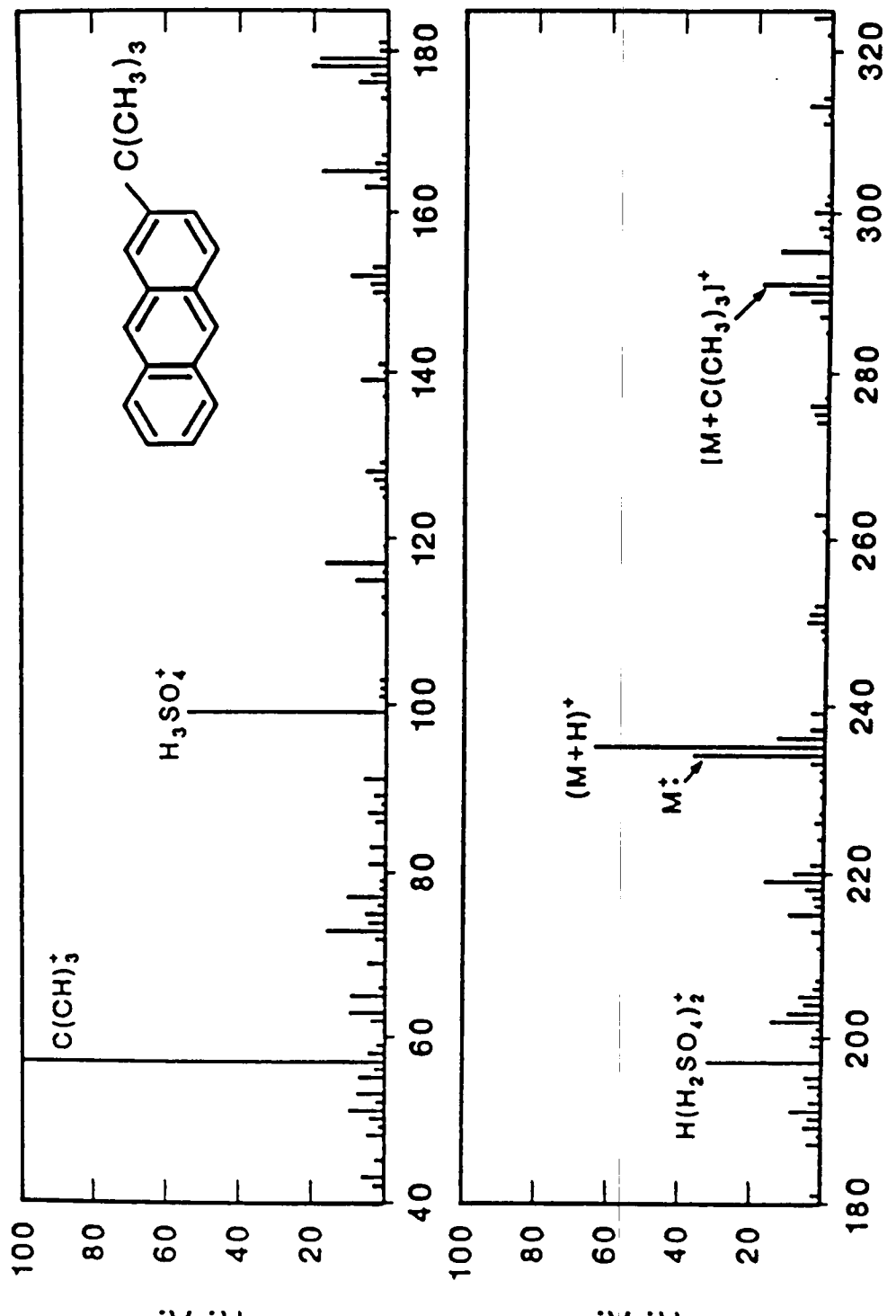


Figure 12. Positive LSIMS spectrum of 2-t-butylanthracene/sulfuric acid solution.

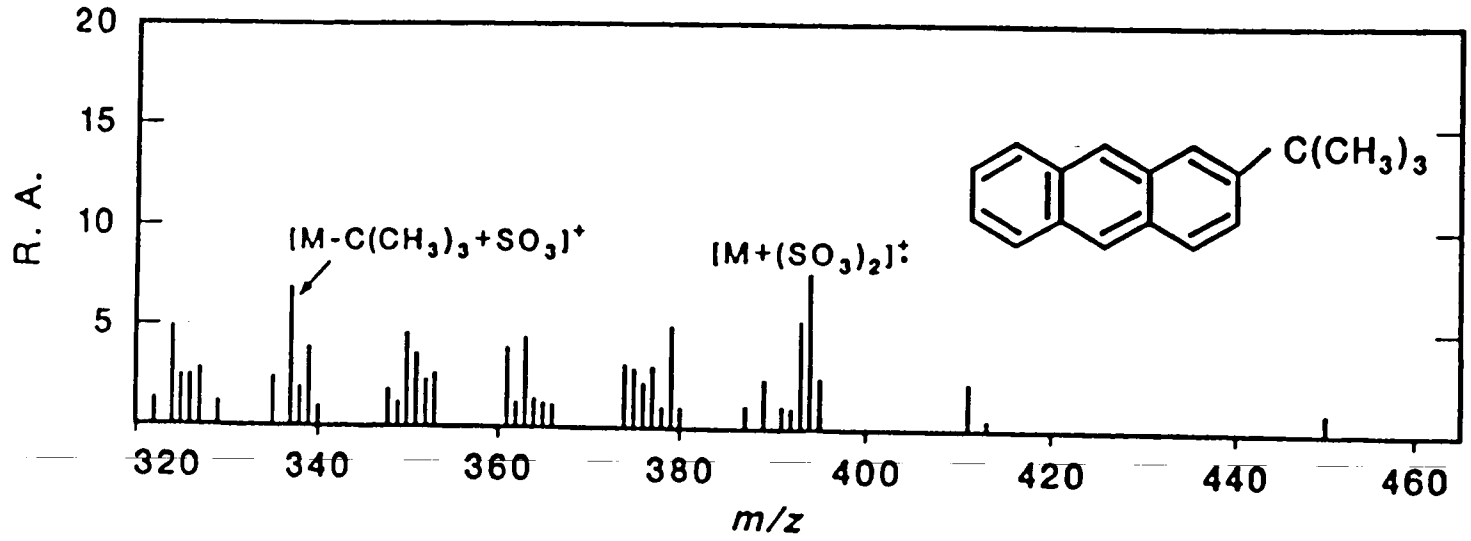


Figure 12 (continued).

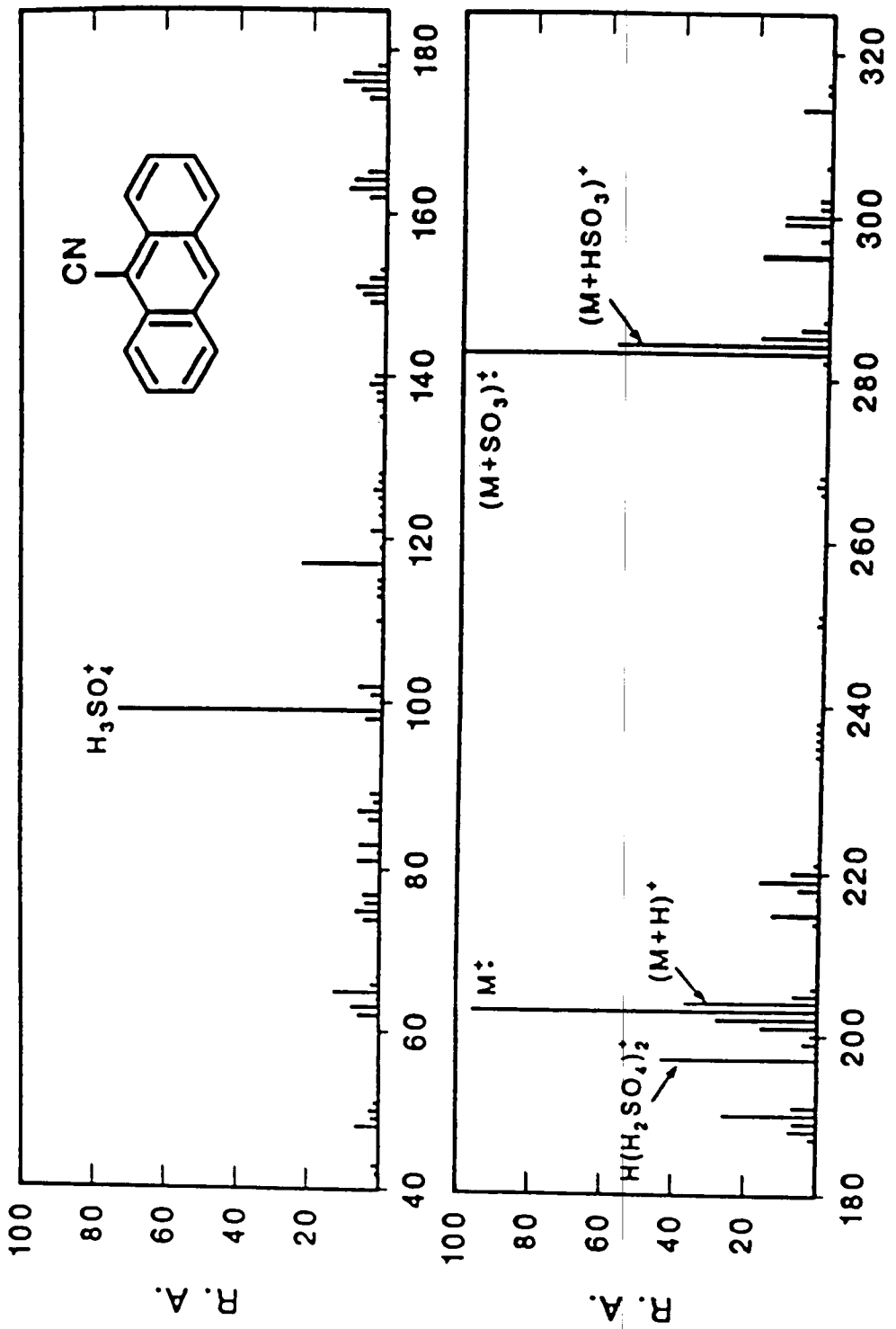
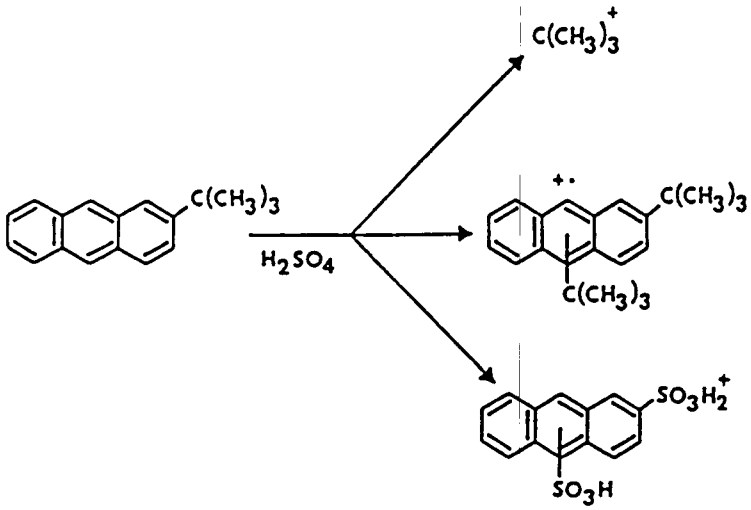


Figure 13. Positive LSIMS spectrum of 9-anthracenecarbonitrile/sulfuric acid solution.



Scheme I

Characteristic fragment ions in the SIMS spectrum of 9-anthracenecarbonitrile at m/z 190, 177, and 176 correspond to $(M-CH)^+$ $(M-CN)^+$, and $(M-HCN)^+$, respectively. The radical cation and protonated sulfonic acids are observed at m/z 283 and 284, respectively. No ions characteristic of the sulfonic acid products are observed in the SIMS spectrum of 1-naphthalenecarbonitrile (Appendix B, p. 164).

Relative to other compounds discussed above, aromatic nitriles are "weak" bases. The K_B for benzonitrile in H_2SO_4 is reported as 0.069 (124). While for sulfuric acid solutions this is a relatively small value, it is orders of magnitude larger than projected values of K_B for many bases dissolved in glycerol (87), solutions of which yield intense

secondary protonated molecules characteristic of the dissolved base. Thus it is not surprising that protonated nitrile secondary ions are observed using H_2SO_4 solutions.

Nitrogen Heteroaromatics.

The SIMS spectrum of acridine, presented in Figure 14, is representative of SIMS spectra of nitrogen heteroaromatic/sulfuric acid solutions. In addition to abundant $(M+H)^+$, abundant $M^{+\cdot}$ and $(M+2H)^+$ are observed at m/z 179 and 181 as well. Ions observed at m/z 167, 166, 152, and 139 correspond to $(MH_2-N)^+$, $(MH-N)^+$, or $(M-CH)^+$, $(M-CHN)^+$ and $(M-C_2H_2N)^+$.

The base peaks in SIMS spectra of the representative compounds 2-methylindole, phenazine, benzo(c)cinnoline, acridine, and dibenz(a,j)acridine dissolved in H_2SO_4 (Appendix B, p. 165-166) correspond to the respective protonated aromatic. The base peak in the SIMS spectrum of carbazole (Appendix B, p. 165), however, corresponds to $M^{+\cdot}$. Fragment ions for this compound class are typically < 10% as abundant as the parent ion.

Aromatic Amines.

LSIMS spectra of aromatic amines dissolved in H_2SO_4 show pronounced temporal variation. This behavior is demonstrated by LSIMS spectra of 9-aminophenanthrene obtained after 5 minutes (Figure 15) and 24 minutes (Figure 16) of continuous primary ion bombardment. The base peak in

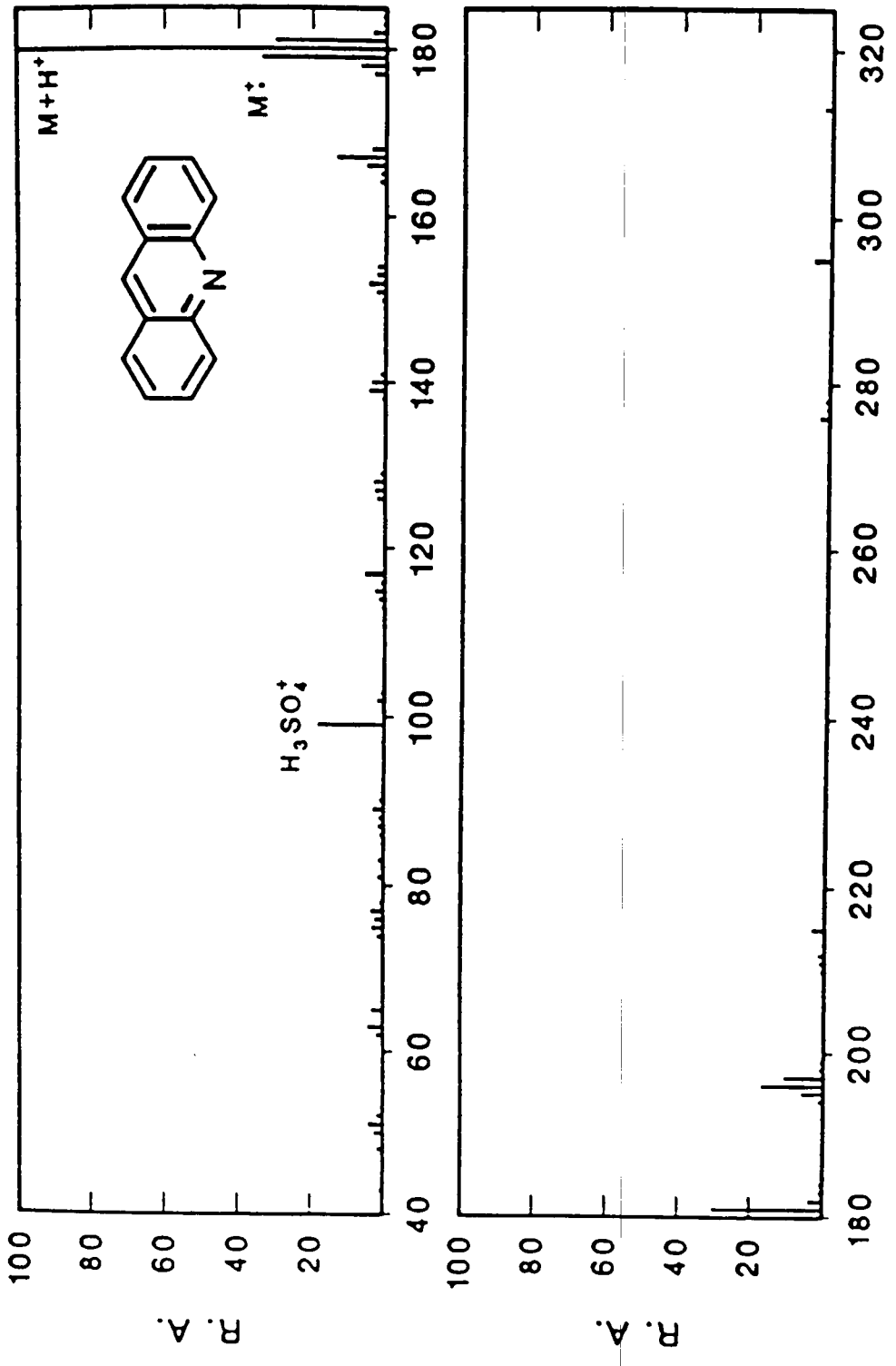


Figure 14. Positive LSIMS spectrum of acridine/sulfuric acid solution.

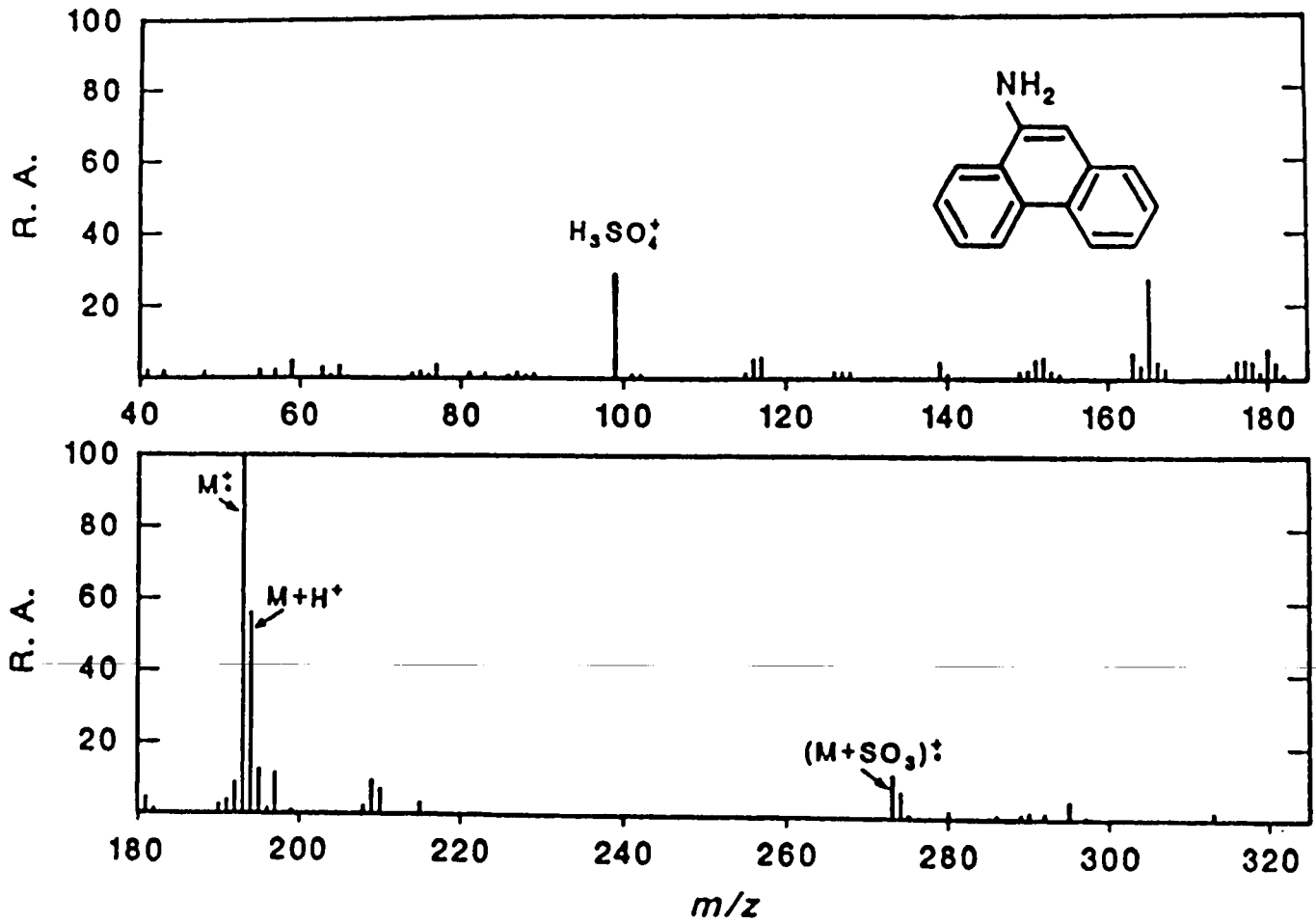


Figure 15. Positive LSIMS spectrum of 9-aminophenanthrene/sulfuric acid solution obtained 5 minutes after initiation of primary ion bombardment.

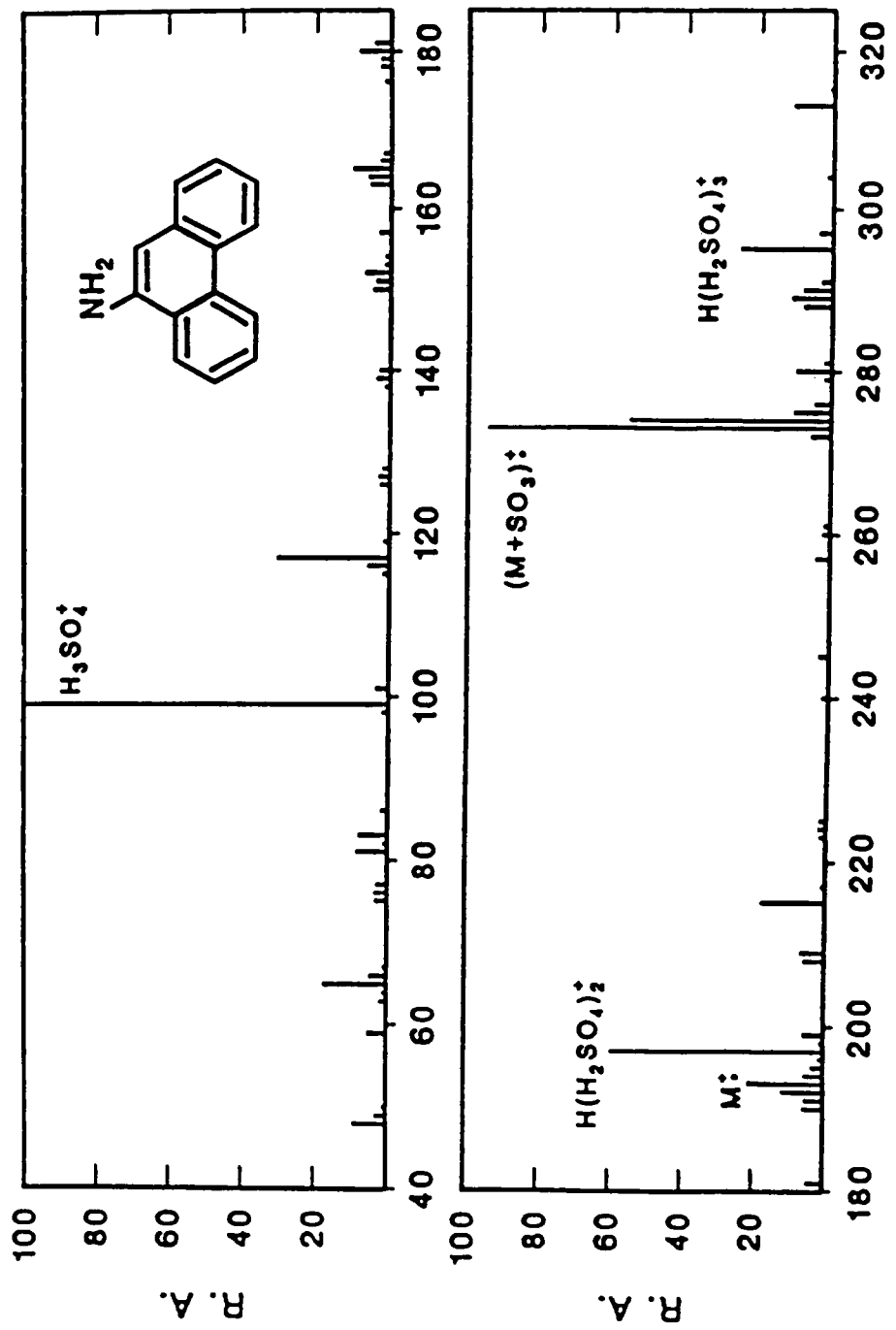


Figure 16. Positive LSIMS spectrum of 9-aminophenanthrene/sulfuric acid solution obtained 24 minutes after initiation of primary ion bombardment.

Figure 15 is the molecular radical cation ($M^{+\cdot}$) while the protonated molecule $(M+H)^+$ is 40% as abundant if corrections for ^{13}C contributions from $M^{+\cdot}$ are made. Sulfonation products are observed at m/z 273 and 274. Figure 16 shows that 19 minutes later the base peak is now $H_3SO_4^+$ while the sulfonation product of 9-aminophenanthrene is the base aromatic peak. The protonated molecule, $(M+H)^+$, is now only 2% as abundant as $M^{+\cdot}$ after corrections for ^{13}C contributions from $M^{+\cdot}$

Nitroaromatics.

Moderately intense ions observed at m/z 173 and 174 in the LSIMS spectrum of 1-nitronaphthalene, shown in Figure 17, correspond to the molecular ion and protonated molecule, respectively. However, neither molecular ions nor protonated molecules were abundant in LSIMS spectra of other nitroaromatic/sulfuric acid solutions investigated (Appendix B, p. 167). For these solutions, either fragment ions or ions arising from condensed phase products constitute the base organic peak in the LSIMS spectra.

The base analyte-characteristic peak in the LSIMS spectrum of 9-nitroanthracene corresponds to $(M-14)^+$. Base organic-characteristic peaks in spectra of 3-nitroperylene and 3-nitropyrene correspond to $(M-15)^+$. The identity of these ions is not known. It is likely that these ions arise from condensed phase reaction as such losses cannot be explained by reasonable unimolecular decompositions.

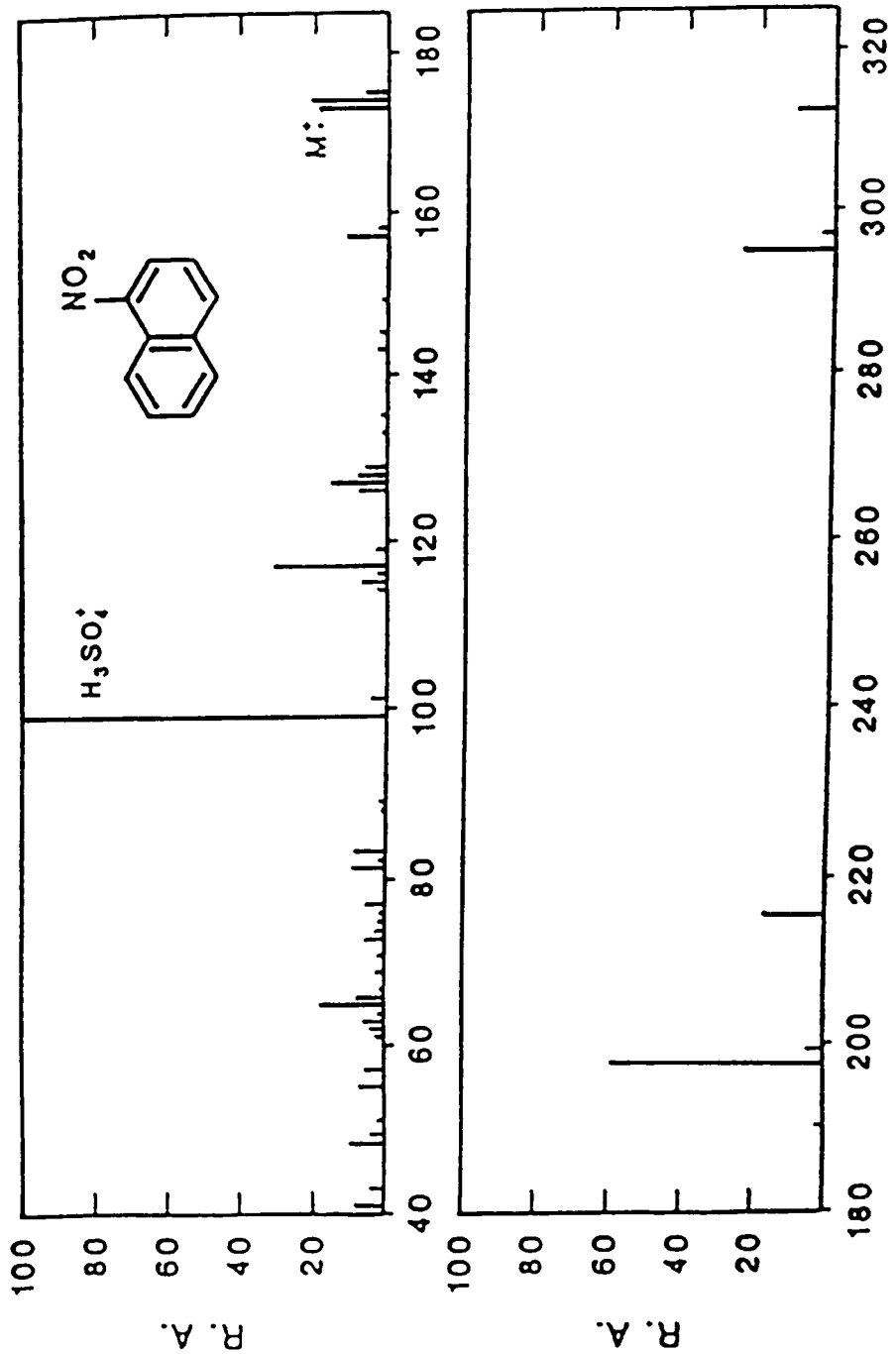


Figure 17. Positive LSIMS spectrum of 1-nitronaphthalene/sulfuric acid solution.

General Features of LSIMS Spectra of Substituted Aromatic/Sulfuric Acid Solutions.

Aromatic ketones, aldehydes, carboxylic acids, amines, and nitrogen heterocycles are nearly completely ionized and are all strong bases in H_2SO_4 (60-63). Nitriles and nitroaromatics are substantially less basic (124,125), but differences in solute basicity do not correlate with differences in secondary aromatic ion emission; almost all aromatic/H_2SO_4 solutions yield intense parent ions.

Generally, base peaks in SIMS spectra of substituted arene/sulfuric acid solutions correspond to the molecular ion or the protonated molecule of the substituted aromatic. Simultaneously abundant $(M+H)^+$ and $M^{\cdot+}$ peaks are rare in SIMS spectra of most analyte/protic matrix solutions, but are common in SIMS spectra of substituted aromatic/H_2SO_4 solutions. In some cases the base peak corresponds to the molecular ion or protonated molecule of apparent sulfonation products of the substituted aromatic.

The fraction of the total secondary ion current carried by respective aromatic molecular ions and protonated aromatic molecules, for approximately 2 mole % solutions is listed in Table 1 as a rough measure of the sensitivity of the technique for differently substituted aromatics. The range of values listed in Table 1 is generally within the experimental uncertainty associated with preparation of samples. A number of factors including mass transport,

Table 1.

Relative Intensities of Secondary Parent Ions from Sulfuric Acid Solutions.

Solute	$\frac{[M+H^+]+[M^{+\cdot}]}{[M+H^+]+[M^{+\cdot}]+\Sigma[H_2SO_4]^+}$ [a], %
1-Naphthol	58
9-Phenanthrol	18
2-Methoxynaphthalene	11
2-Acetonaphthone	68
Anthrone	98
1,9-benzanthr-7-one	25
2-Naphthalenecarboxaldehyde	27
9-Anthracenecarboxaldehyde	21
9-Phenanthrenecarboxaldehyde	13
1-Pyrenecarboxaldehyde	14
6-benzo(a)pyrene-carboxaldehyde	2
Benzoic acid	27
2-Naphthoic acid	67
9-Anthracene carboxylic acid	62
3-Methylindole	95
Carbazole	90
Acridine	65
Phenazine	76
Benzo(c)cinnoline	86
Dibenz(a,j)acridine	29
1-Naphthalenecarbonitrile	37
9-Anthracenecarbonitrile	29
9-Phenanthrenecarbonitrile	24
2-Nitronaphthalene	13
1-Chloroanthracene	8[b]

a $\Sigma(H_2SO_4]^+ = [SO^+] + [HSO_2^+] + [HSO_3^+] + [H_3SO_3^+] + [H(H_2SO_4)_n^+] + [H(H_2SO_4)_n \cdot H_2O)^+]$, where $1 < n \leq 3$

b Intensities from ions containing ^{35}Cl and ^{37}Cl are summed.

surface effects, and sample volatility affect analyte surface concentration, and thus fractional ion current carried by analyte ions (115,127). While these effects are not addressed here, it is noteworthy that, for approximately 2 mole % analyte solutions, the mean of the fractional ion currents carried by aromatic-characteristic secondary ions reported in Table 1 is greater than 40%. For a number of compounds, such as 1-chloroanthracene, a relatively weak protonated molecule peak is observed; the relative abundance of this ion compared to the abundance of protonated sulfuric acid is about the same as the concentration of the compound, 2 mole %.

A loose correlation exists between the $[M^{+\cdot}]/[(M+H)^+]$ ratios observed in LSIMS spectra of a series of similarly substituted aromatic hydrocarbons and the oxidation potentials of the corresponding unsubstituted aromatics. As indicated in Table 2, the $[M^{+\cdot}]/[(M+H)^+]$ ratios observed in LSIMS spectra of individual compound classes generally increase as the oxidation potential of the unsubstituted analog decreases. Thus, the greater the ease of oxidation of the aromatic ring, the greater the relative abundance of the molecular ion. For example, this correlation is indicated in Table 2 by comparison of the $[M^{+\cdot}]/[(M+H)^+]$ ratios for the series of aromatic acids investigated to the oxidation potentials of benzene, naphthalene, and anthracene.

Table 2.

Comparison of [Molecular Ion]/[Protonated Molecule] Ratios of Substituted Aromatics to the Oxidation Potentials of the Unsubstituted Analog

Solute	$[M^{+\cdot}]/[M+H^+]$ [a], %	$E^o_{1/2}$ (Volts) [b]
Benzoic acid	26	2.00
2-Naphthoic acid	140	1.31
9-Anthracene carboxylic acid	395	0.84
1-Naphthalenecarbonitrile	125	1.31
9-Phenanthrenecarbonitrile	192	1.23
9-Anthracenecarbonitrile	429	0.84
2-Naphthalenecarboxaldehyde	49	1.31
9-Phenanthrenecarboxaldehyde	55	1.23
9-Anthracenecarboxaldehyde	61	0.84
1-Pyrenecarboxaldehyde	97	0.86
6-benzo(a)pyrene-carboxaldehyde	100	0.76

a Corrected for ^{13}C contribution from $M^{+\cdot}$.

b Polarographic oxidation potentials of aromatic hydrocarbons in acetonitrile solutions carried out at a rotating platinum anode (128).

Fragmentation of parent ions in LSIMS spectra of these compounds can generally be attributed to loss of the functional group and ring cleavages involving the functional group. With few exceptions, SIMS spectra in the mass range of the parent and fragment ions generally parallel electron impact ionization (EI) or chemical ionization (CI) mass spectra where such data are available for comparison.

When the base peak in the LSIMS spectrum corresponds to the molecular radical cation, $M^{+\cdot}$, products indicative of sulfonation are frequently observed. Sulfonic acids produced from sulfonation reactions are manifest in SIMS spectra as radical cations $(M + 80)^{+\cdot}$ or protonated acids $(M + 81)^{+}$. Temporal variation in SIMS spectra is observed when peaks corresponding to sulfonation products are present, though the rate of this variation differs among the various solutions studied.

Oxygen/aromatic adduct ions are typically observed in LSIMS spectra of substituted aromatic/sulfuric acid solutions. These adduct ions are observed as their radical cations $(M + 16)^{+\cdot}$ or protonated forms $(M + 17)^{+}$; in the LSIMS spectrum of 9-oxodihydroanthracene (Figure 6, p. 48) oxygen adducts are observed at m/z 210 $[(M+O)^{+\cdot}]$ and 211 $[(M+H+O)^{+}]$. Oxygen addition to the sulfonic acids is occasionally observed. In general, peaks corresponding to oxygen adducts of the dissolved aromatic are of relatively low abundance (<10%).

C. Chemical Noise in Aromatic/Sulfuric acid Solutions

A notable feature of the sulfuric acid spectrum is the absence of peaks at every integral mass because, unlike glycerol, sulfuric acid lacks a hydrocarbon backbone. As discussed earlier, even when organic analyte ions and matrix ions have the same nominal mass they are readily resolved because of the difference in mass defect between carbon and sulfur (see p. 20). Because sulfuric acid produces few but very characteristic background peaks, very little chemical noise is evident in the spectra. This feature is apparent in Figure 18, which is a partial mass spectrum of 10^{-4} M benzoic acid/sulfuric acid solution reflecting the average of 10 scans over a 1 min. period. The signal-to-electronic noise ratio [S/N (electronic)] is approximately 160:1. Multiple scan averaging could improve S/N (electronic) further, but can do nothing to reduce chemical noise, e.g.,the $NaH_2SO_4^+$ peak (m/z 122.9529). However, this peak is readily separated from the benzoic acid $(M+H)^+$ peak at m/z 123.0446 by any mass spectrometer with a resolving power greater than 1500.

Figure 19 shows the behavior of various parameters which determine sensitivity of the technique. The slope of log $(M+H)^+$ current vs. log concentration benzoic acid is 1.2 over the range of concentrations 0.5 M - 10^{-4} M. Given the numerous sources of error associated with measuring absolute secondary ion currents, this may be taken as a linear

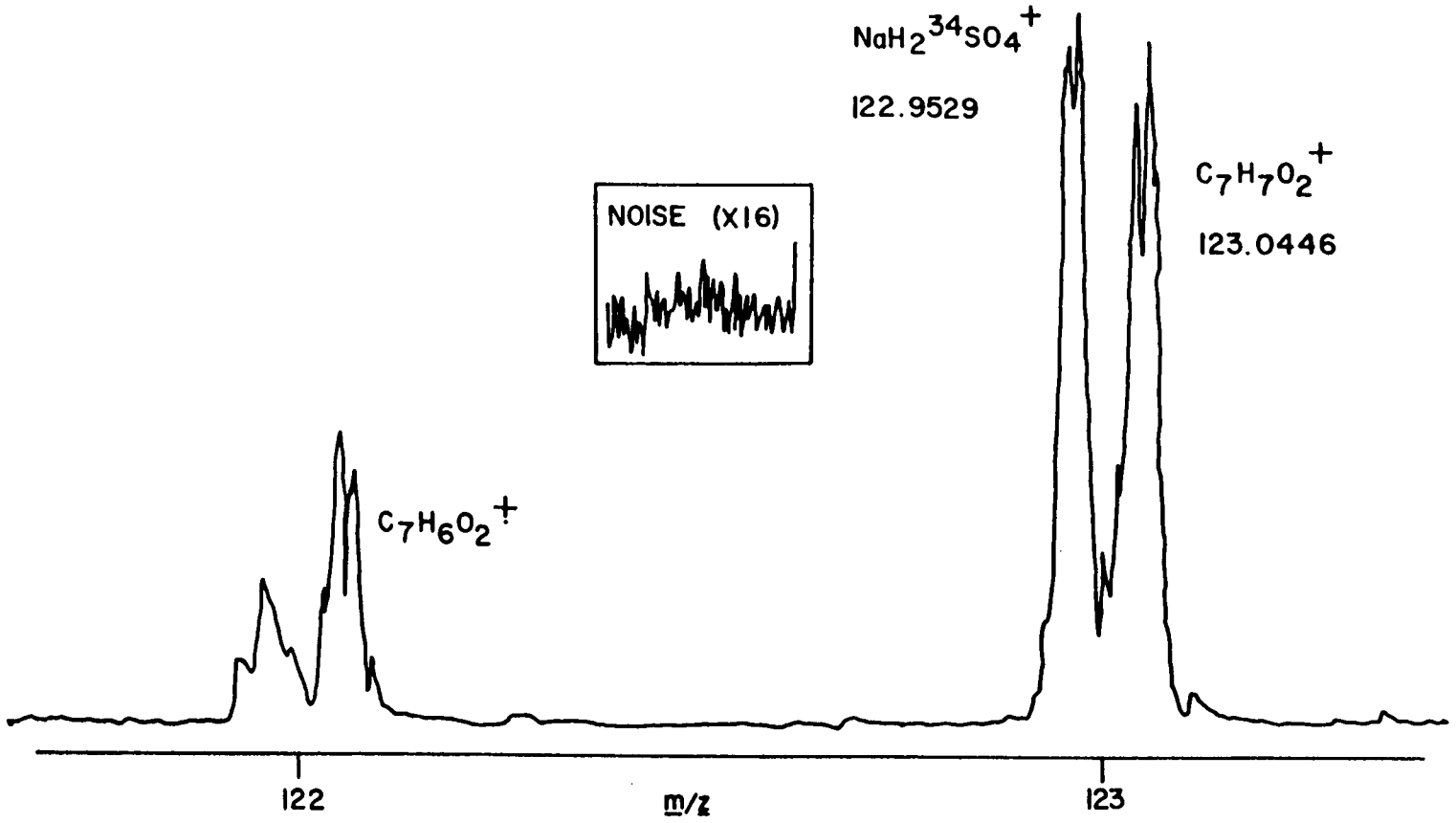


Figure 18. Partial LSIMS spectrum of 10^{-4} M benzoic acid/H_2SO_4 solution in the region of m/z 122-123. The spectrum reflects an average of ten scans taken over a period of 1 minute. $NaH_2SO_4{}^+$ arises from contamination.

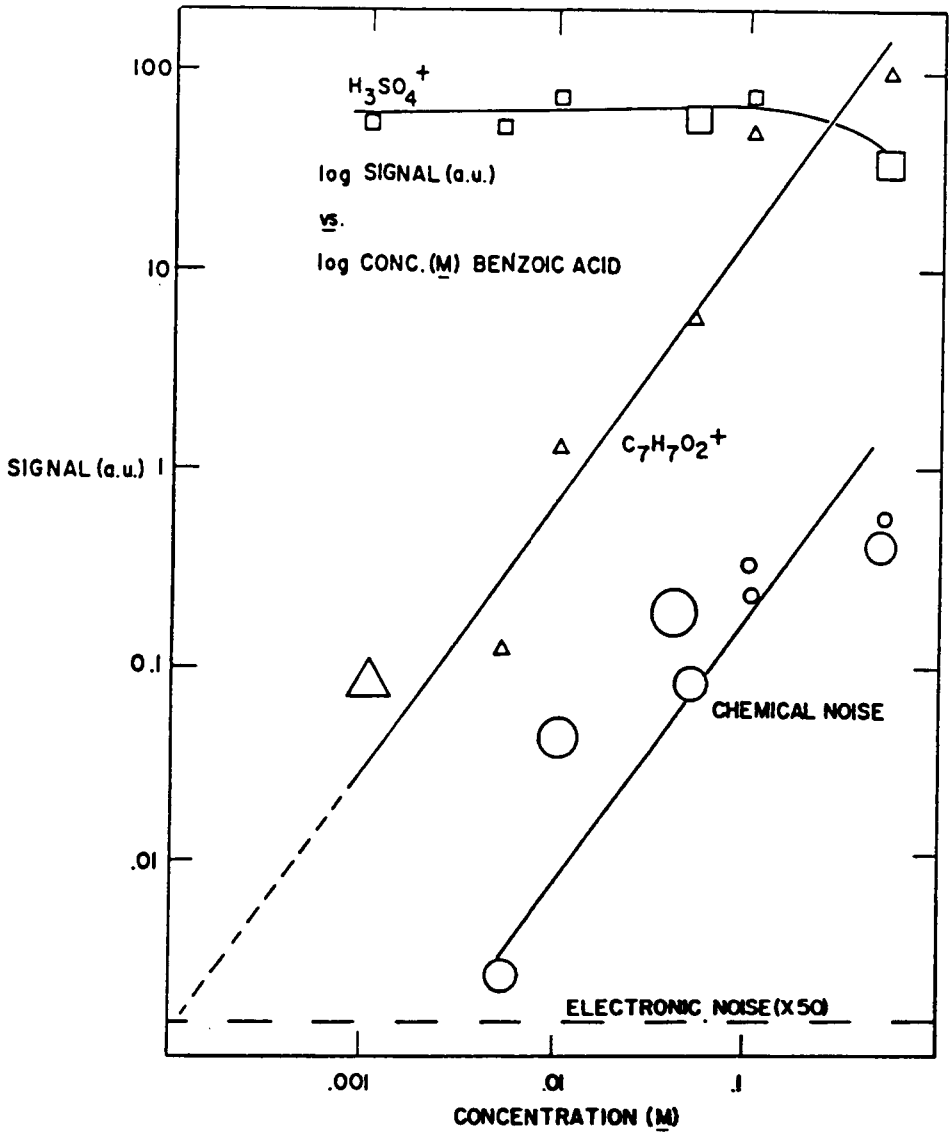


Figure 19. Log-log plots of various parameters which determine the sensitivity of LSIMS with sulfuric acid. Noise signal was defined as the average signal obtained for m/z 104, 108, 111. Symbol size reflects standard deviation in each measurement.

relationship. Chemical noise attributable to organic fragments decreases with analyte concentration, and is virtually undetectable at reduced analyte concentrations. The average of the signal from ions observed at m/z 104, 108, and 111 is used to define the chemical noise. These ions cannot arise from gas phase unimolecular decompositions. They arise from non-specific fragmentation (ion damage) of the sample and provide no information. For the instrumentation employed here, limits of detection are approximately 10^{-6} M at S/N (electronic) = 2:1. For a sample size of 1 μL, this corresponds to a detection limit of about 10^{-12} moles. Typically, a 1 μL sample provides a continuous signal for approximately 20 min., so that multiple scan averaging may reduce the limits of detection further. Intensity of sulfuric acid secondary ions does not vary significantly except at high benzoic acid concentrations.

D. Effect of Current Density on Sensitivity

Studies of the secondary ion emission process for amines introduced as a gas onto glycerol indicate that the abundance of analyte-characteristic ions relative to matrix ions could be enhanced by lowering the primary ion current density (129). Variation of the primary ion beam current density and its effect on abundance of aromatic secondary ions relative to sulfuric acid-characteristic ions was

investigated using a 0.1 M anthraquinone/sulfuric acid solution. A plot of the log of the fractional secondary ion current associated with anthraquinone $\{[(M+H)^+] + [(M+2H)^+]\}$ vs. the primary ion current density is shown in Figure 20. The abundance of the anthraquinone secondary ions relative to the abundance of sulfuric acid-characteristic ions increases exponentially as current density decreases. This effect is illustrated further in Figure 21 which shows the LSIMS spectra of 0.1 M anthraquinone/sulfuric acid solutions obtained at two different primary ion current densities. At lower flux the abundance of protonated anthraquinone relative to the base sulfuric acid peak is significantly enhanced over the higher flux spectrum. The abundance of analyte-characteristic ions relative to each other is unaffected by changes in primary ion current density. The total secondary ion current is lower when a lower primary ion current density is used. A low primary ion current density minimizes chemical noise. The minimum primary ion current which can be used is dependent on the primary ion source employed.

E. Mechanistic aspects

1. Gas Phase Reactions

Secondary ion emission from liquid solution into the gas phase is accompanied by simultaneous sputtering of a

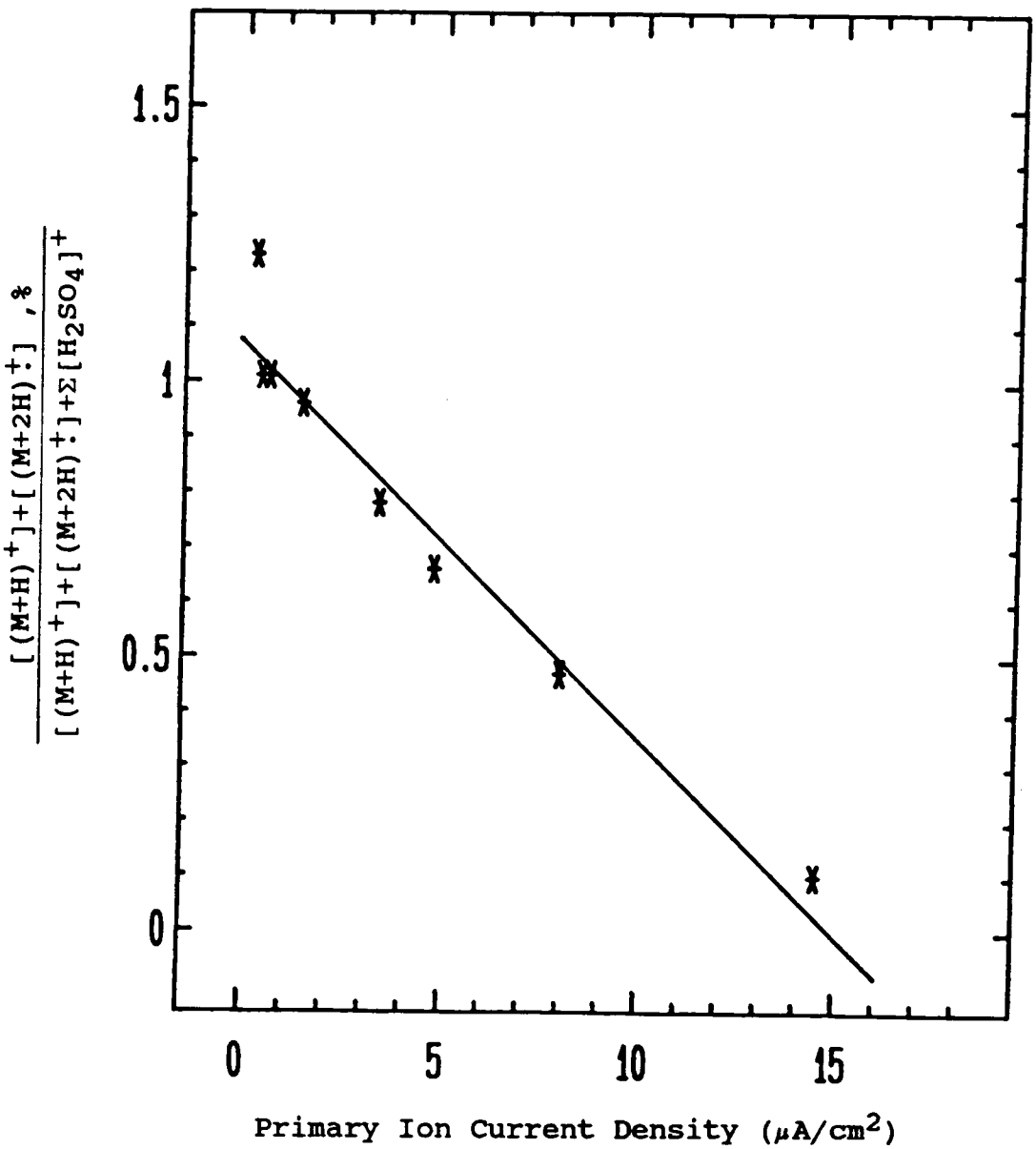


Figure 20. Plot of the log of the fractional secondary ion current associated with anthraquinone ($[(M+H)^+] + [(M+2H)^+]$) vs. the primary ion current density.

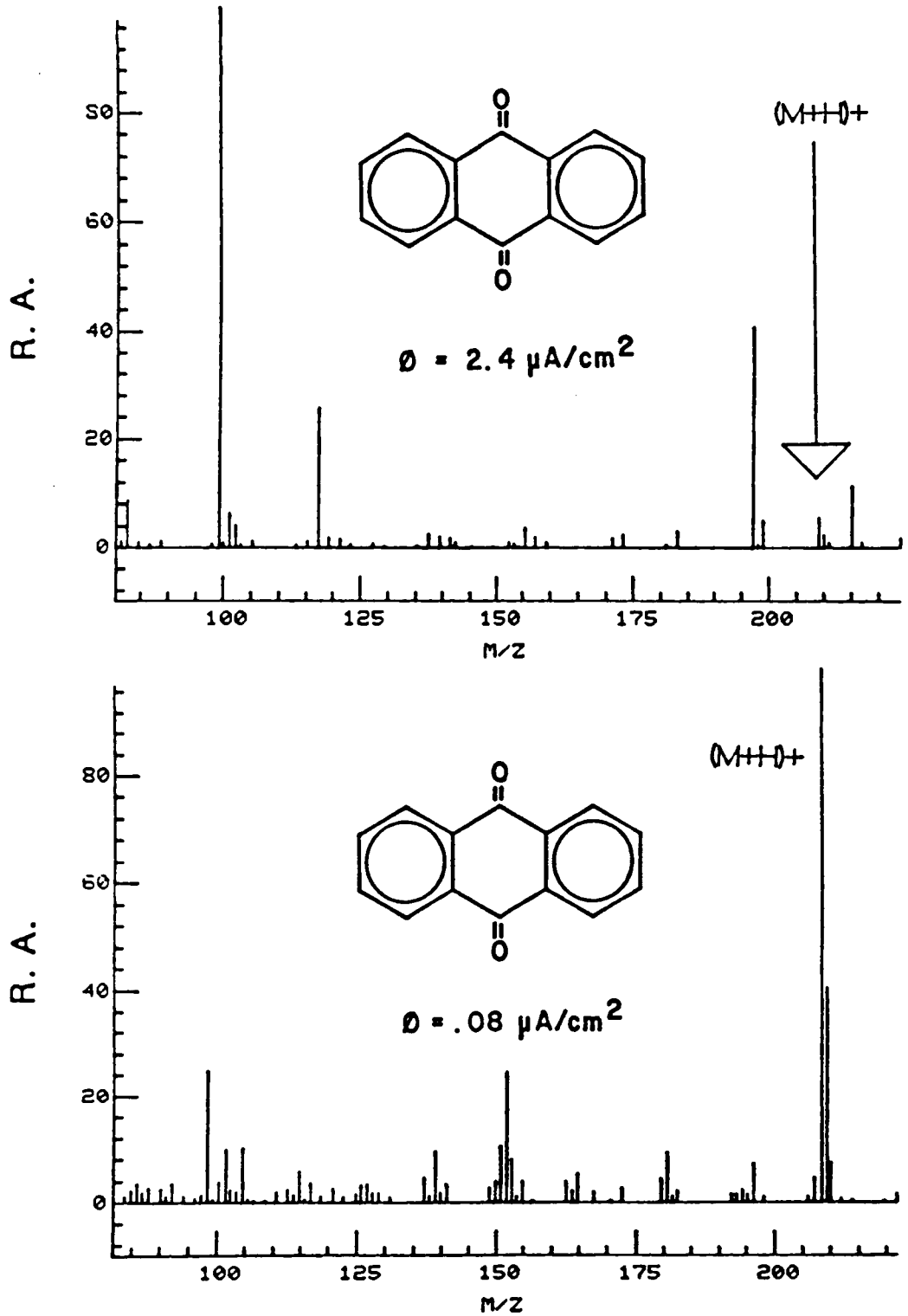


Figure 21. Positive LSIMS spectra of 0.1 M anthraquinone/sulfuric acid solutions at primary ion current densities of 2.4 $\mu A/cm^2$ and 0.08 $\mu A/cm^2$.

greater number of neutral molecules and fragments. This has been demonstrated by weight loss/secondary ion current measurements, and is a common feature of secondary ion emission from all substances. Collisions will occur between species sputtered from the condensed phase as they are transferred into the high vacuum. With the exception of unimolecular decompositions, reactions resulting from bimolecular collisions in the gas phase above the surface are the last events effecting the LSIMS spectrum.

The fact that sputtering occurs so rapidly severely limits the kinds of reactions which can occur during the estimated 10^{-12} s of a sputtering event. It is reasonable to consider gas phase proton transfer reactions only because they (a) can occur at rates equal to bimolecular collision frequency (130), (b) occur only if the reaction is exothermic; that is, the direction of proton transfer can be anticipated from thermodynamic information. Consequently, it is possible to determine experimentally whether a particular proton transfer reaction is likely to occur by comparison of analyte and matrix abundances in LSIMS spectra to their respective proton affinities.

By using this approach, Sunner et al. demonstrated that proton transfer reactions can and do occur during sputtering events (35,36). The conclusion is based on the fact that enhanced emission of protonated solute molecules is suppressed if the solute proton affinity is less than

that of the solvent. For dilute analyte/matrix solutions, most of the molecules sputtered in any single sputtering event will arise from the matrix. For an analyte with proton affinity less than that of the matrix, a protonated analyte molecule would be deprotonated by collision with any matrix molecule during the transition into the gas phase. Alternatively, endothermic protonation of such an analyte molecule by a protonated solvent molecule is precluded. In either case, the intensity of secondary protonated analytes would be substantially reduced if analyte proton affinity is less than matrix proton affinity, a conclusion consistent with observed spectra. Substituted aromatic compounds have proton affinities substantially greater than that of sulfuric acid (PA=170 kcal/mole) (59), and abundances of secondary protonated aromatic molecules detected from aromatic/sulfuric acid solutions are consistent with the conclusion of Sunner et al. (35,36).

A similar argument should be applicable to any molecular ions which might be sputtered. That is, the proton affinity of the radical (M - H·) must be greater than the proton affinity of the matrix molecules if the molecular ion is to survive the transition into the gas phase. Consider reactions 10-12, where ArYH is to be taken as a substituted aromatic compound. The homolytic bond dissociation of the weakest σ-bond containing hydrogen in the ArYH molecule is defined as D(ArY-H), and IP is the ionization

$$ArYH \longrightarrow ArY\cdot + H\cdot \qquad \Delta H = D(ArY\text{-}H) \quad (10)$$

$$H\cdot \longrightarrow H^{+} \qquad \Delta H = IP(H\cdot) \quad (11)$$

$$ArYH \longrightarrow ArYH^{+}\cdot \qquad \Delta H = IP(ArYH) \quad (12)$$

energy of the indicated species. From tabulated values of the enthalpies of reactions (10) - (12), the enthalpy of reaction (13) can be calculated. From the cycle (10) - (13),

$$ArYH^{+}\cdot \longrightarrow ArY\cdot + H^{+} \qquad \Delta H = PA(ArY\cdot) \quad (13)$$

$PA(ArY\cdot) = IP(H\cdot) + D(ArY\text{-}H) - IP(ArYH)$. $PA(ArY\cdot)$ is the proton affinity of the aromatic radical formed by loss of $H\cdot$. Taking the ionization energies of benzoic acid and $H\cdot$ as 224.2 kcal/mole (9.73 eV) (131) and 313.6 kcal/mole (13.6 eV) (131), respectively, and D(COO-H) as 110 kcal/mole (4.77 eV) (132), PA(benzoic acid - $H\cdot$) is 199 kcal/mole. For all other aromatic acids, D(COO-H) should be nearly constant, and acids of larger ring systems should presumably have lower ionization energies than benzoic acid. Consequently, the proton affinities of the corresponding radicals should be greater than those of (benzoic acid - $H\cdot$) and thus, sulfuric acid. As a rule, a lower limit of bond dissociation energies of 80 kcal/mole can be assumed, so that if a compound has an ionization energy less than

9.7 eV, the molecular ion of that compound should survive the transition from condensed phase into gas phase via sputtering from sulfuric acid. Even though the IP of benzoic acid is above this limit, D(COO-H) and D(Ar-H) are both approximately 30 kcal/mole greater than the minimum assumed in the above calculation.

To summarize, for the compounds investigated, neither aromatic molecular ions nor protonated aromatic molecules should suffer deprotonation by collision with sulfuric acid molecules during sputtering. This should not be taken to mean that either the protonated aromatics or the aromatic molecular ions are formed by gas phase protonation of neutral precursors. The compounds studied here are universally basic in 98% sulfuric acid, so that it is reasonable to believe that the protonated aromatic molecules detected were protonated <u>before</u> suffering any collisions with sulfuric acid molecules during sputtering; that is, the aromatic molecules were "pre-ionized". The origin of abundant secondary aromatic molecular ions is not so obvious as radical cations of substituted aromatic compounds are not known to exist in appreciable concentrations in sulfuric acid solutions.

Sunner <u>et al</u>. noted that the abundance of major analyte fragment ions observed in LSIMS spectra of glycerol solutions relative to the abundance of protonated analyte molecules was constant and independent of the abundance of

protonated glycerol molecules (35). From this, it was concluded that fragment ions arose from gas phase decomposition. Such an explanation (that $M^{+\cdot}$ arise from fragmentation of $(M+H)^+$) for the intense molecular ions and constant $[M^{+\cdot}]/[(M+H)^+]$ ratios observed here is not justified. Protonated analyte molecules could lose H· by unimolecular decomposition to yield secondary molecular ions; however, decompositions of even electron ions to yield odd electron fragment ions are relatively rare, and are not general phenomena (121). In the few unimolecular decompositions in which H· is lost from an even electron species, the loss is an intermediate step of a consecutive ion decomposition (133). Alternatively, highly energetic collisions between protonated aromatic molecules and sulfuric acid molecules during sputtering can cause loss of H· by protonated aromatic molecules. However, measurements of fragment ion intensities from collisionally activated decompositions, or CAD spectra, of parent ions having keV kinetic energies, invariably show that loss of H· by even electron parent ions yield daughter ions of low abundance (15). Low energy collisions between protonated aromatic ions and sulfuric acid molecules or their fragments during sputtering can cause loss of H· by protonated aromatic molecules, but hydrogen abstraction reactions are <u>slow</u> reactions and require particular orientations between reactants to occur (134). Such reactions would be unlikely

to have a significant effect on the distribution of ions observed in these spectra.

Gas phase formation of $M^{+\cdot}$ via ion impact of neutral species has been indicated in a limited number of studies (51,52). The steps involved in this gas phase ionization are shown in reactions 14 and 15. In the first step, 14, the neutral aromatic (M) evaporates or is sputtered into the gas phase following primary ion impact with the liquid surface. Subsequent to ejection of the neutral aromatic, another keV argon ion collides with M to produce the molecular radical cation of the aromatic as indicated in 15.

$$M_{(l)} \longrightarrow M_{(g)} \qquad (14)$$

$$M_{(g)} \xrightarrow{Ar^+} M^{+\cdot} + e^- \qquad (15)$$

Such a process is not supported by comparison of the kinetic energy spread observed for the molecular ion of 9-anthracenecarbonitrile to the protonated sulfuric acid molecule. The kinetic energy spread of secondary ions was determined by ramping the accelerating potential of the secondary ion source so as to selectively transmit ions of only a discrete kinetic energy (K.E.). The slits on the electrostatic sector, the kinetic energy filter, were reduced to limit ΔK.E. As shown in Figure 22, the kinetic energy distributions for the molecular ion of

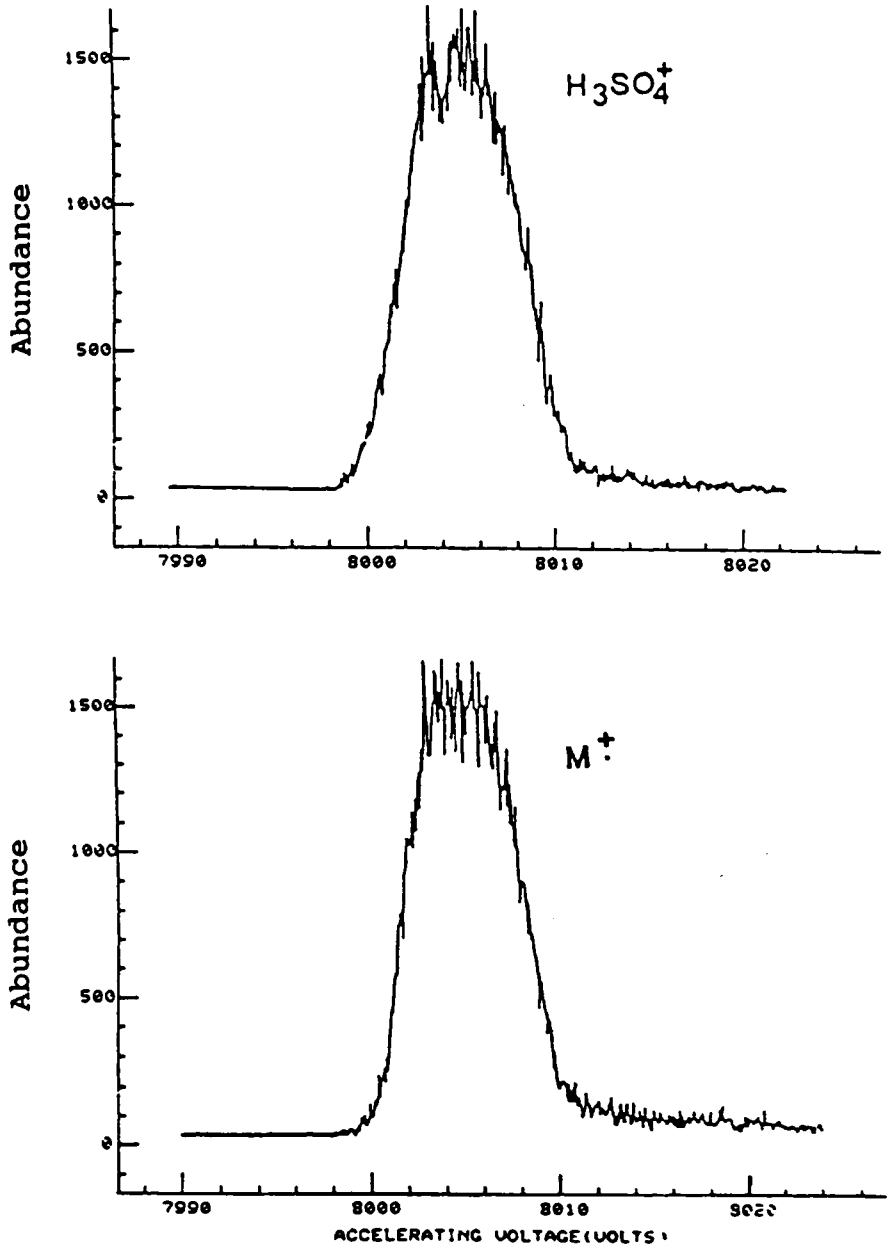


Figure 22. Kinetic energy distributions for the molecular ion of 9-anthracenecarbonitrile and protonated sulfuric acid.

9-anthracenecarbonitrile and protonated sulfuric acid are virtually the same, indicating that both ions are formed within the same region of the secondary ion source. The same kinetic energy distribution is observed for the protonated nitrile. The 10 volt energy width corresponds to a 100 micron region in the secondary ion source since the electric field in the sample region is approximately 1000 V/cm. Since the self dissociation of concentrated sulfuric acid is extensive (see p. 20), protonated sulfuric acid exists at an appreciable concentration in concentrated sulfuric acid. Protonated sulfuric acid secondary ions are probably protonated in solution and sputtered directly from solution. Consequently, ion formation [$(M+H)^+$ and $(M^{+\cdot})$] is within 100 microns of the sample surface. If gas phase ion impact were responsible for molecular ion formation, tailing would be observed in the kinetic energy distribution for the molecular ion since the diffuse primary beam used extends well above 100 microns from the surface.

Additional observations indicate that reactions 14 and 15 cannot contribute substantially to $[M^{+\cdot}]$. The $[M^{+\cdot}]/[(M+H)^+]$ ratio was found to be independent of the primary ion beam current density. This is shown in Figure 23, where the $[M^{+\cdot}]/[(M+H)^+]$ ratio for benzoic acid is the same at different primary ion current densities. If $M^{+\cdot}$ was formed in the gas phase from ion impact ionization of a gas phase neutral, whereas $(M+H)^+$ was formed in the

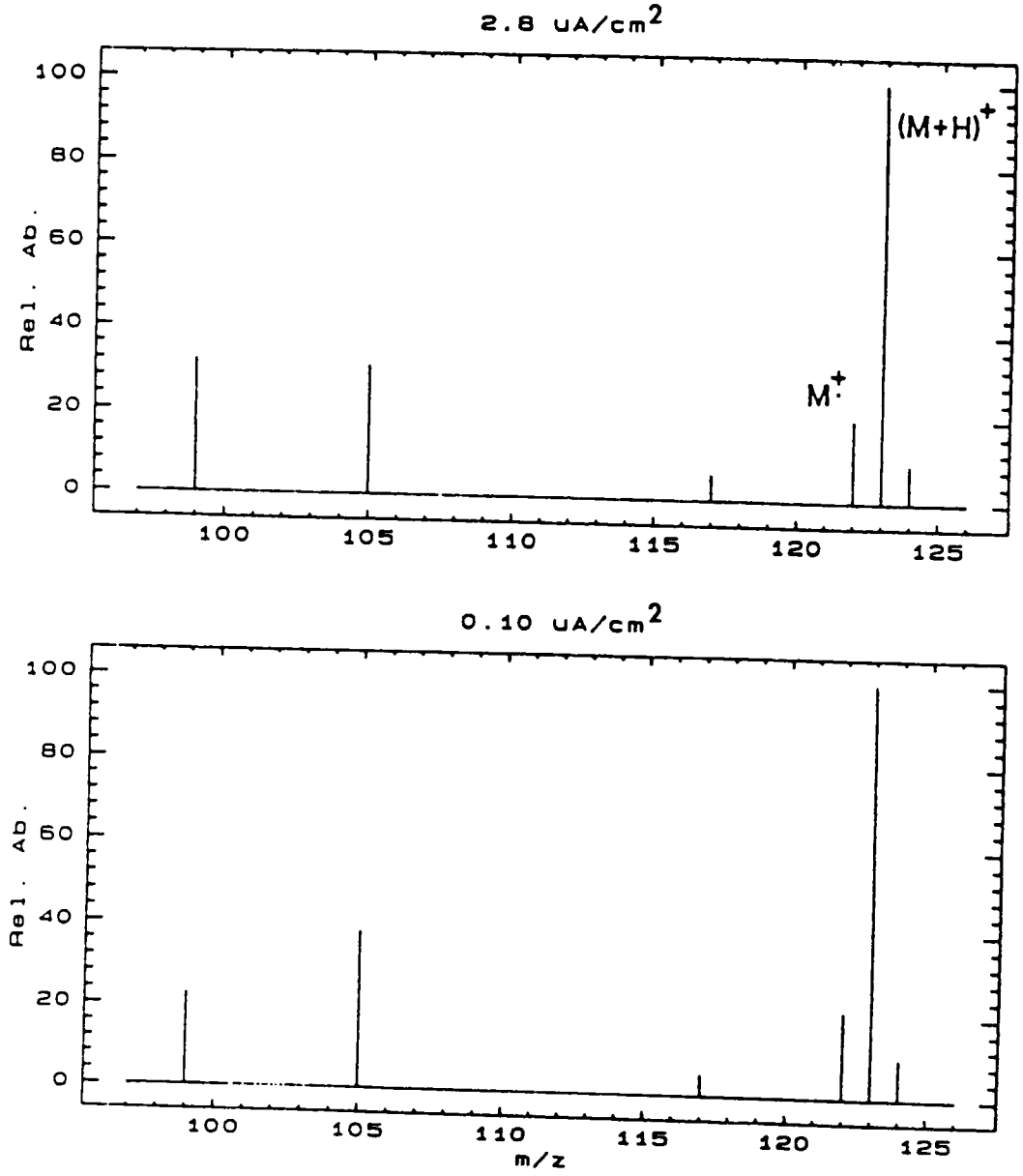


Figure 23. Partial LSIMS spectra of a benzoic acid/H_2SO_4 solution obtained with primary ion current densities of 2.8 and 0.1 $\mu A/cm^2$.

condensed phase and sputtered from solution directly, the $[M^{+\cdot}]/[(M+H)^+]$ ratio would be a function of the primary ion current density. It is unlikely that very different reactions for formation of $(M+H)^+$ and $(M^{+\cdot})$ secondary ions could occur with equal probability. The fact is that no reasonable, general gas phase reaction can be invoked to explain the high abundance of molecular ions observed in the spectra reported here.

2. Condensed Phase Reactions.

The relative intensities of aromatic molecular ions compared to the intensities of protonated aromatic molecules, $[M^{+\cdot}]/[(M+H)^+]$, follow a pattern. Table 2 (p. 76) shows a listing of the $[M^{+\cdot}]/[(M+H)^+]$ intensity ratios observed in respective SIMS spectra. For the aromatic acids studied, the ratio increases for the series benzoic acid, naphthoic acid, and anthracene carboxylic acid. From spectra of this series of compounds, which are strong bases in concentrated sulfuric acid, it appears that for compounds having a single common substituent, the number of rings has a significant effect on $[M^{+\cdot}]/[(M+H)^+]$. Spectra of compounds such as nitriles, which are weak bases in sulfuric acid, show similar behavior, although the $[M^{+\cdot}]/[(M+H)^+]$ is greater than unity.

For a homologous series of unsubstituted aromatic hydrocarbons, basicity in sulfuric acid solution increases

with the number of rings. This can be deduced from the localization energies of the hydrocarbons, which decrease with increasing number of rings. Localization energy is a measure of the π bonding energy required to isolate 2 electrons at a position in an aromatic ring system from the remainder of the π system (128). These former π electrons are required to form a σ-bond with the proton (or other electrophile), and can no longer participate in the aromatic π system. A reasonable expectation from this knowledge is that, for a homologous series of substituted aromatic compounds, the viability of ring protonation, or more generally, the susceptibility of the aromatic ring system to electrophilic attack, increases with the number of rings. From LSIMS spectra of the compounds studied, it appears that susceptibility of the aromatic portion of the molecules to electrophilic attack, compared to susceptibility of the substituent to protonation determines the $[M^{\cdot+}]/[(M+H)^+]$ ratio. Put more bluntly, the more likely that ring protonation occurs in solution, the greater is the $[M^{\cdot+}]/[(M+H)^+]$ ratio.

Evidence that the susceptibility of ring vs. substituent protonation determines the $[M^{\cdot+}]/[(M+H)^+]$ ratio is provided by LSIMS spectra of nitrogen heterocycles. For these compounds, the secondary protonated molecule is generally the more intense species. The nonbonding orbitals of nitrogen in nitrogen heterocycles are orthogonal to the

aromatic π system; consequently, nitrogen protonation does not require that π electrons to be isolated from the aromatic system. In most nitrogen heterocycles, protonation at the nitrogen is known to predominate (87) over ring protonation, and the observed $[M^{+\cdot}]/[(M+H)^+]$ ratios for the nitrogen heterocycles presented in Appendix B (pp. 165-166) are consistent with this and the above hypothesis. The spectrum of carbazole is unique among those of nitrogen heterocycles studied in that the $M^{+\cdot}$ ion is more intense than the $(M+H)^+$ ion.

Difference in protonation sites between carbazole and the other nitrogen heterocycles is indicated by measurements of the extent of protonation as a function of acid strength. The extent to which a compound is protonated in solution can, in some cases, be determined with optical spectroscopic methods. Spectrophotometric determination of the extent of protonation of weakly basic indicators (B) in solution is the basis of a quantitative acidity scale developed by Hammett and Deyrup (135). These authors defined an acidity function, H_o, by equation 16, where K_{BH^+} is the acid

$$H_o = pK_{BH^+} - \log [BH^+]/[B] \qquad (16)$$

dissociation constant of BH^+, the conjugate acid of B. The ratio of the concentration of the protonated base to the neutral base, $[BH^+]/[B]$ is determined

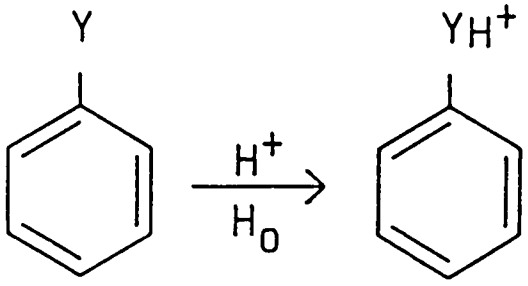
spectrophotometrically. Equation 16 can be reduced to equation 17 where a_{H^+} is the activity of hydrogen ions in solution with y_B and y_{BH^+} being the activity coefficients for the neutral and protonated base, respectively. From

$$H_o = -\log (a_{H^+} y_B / y_{BH^+}) \qquad (17)$$

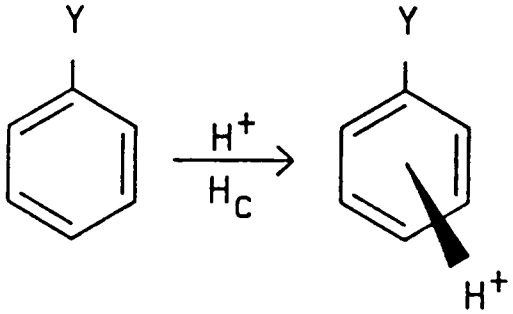
equation 17 it can be seen that H_o will be independent of the particular indicator used provided (y_B/y_{BH^+}) is identical for all indicator bases in the same acid solution. Acidity functions are necessarily defined with a particular set of bases. For bases of similar structure similar acidity functions will be observed. There can be dramatic differences in the acidity functions defined when bases with different structure are used because the protonation reactions may be completely different. Only if a particular compound, B, is protonated in an identical manner to the indicator bases used to define a particular acidity function, will a plot of log $[BH^+]/[B]$ vs. the acidity function be linear with unit slope. If a compound is not protonated in a manner identical to that of the reference indicators, a plot of log $[BH^+]/[B]$ vs. H_o will not have unit slope.

Compounds which are protonated on an aromatic carbon will define different acidity functions from those protonated on the nitrogen of an aromatic heterocycle. This

fact is illustrated in reactions 18 and 19, which shows substituent protonation and ring protonation, respectively. Measurements of protonation of carbazole (136) as a function of acid strength, fit best with the acidity function H_C (137), which is a measure of the ability of an acid solution to protonate an aromatic ring structure.



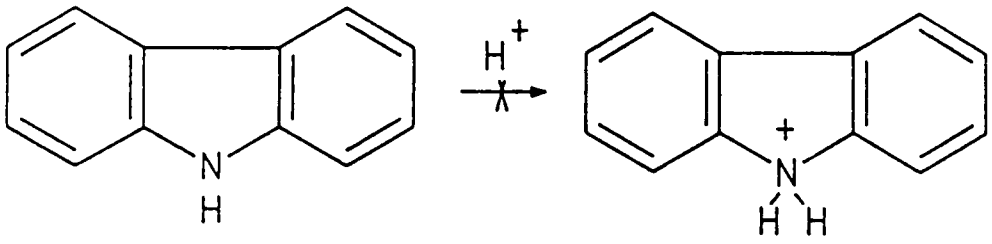
(18)



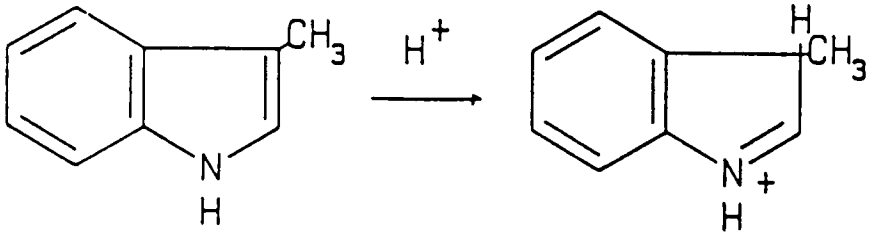
(19)

As shown in reaction 20, protonation of carbazole at the nitrogen is unfavorable, due to formation of a cationic cyclopentadienyl structure (128). Protonation of 3-methylindole, reaction 21, does not occur on the nitrogen either, but the structure generated by protonation does not require localization of aromatic π electrons; the LSIMS spectrum of

3-methylindole/sulfuric acid shows $[M^{+\cdot}]/[(M+H)^+]$ less than unity.



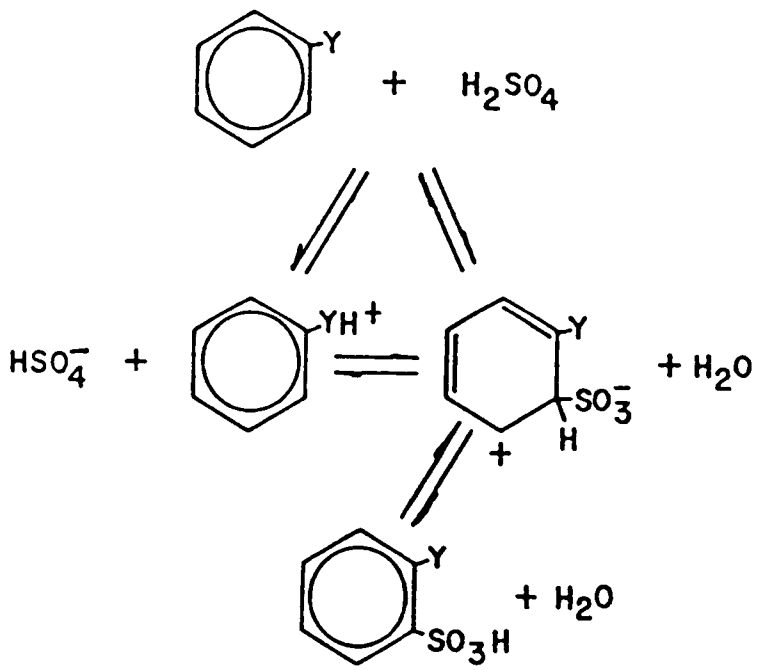
(20)



(21)

Exactly why $[M^{+\cdot}]/[(M+H)^+]$ reflects the viability of ring protonation over substituent protonation is not clear, but it seems to be a general phenomenon. In previous work, secondary emission of aromatic molecular ions from solutions has been related to complex formation of one form or another (43-45). Presumably, such complexes are excited by primary particle impact and dissociate to yield aromatic molecular ions. Alternatively, ionized complexes, even if they are even electron ions, might undergo gas phase unimolecular decomposition to lose the electrophile, a reaction driven by the return of aromaticity to the ring structure and the relative weakness of the complex σ-bond (128).

It is known from kinetic studies of aromatic sulfonation that substituted aromatic compounds form σ-complexes in sulfuric acid solution (89). Reaction Scheme II summarizes the salient features of sulfonation of substituted aromatic compounds by sulfuric acid. Upon dissolution, equilibrium is established between the neutral aromatic, the substituent-protonated aromatic and the σ-complex (89). In 98% sulfuric acid, for all compounds investigated, only the latter two are of significant concentration. The rate-determining and final step to sulfonation is aromatic-to-sulfonic group proton transfer (80-82,89). Under the experimental conditions employed here the rate of this proton transfer is so slow as to be unimportant. To be



SCHEME II

consistent with kinetic studies (89), we have indicated only the aromatic SO_3 σ-complex above, although other σ-complexes involving H^+ or $H_2S_2O_7$ exist in solution to some extent. For those aromatic compounds in which the substituent is strongly basic in sulfuric acid, protonation is mainly confined to the substituent. UV spectra, for example, show the disappearance of the n,π^* transition in the spectrum of benzophenone when it is dissolved in acid media, consistent with O-protonation (87). For compounds such as carbazole, where protonation external to the ring structure is precluded, σ-complex formation is favored. The surprising feature of the SIMS spectra of the aromatic acid/sulfuric acid solutions is that the $[M^{+\cdot}]/[(M+H)^+]$ ratio increases in the same manner as would the concentration of the σ-complex relative to that of the substituent-protonated tautomer. This behavior leads to speculation that precursors to the aromatic molecular ions detected were mainly σ-complexes in solution whereas the precursors to the detected secondary aromatic molecules were protonated on the substituent in solution.

F. Effects of Matrix Modification on SIMS Spectra

Modifications of the sulfuric acid matrix were attempted to expand the number of compounds amenable to LSIMS analysis to include unsubstituted aromatics, compounds for which LSIMS spectra could not generally be

obtained using sulfuric acid. Matrix modification was attempted by adding compounds to the matrix which would promote specific condensed phase reactions. Such promotion reactions could enhance the emission of analyte-characteristic secondary ions.

In an effort to improve the sensitivity for weakly basic substituted PAHs (nitroaromatics and aromatic nitriles), attempts were made to increase the acidity of the matrix. A superacid, tetra(hydrogen sulfato) boric acid in H_2SO_4 (reaction 5, p. 35), was employed in an attempt to increase the extent to which nitroaromatics and aromatic nitriles were protonated. It was hoped that more of the aromatic-characteristic ion signal would be associated with the protonated molecule [$(M+H)^+$] in the LSIMS spectrum of super acid solutions.

Organic-characteristic ions in the LSIMS spectra of 9-nitroanthracene and 9-anthracenecarbonitrile/super acid solutions are of the same absolute and relative abundance as obtained when concentrated $H2SO_4$ is employed as the liquid matrix. The failure of the tetra(hydrogen sulfato) boric acid matrix to improve the sensitivity for nitroaromatics or aromatic nitriles suggests that the matrix may not be stable under vacuum. SO_3 evolution would reduce the acidity of the matrix. When the superacid is placed under vacuum with a roughing pump, substantial gas evolution from solution occurs. Condensation of this gas in a trap cooled with

liquid nitrogen gives a white solid which, when mixed with water, produces an acidic solution, suggesting that the evolved gas is SO_3. While other superacid systems exist, none is amenable to the vacuum requirements of the secondary ion source.

The inability to increase the intensity of the protonated molecule suggests improving sensitivity by increasing the molecular ion intensity. If work showing complex formation as an important aspect of molecular ion formation in other matrices is also applicable to the sulfuric acid matrix, addition of complexing agents to aromatic/sulfuric acid solutions may enhance molecular secondary ion emission. A variety of inorganic and organic complexing agents have been selected based on their ability to form π complexes with aromatic compounds. These complexing agents have been added to benzoic acid/sulfuric acid solutions in an attempt to increase the $[M^{\cdot+}]/[(M+H)^+]$ ratio observed for benzoic acid. The inorganic complexing agents used ($AlCl_3$, $ZnCl_2$, $FeCl_3$, $SbCl_3$, I_2) are insoluble in concentrated sulfuric acid and no change in the $[M^{\cdot+}]/[(M+H)^+]$ ratio of benzoic acid is observed upon their addition. Attempts to use metal chlorides to form complexes with unsubstituted aromatics prior to dissolution in sulfuric acid were of limited success. Anthracene was successfully complexed with $SbCl_3$ by heating the two together to produce a green melt which was soluble in

sulfuric acid. The resulting green solution was not stable in the secondary ion source. The green color was quickly lost, presumably from evaporation of $SbCl_3$ which is a volatile solid.

Trinitrophenol (picric acid) and 7,7,8,8-tetracyanoquinodimethane (TCNQ) were selected as organic complexing agents since both are known to form complexes with aromatic compounds (138). Both organic complexing agents exhibited limited solubility in sulfuric acid. The $[M^{+\cdot}]/[(M+H)^+]$ ratio observed for benzoic acid was unaffected by dissolution of the organic complexing agent.

Since impurities are often found in "real" samples, the effect of impurities on the LSIMS spectra of target compounds dissolved in sulfuric acid solutions was investigated. Inorganic impurities, such as alkali metal cations, are common contaminants of biological samples. In addition, inorganic salts are found in soils and flyash samples which may be laden with aromatic compounds. Potassium, sodium, and ammonium bisulfate were selected as representative contaminants and added individually to aromatic/sulfuric acid solutions. Since HSO_4^- is a strong base in H_2SO_4, it can be determined if base addition reduces the effectiveness of concentrated sulfuric acid as a LSIMS matrix. Addition of the bisulfate salts did not alter the relative abundances of organic secondary ions. As shown in Figure 24, addition of ammonium bisulfate to a

9-phenanthrenecarbonitrile/sulfuric acid solution dramatically changes the inorganic portion of the spectrum; $NH_4H_2SO_4^+$ is now the base peak. However, there is no change in the relative abundances of organic secondary ions. Similar results were obtained when the other salts were used. The implication is that LSIMS spectra of organics obtained from concentrated sulfuric acid are largely independent of inorganic impurities.

G. Analytical Applications for Concentrated Sulfuric Acid

1. Pterins

Pterins form stable solutions in concentrated sulfuric acid from which abundant and persistent pterin characteristic secondary ions can be observed. Molecular weights of pterins investigated are given in Table 3. LSIMS spectra from the pterin/sulfuric acid solutions investigated are shown in Figures 25 - 32. Generally, the base peaks in pterin/sulfuric acid spectra correspond to the protonated pterin. This is expected since abundant protonated molecules are observed in LSIMS spectra of aromatic carbonyls and nitrogen-containing aromatics dissolved in H_2SO_4. The base analyte peak in the LSIMS spectrum of 6-hydroxy-methylpterin, shown in Figure 32, corresponds to the apparent protonated sulfonation product (observed at m/z 274). A feature of the pterin/sulfuric acid spectra distinct from those of aromatics containing a single

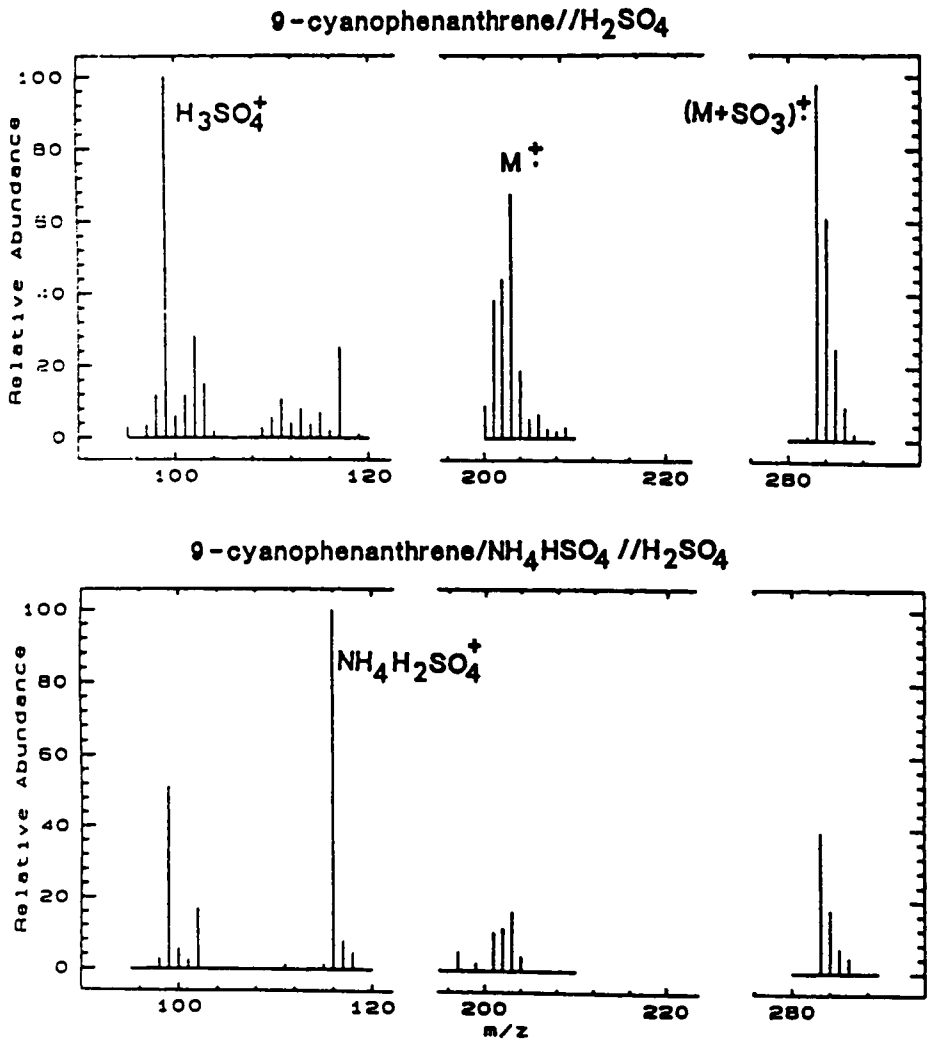


Figure 24. Positive LSIMS spectra obtained from 9-phenanthrene/H_2SO_4 and 9-phenanthrene/NH_4HSO_4/H_2SO_4 solutions.

Table 3.

Molecular Weights of the Pterins Investigated

Compound	M.W.
Pterin	163
Lumazine	164
6-Methylpterin	177
Xanthopterin	179
6-Formylpterin	191
Leucopterin	195
Pterin-6-carboxylic acid	207
6-Hydroxymethylpterin	193

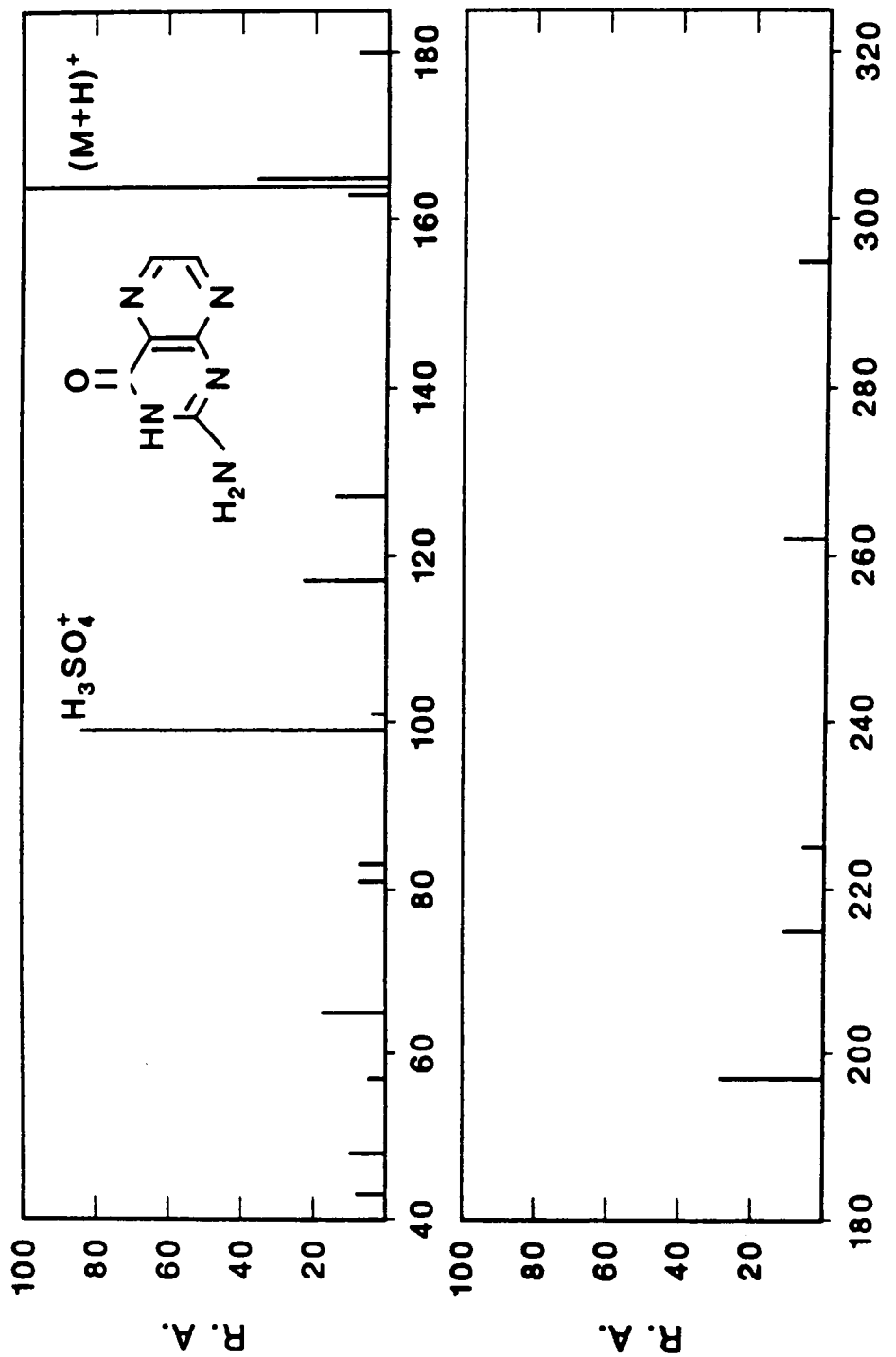


Figure 25. Positive LSIMS spectrum of a 2 mole % pterin/sulfuric acid solution.

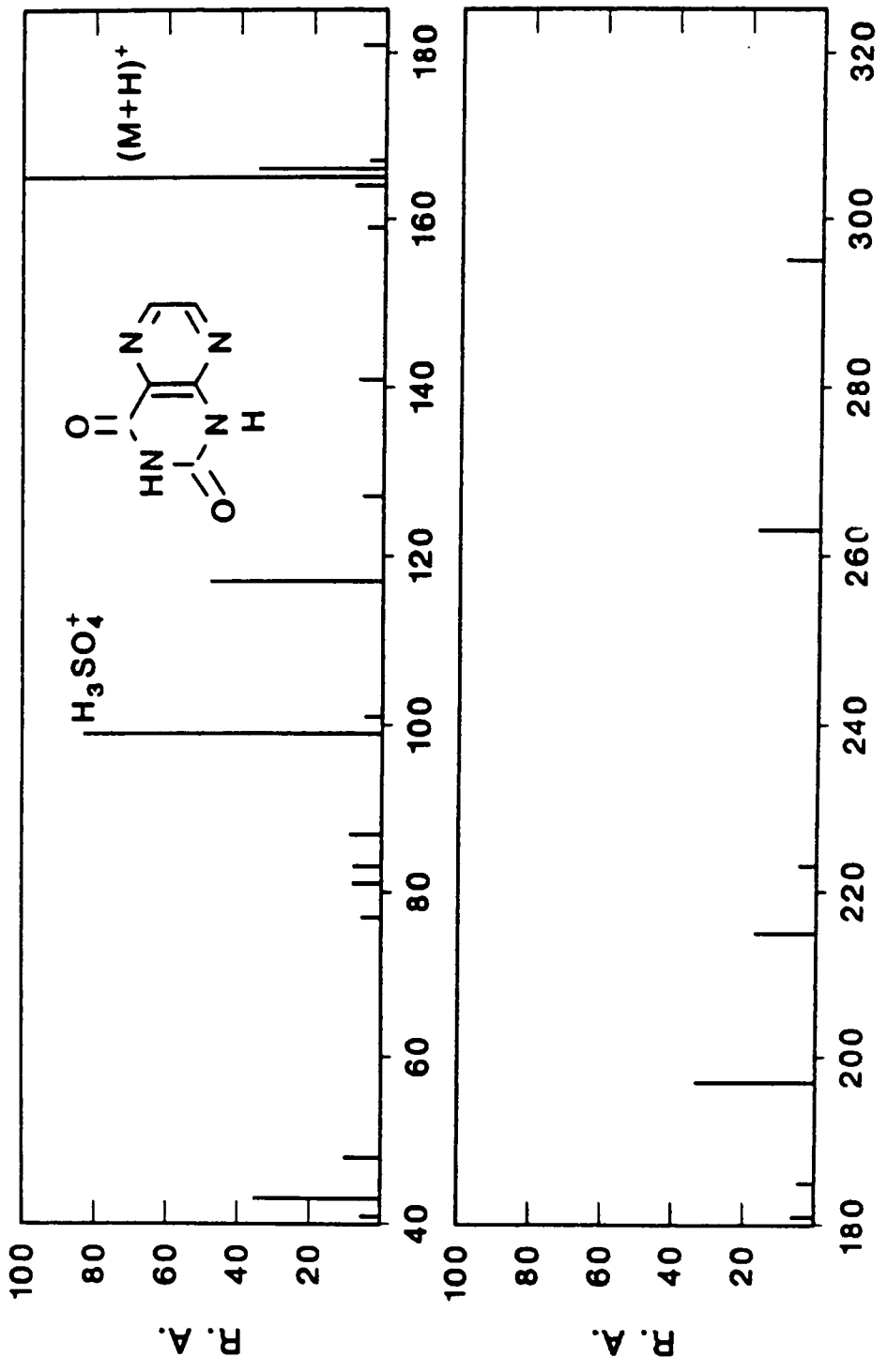


Figure 26. Positive LSIMS spectrum of a 2 mole % lumazine/sulfuric acid solution.

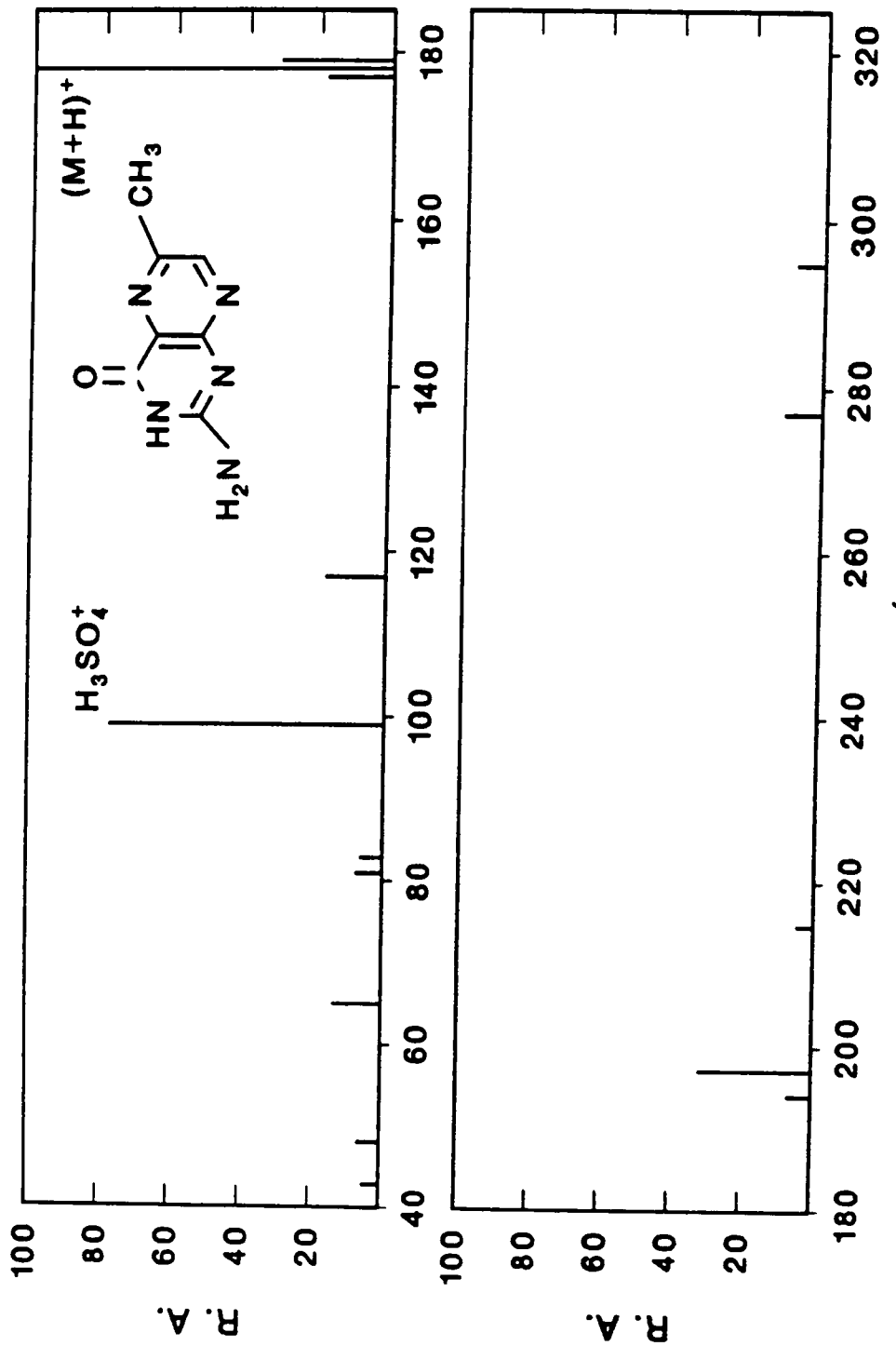


Figure 27. Positive LSIMS spectrum of a 2 mole % 6-methylpterin/sulfuric acid solution.

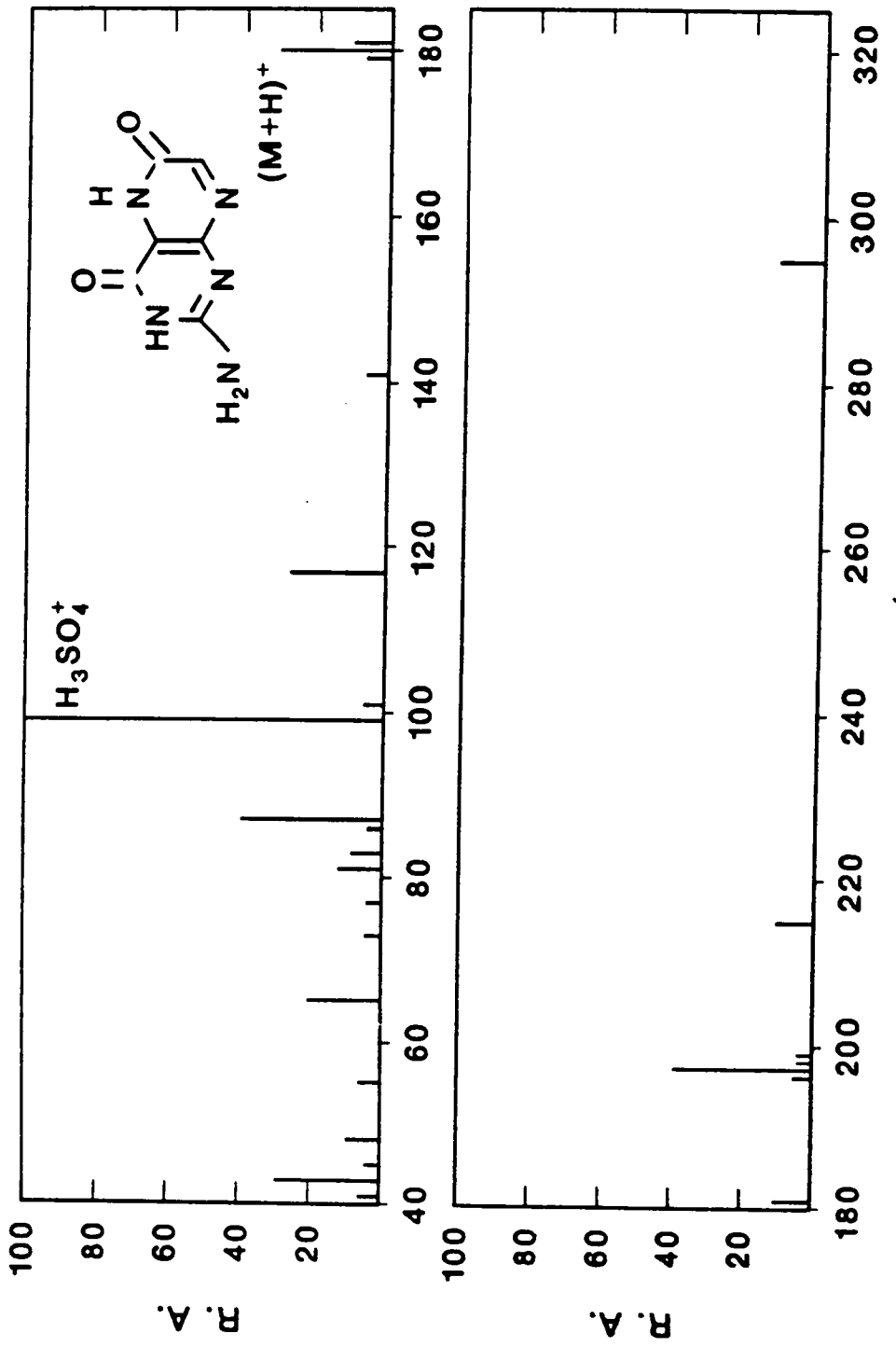


Figure 28. Positive LSIMS spectrum of a 2 mole % xanthopterin/sulfuric acid solution.

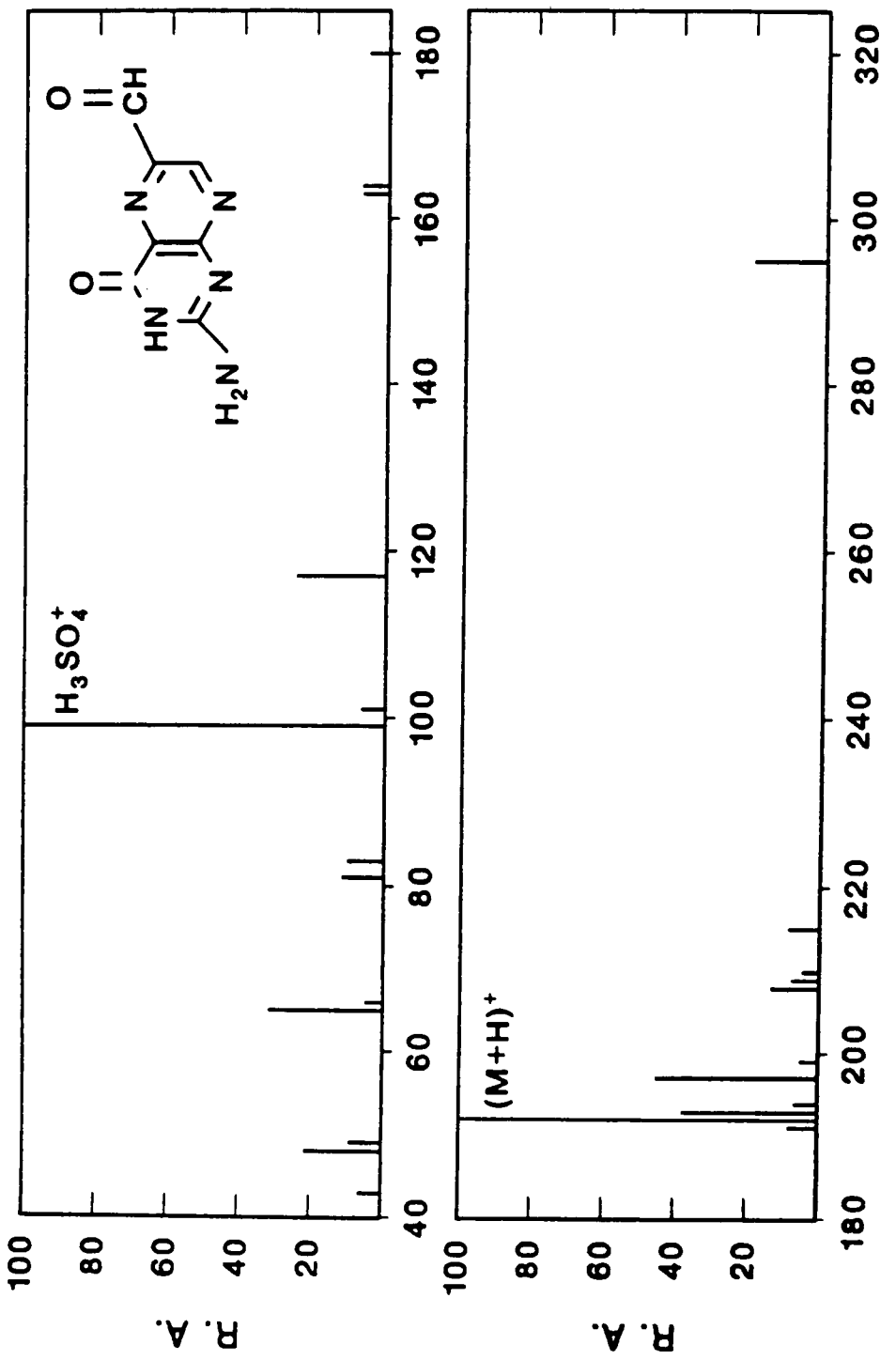


Figure 29. Positive LSIMS spectrum of a 2 mole % 6-formylpterin/sulfuric acid solution.

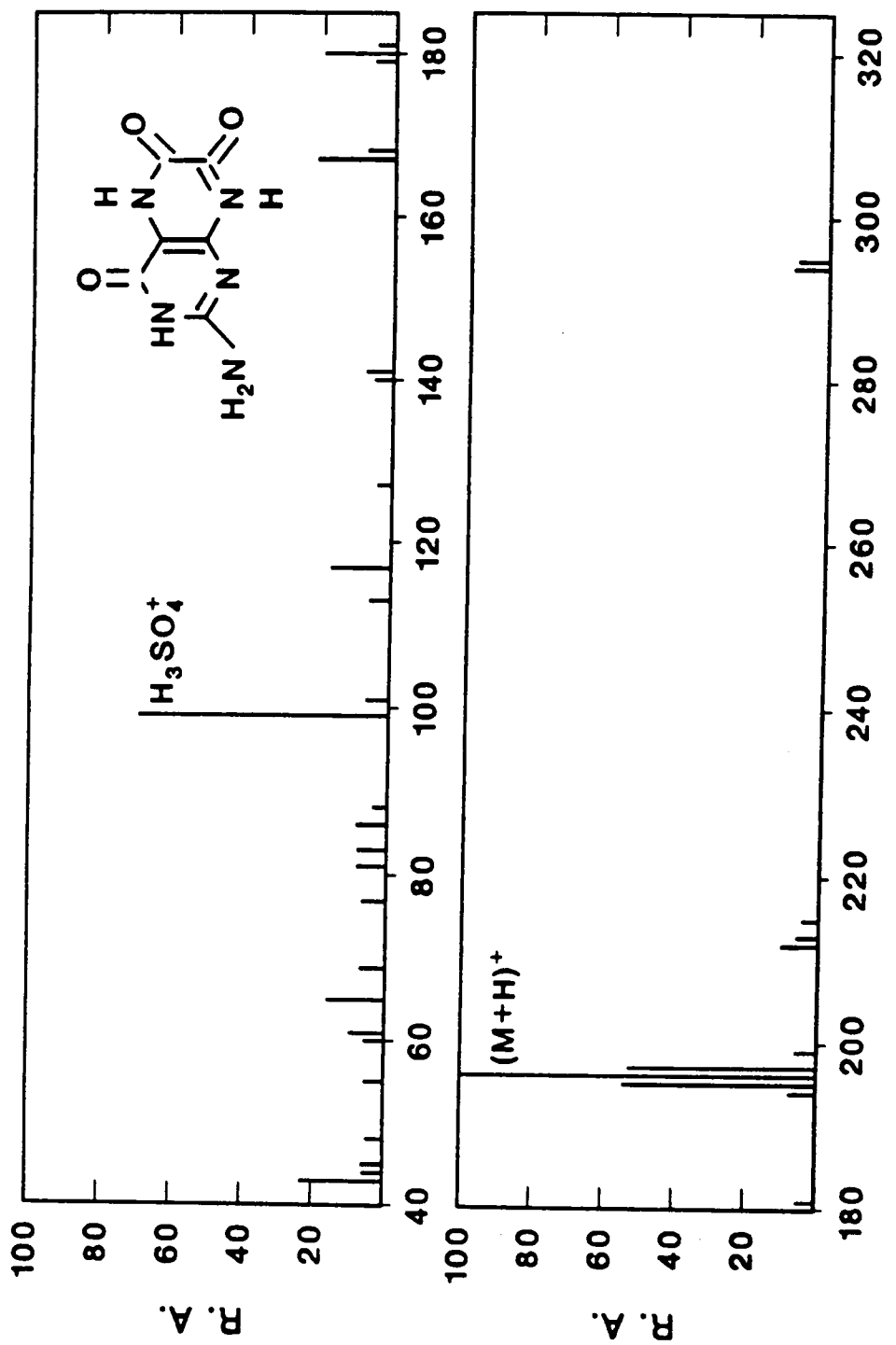


Figure 30. Positive LSIMS spectrum of a 2 mole % leucopterin/sulfuric acid solution.

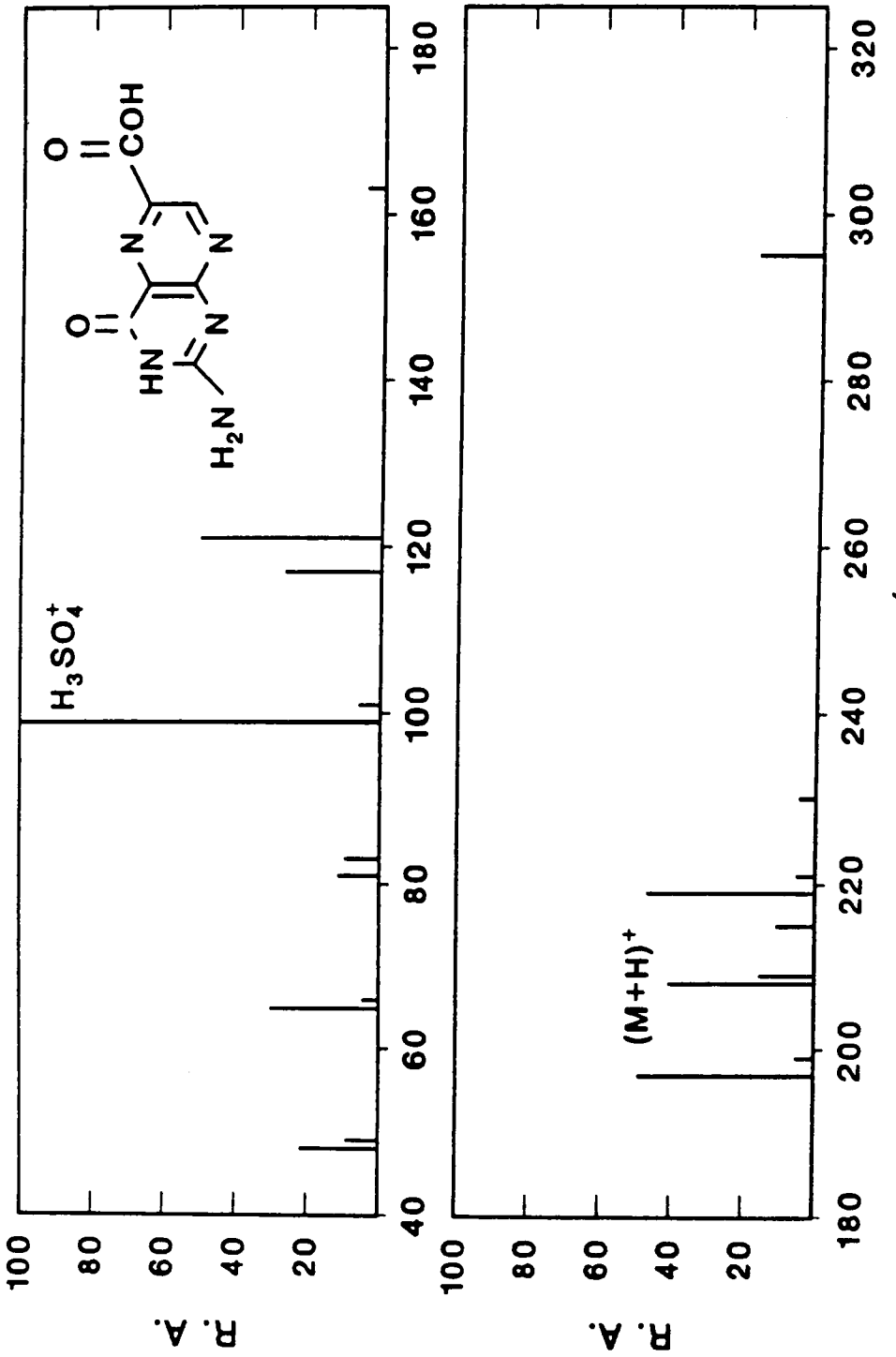


Figure 31. Positive LSIMS spectrum of a 2 mole % pterin-6-carboxylic acid/sulfuric acid solution.

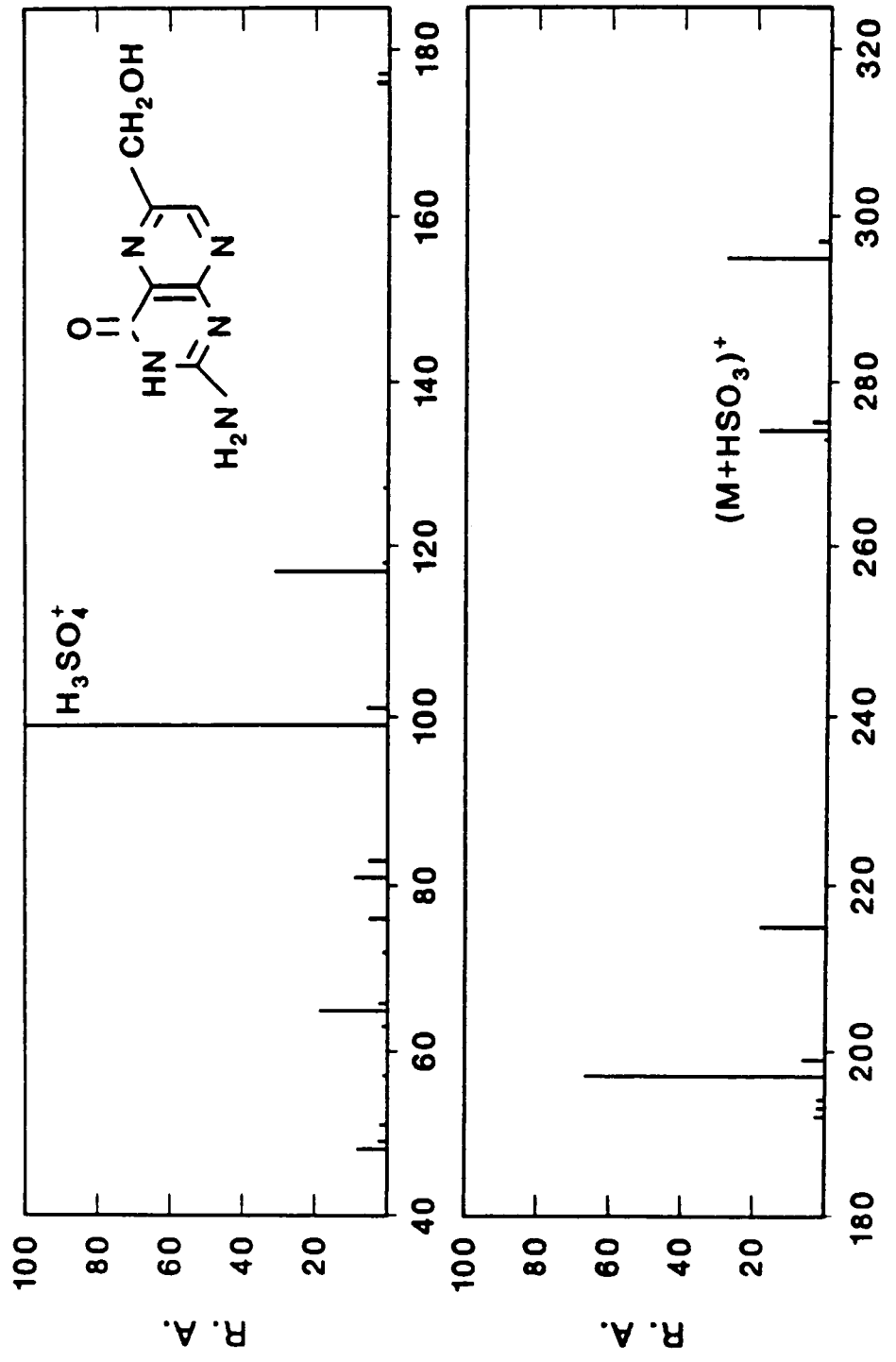


Figure 32. Positive LSIMS spectrum of a 2 mole % 6-hydroxymethylpterin/sulfuric acid solution.

functional group is that abundant M+2 ions are observed in the pterin spectra. The abundance of the M+2 ion is in excess of that which can be attributed to ^{13}C, ^{15}N, and ^{17}O isotope contributions from $(M+H)^+$. The origin of the M+2 ion is unknown. The relative abundance of fragment ions in the LSIMS spectra of pterin/sulfuric acid solutions is low. In some of the spectra a moderately intense peak is observed at m/z 43 which corresponds to $HNCO^+$. The LSIMS spectrum of pterin-6-carboxylic acid dissolved in sulfuric acid (Figure 31) is noteworthy in that sodium contamination of the sample is indicated in the spectrum by the appearance of $NaH_2SO_4^+$ and $Na(H_2SO_4)_2^+$ at m/z 121 and 219, respectively. The abundance of the $(M+Na)^+$ adduct, observed at m/z 230, relative to the $(M+H)^+$ abundance, is less than the abundance of the $NaH_2SO_4^+$ relative to the $H_3SO_4^+$ abundance. Sulfuric acid apparently scavenges sodium cations. Sodium contamination is frequently encountered in biological samples and abundant $(M+Na)^+$ peaks are generally observed in the LSIMS spectra from such samples when other matrices are used. An advantage of H_2SO_4 as a matrix is that $(M+Na)^+$ peaks are of minimal intensity.

2. Adsorbed Aromatics

Application of SIMS to *in situ* detection of substituted aromatics adsorbed on substrates was investigated. Concentrated sulfuric acid was used to serve

the dual role of extraction solvent and matrix for enhanced secondary ion emission of desorbed substituted aromatics. Alumina, silica gel, filter paper, and fly ash were the substrates used for these investigations. Acridine was selected as the substituted aromatic for this investigation since the sensitivity of LSIMS for azaarenes dissolved in concentrated sulfuric acid is high (see Table 1, p. 74). The quantities of acridine deposited on the substrates investigated are listed in Table 4. The acridine concentration of solutions prepared for LSIMS analysis, as described on page 37, are listed in Table 4. LSIMS spectra of solutions produced from room temperature extractions were the same as those obtained from the extractions performed at 90°C.

Acridine was only evident in the LSIMS spectra of the supernatant obtained from silica gel/H_2SO_4 and the filter paper/H_2SO_4 paste. Acridine was identified based on its characteristic $[M^{\cdot+}]/[(M+H)^+]$ ratio (Appendix B, p. 166). Protonated acridine was approximately 2% the abundance of $H_3SO_4^+$ in the LSIMS spectrum obtained from the silica gel/H_2SO_4 supernatant. This relative abundance is the same as that obtained from a 10 m<u>M</u> acridine solution, indicating that the extraction of acridine from silica gel using sulfuric acid is <u>ca</u>. 100%. The filter paper decomposed when mixed with sulfuric acid to give a black paste from which abundant acridine characteristic secondary ions were

Table 4.[a]

Amounts of Acridine Deposited on Substrates and Concentrations of Extracts

Substrate	Acridine Loading (μg/g substrate)	Sample Size (mg)[b]	Concentration Acridine/H_2SO_4 Solution[c]
Texas Ash	194	17.2	1.9 mM
Kaneb Ash	215	21.0	2.5 mM
Silica Gel	880	21	10.0 mM
Alumina	236	22.7	3 mM
Filter Paper	50 mg/g	6	170 mM

a Data given reflect room temperature extraction experiments.

b Mass of substrate loaded with acridine mixed with 10 μL concentrated sulfuric acid.

c Assumes 100% extraction efficiency.

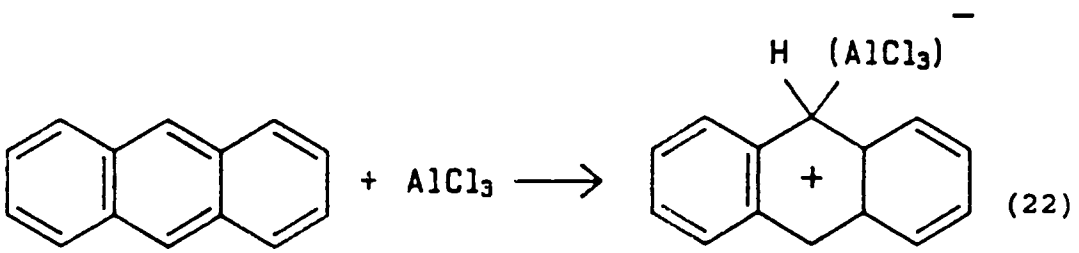
detected. The background signal from this paste was high; a peak was observed at every mass.

The $[M^{+\cdot}]/[(M+H)^+]$ ratio characteristic of acridine could not be discerned from the background signal observed in LSIMS spectra of the supernatants obtained from alumina, Texas Ash, or Kaneb Ash/H_2SO_4 mixtures. Acridine could not be detected in SIMS spectra of the paste of the sulfuric acid wetted substrates. Approximately 7 μL of sulfuric acid were required to wet 20 mg of fly ash. Gas evolution and heating occurred when fly ash was mixed with concentrated sulfuric acid.

While concentrated sulfuric acid is not suitable for in situ detection and identification of substituted aromatics adsorbed on fly ash, it can be used for analysis of PAH transformation products present in solvent extracts. Many of the suspected products from photochemical and non-photochemical transformation of PAH's adsorbed on fly ash belong to compound classes whose sulfuric acid solutions yield abundant aromatic-characteristic secondary ion currents. Involatile aromatics, which to date have been intractable with mass spectrometry, can possibly be detected and identified using concentrated sulfuric acid as an LSIMS matrix.

H. Metal Chlorides and Ambient Temperature Melts

Some metal chlorides behave as oxidizing agents toward aromatic compounds, producing aromatic radical cations (91,139) while other metal chlorides react with aromatic compounds to form σ-complexes (140). Formation of a σ-complex between anthracene and $AlCl_3$ is shown in Reaction (22) (140).



(22)

Because Reaction (22) is very similar to Reaction (3) (p. 22) of aromatic compounds with H_2SO_4, several metal chlorides were investigated as SIMS matrices for enhanced aromatic secondary ion emission. Some of the metal chlorides used in this investigation have vapor pressures incompatible with the vacuum requirements of the ion source. The neat metal chlorides investigated, the temperature at which their vapor pressure is 1 torr (141), and the temperature at which their SIMS spectra were obtained are given in Table 5.

The SIMS spectra of $AlCl_3$, $SnCl_2$, $ZnCl_2$, and $SbCl_3$, presented in Figures 33 - 36, respectively, are representative of the salts investigated. In some SIMS

Table 5.

Operating Temperatures for SIMS Spectra of Metal Chlorides

MCl_x	Temperature (^oC) Pressure = 1 torr	SIMS Temperature (^oC)
$AlCl_3$	100	31
$BiCl_3$	-	31
$HgCl_2$	136	31
$ZnCl_2$	428	31
$TeCl_4$	-	31
$InCl_3$	-	31
$PbCl_2$	547	31
$SbCl_3$	49	- 35
$SbCl_5$	23	- 47
$SnCl_2$	316	31
$SnCl_4$	- 23	- 48

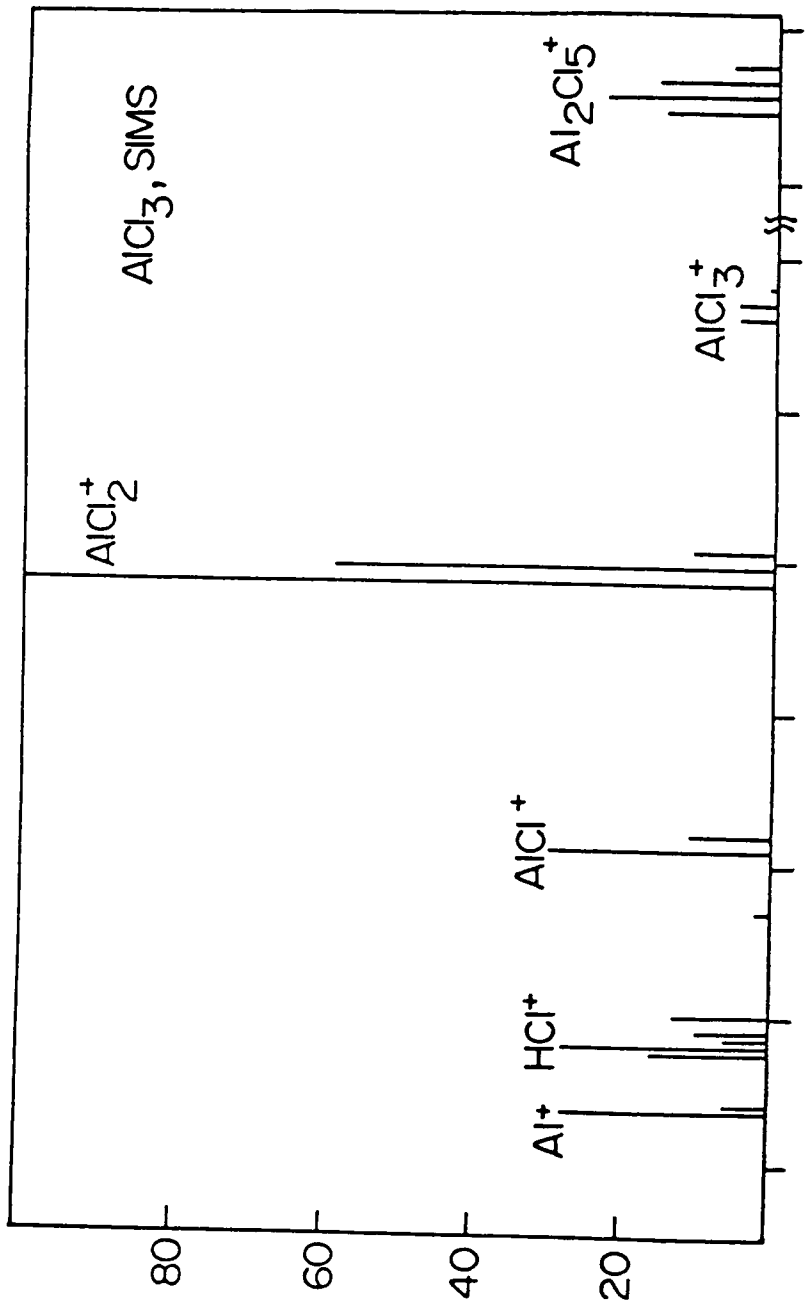


Figure 33. Positive SIMS spectrum of $AlCl_3$.

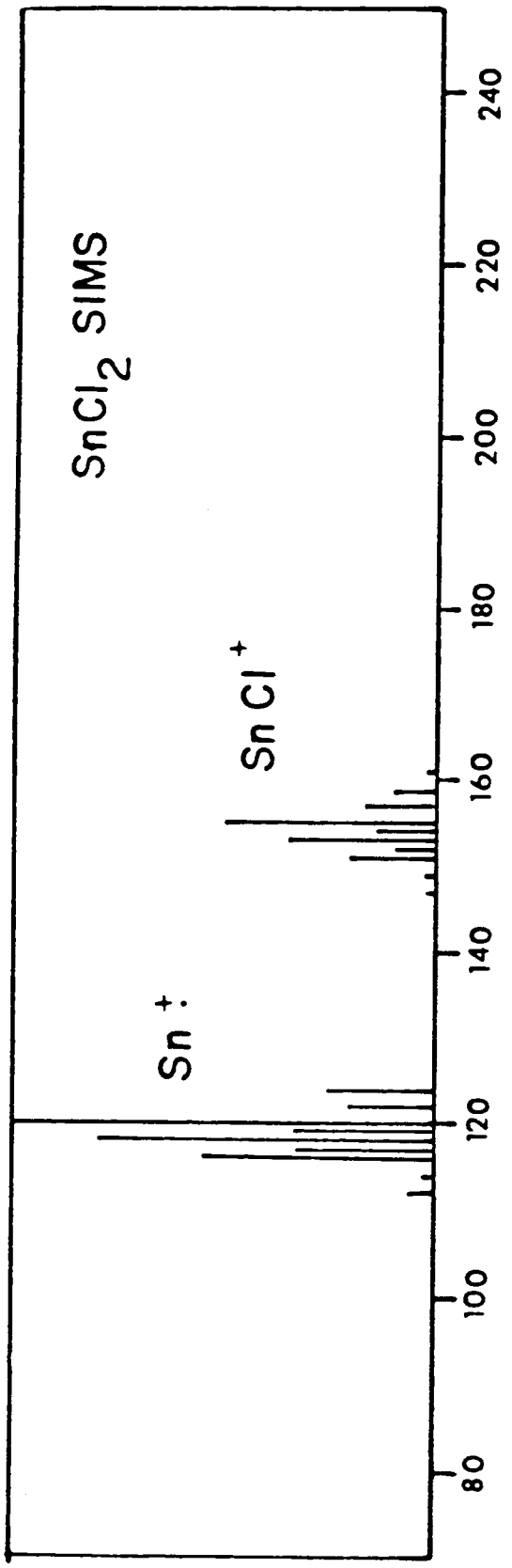


Figure 34. Positive SIMS spectrum of $SnCl_2$.

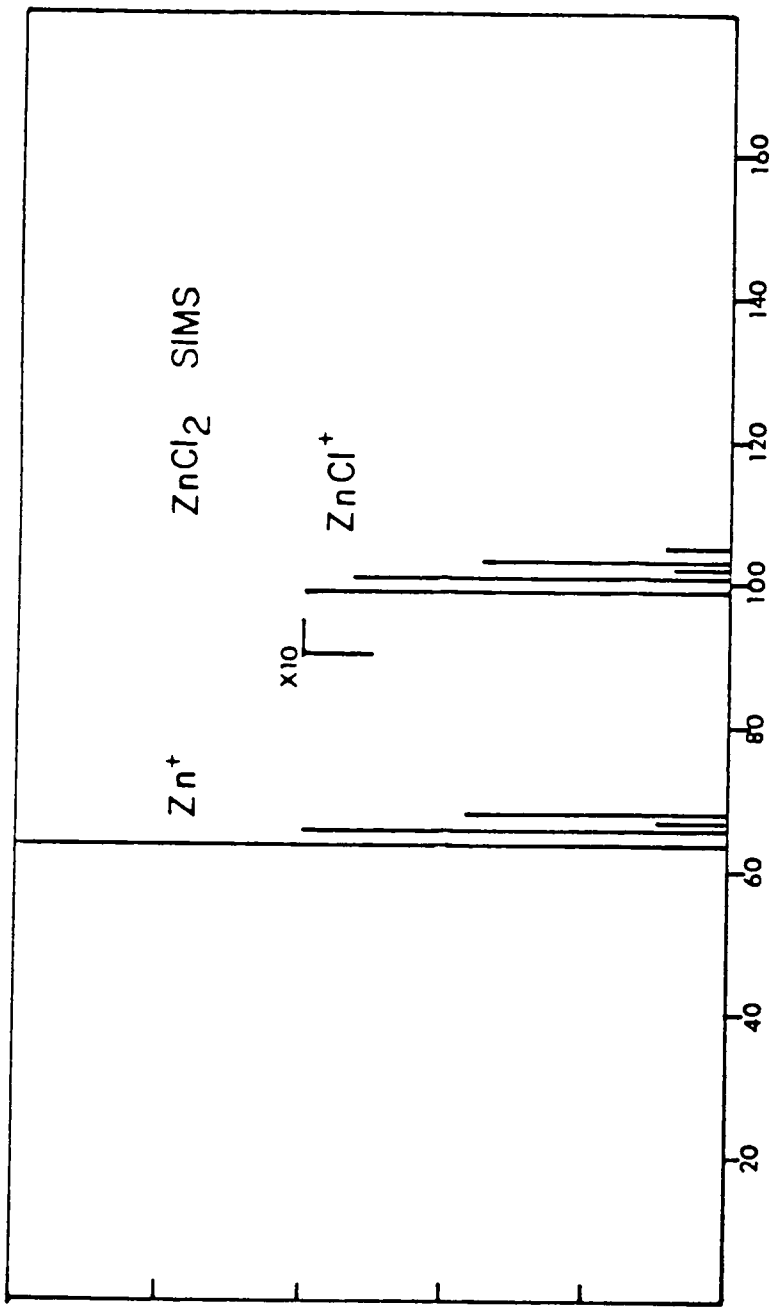


Figure 35. Positive SIMS spectrum of $ZnCl_2$.

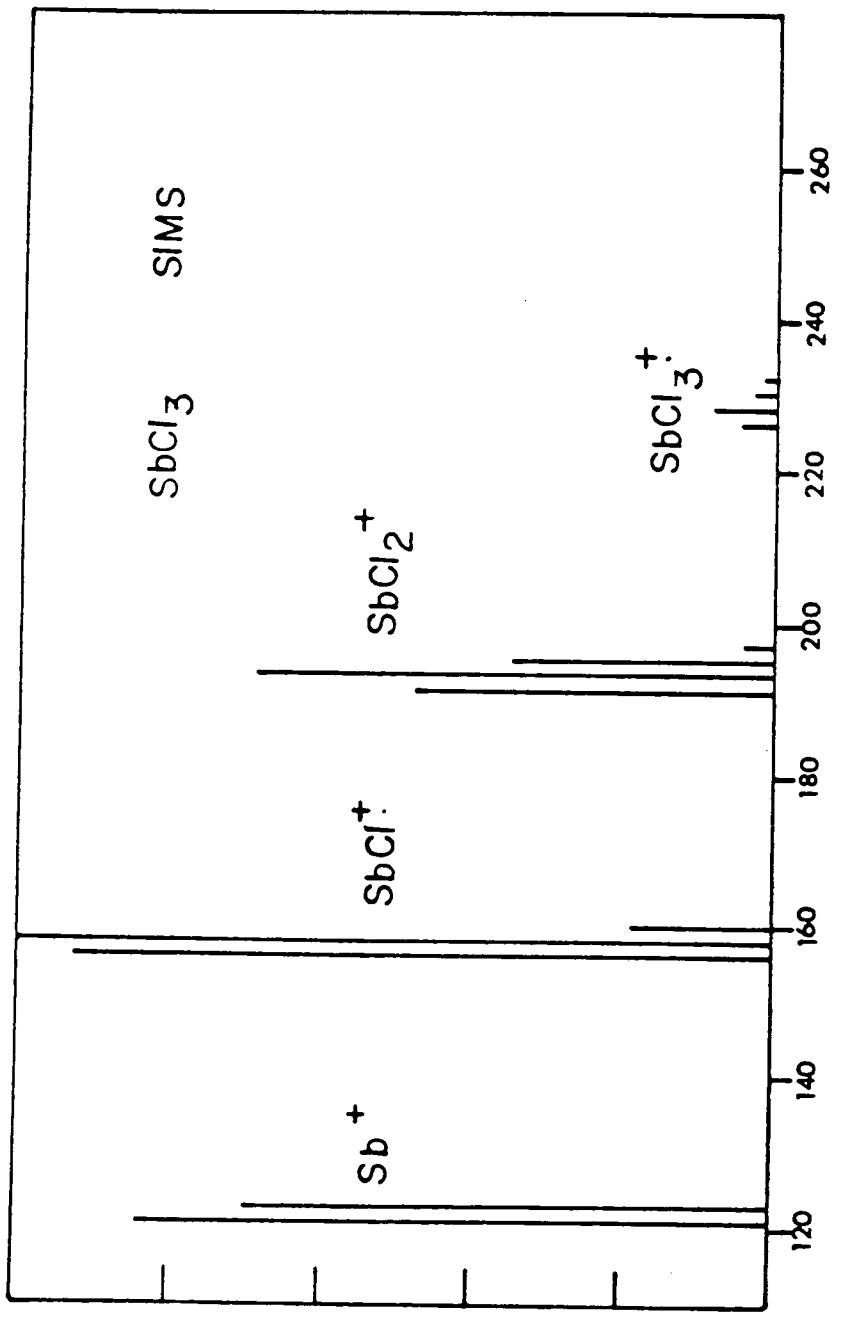


Figure 36. Positive SIMS spectrum of $SbCl_3$.

spectra the base salt-characteristic ion corresponds to the metal cation. In others a chloride-containing cation predominates. It must be noted that the mass spectrometer is subject to attack by these corrosive salts. Insertion of metal chlorides into the secondary ion source resulted in the cracking of diffusion pump oil, attack of the seals in the mechanical pumps backing the diffusion pumps, and corrosion of secondary ion source components and electrodes in the electrostatic analyzer.

For this investigation metal chlorides were used neat, as components in salt melts or mixed with nonvolatile liquids. The effectiveness of metal chlorides as SIMS matrices was evaluated using volatile and non-volatile aromatics.

Though SIMS is generally associated with non-volatile compounds, adsorbed organophosphorus compounds have been detected by using SIMS when they were introduced onto a polyphosphoric acid (PPA) matrix subject to primary ion bombardment (32). For comparison, LSIMS spectra of organophosphorus/PPA solutions exhibited slightly less fragmentation than when the organophosphorus compounds were introduced via the gas phase, but for the most part, the results were similar. The study suggested that secondary ion emission is more dependent on analyte-matrix interactions than on the mode of sample introduction. If the analyte-matrix interaction which leads to enhanced secondary ion

emission is the same for compounds of the same compound class, volatile analytes can be used to evaluate the effectiveness of a particular matrix for enhanced emission of compounds of the same class.

If a matrix enhances the secondary ion emission of a gaseous analyte, analyte-characteristic secondary ions are observed as long as the analyte is introduced onto the surface of the matrix (32). Analyte-characteristic secondary ion emission ceases within a few minutes after the inlet system is evacuated and gaseous introduction stops. No memory effects are observed when samples are introduced in this manner. Use of this technique permits rapid screening for the effectiveness of a particular matrix for a number of compound classes, because individual analyte/matrix solutions need not be prepared to test representative analyte/matrix systems.

Gaseous introduction of aromatics was one method used to assess the effectiveness of a particular metal chloride for enhanced aromatic secondary ion emission. Aluminum chloride was the salt most frequently employed in these investigations since 1) high purity $AlCl_3$ was readily available, 2) the vapor pressure of $AlCl_3$ at room temperature is low, 3) and aromatic secondary ion emission from $AlCl_3$ was more reproducible than that from the other salts investigated. When aromatic compounds were introduced onto an $AlCl_3$ matrix subject to primary ion bombardment,

molecular ions and fragment ions characteristic of the aromatic were generally observed. Generation of secondary ions from gas phase ion impact of neutrals was not indicated since no secondary ions were observed when gaseous analytes were introduced onto a bare gold target subject to primary ion bombardment. SIMS spectra of benzene, aniline, and anisole obtained from an $AlCl_3$ matrix are shown in Figures 37 - 39, respectively. Molecular ions and fragment ions characteristic of gaseous analytes were of only moderate abundance. Further, spectra obtained from gaseous analytes introduced onto a salt matrix were difficult to reproduce.

Aluminum chloride was also used as a SIMS matrix for non-volatile aromatics. Samples were prepared by depositing PAH/benzene solutions onto $AlCl_3$ matrices. Benzene was removed from the sample when the sample was evacuated in the insertion lock of the secondary ion source. Dried samples were ca. 10 mole % PAH. No organic characteristic secondary ions were observed for the samples investigated: naphthalene, anthracene, pyrene, and perylene deposited on $AlCl_3$. Secondary ion emission observed from solid metal chlorides was neither as stable nor as abundant as that generally associated with liquid matrices.

Room temperature salt melts containing $AlCl_3$ were investigated as possible LSIMS matrices to see if incorporation of $AlCl_3$ in a liquid matrix would increase the abundance and stability of aromatic secondary ion emission.

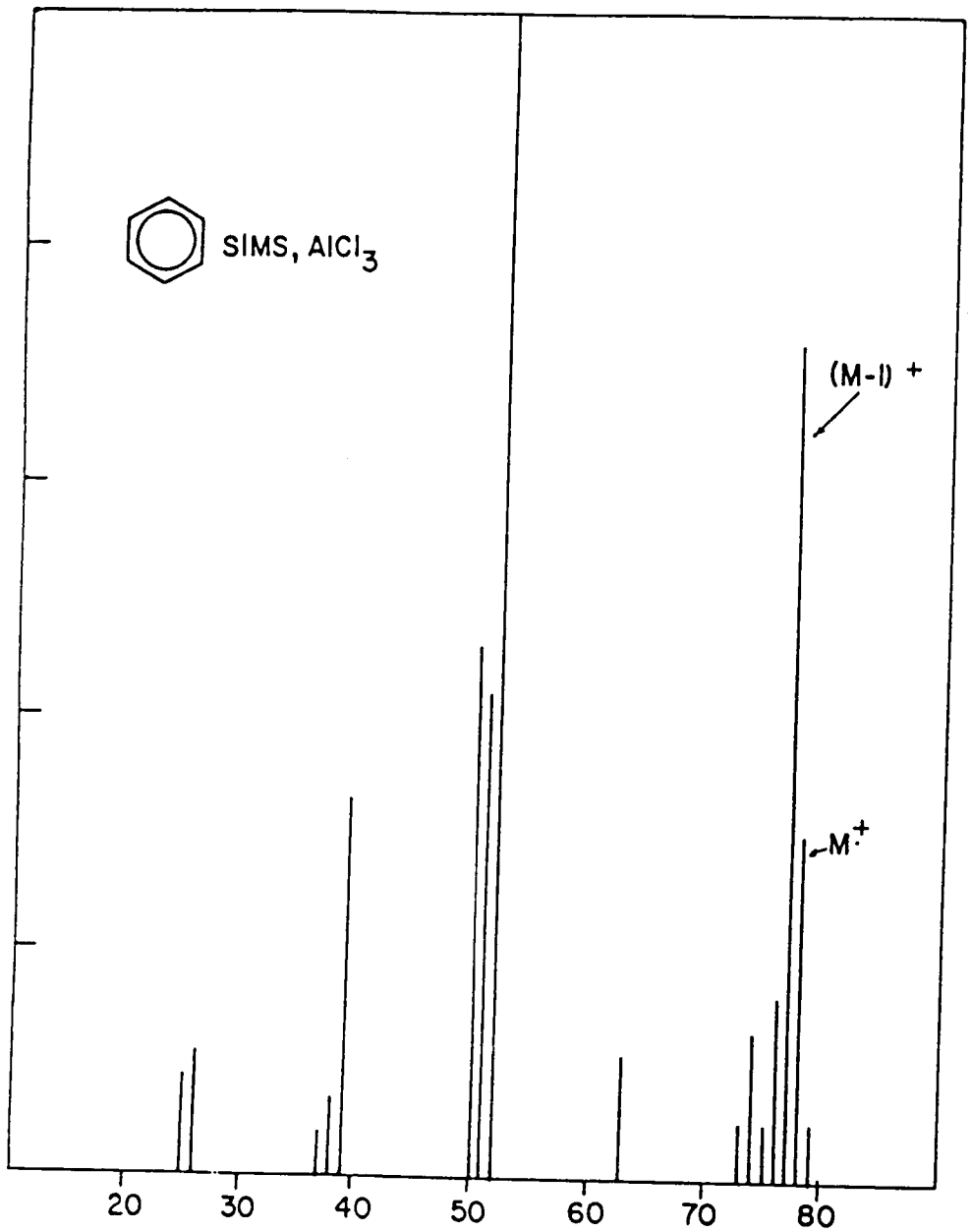


Figure 37. Positive SIMS spectrum of benzene obtained using $AlCl_3$ matrix. $AlCl_3$ characteristic ions have been subtracted from the spectrum.

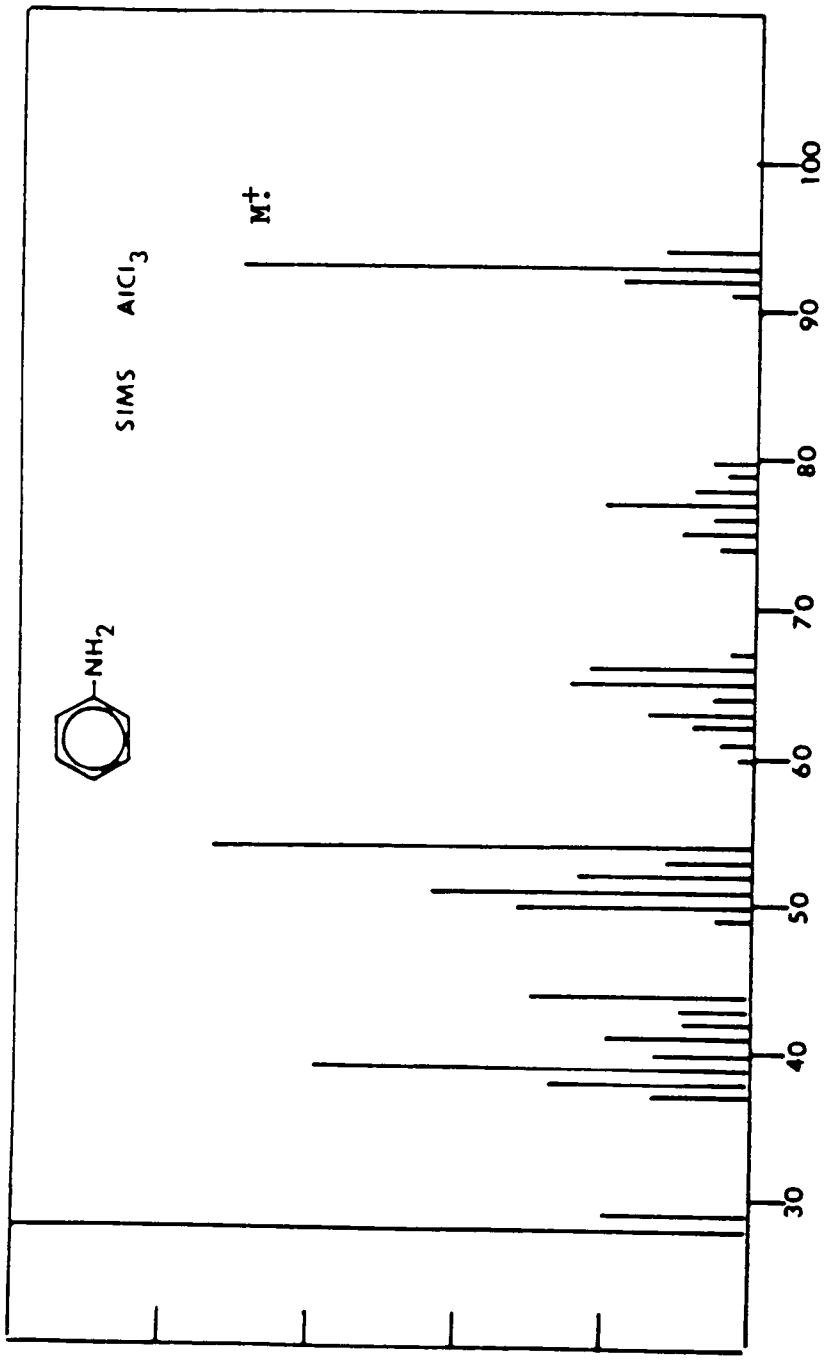


Figure 38. Positive SIMS spectrum of aniline obtained using $AlCl_3$ matrix. $AlCl_3$ characteristic ions have been subtracted from the spectrum.

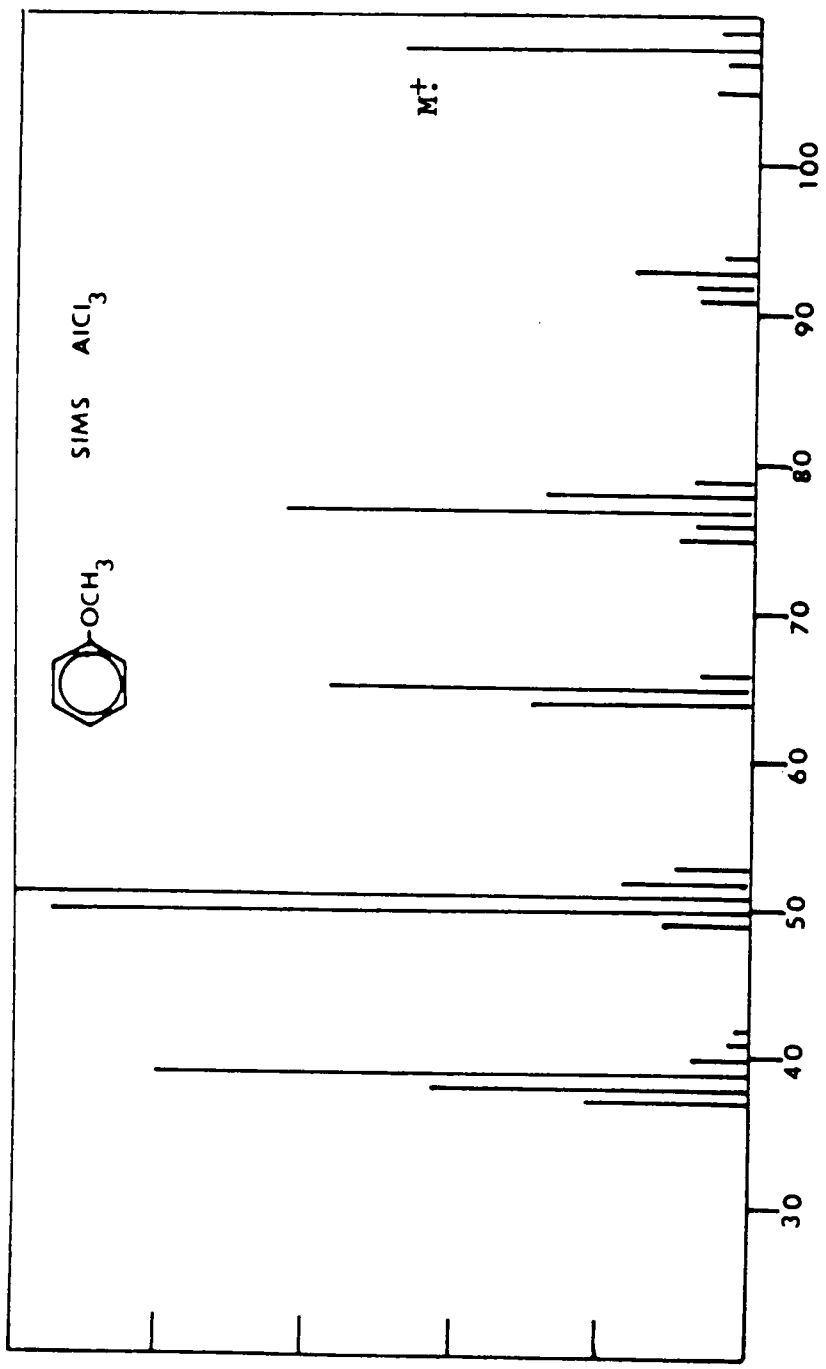


Figure 39. Positive SIMS spectrum of anisole obtained using $AlCl_3$ matrix. $AlCl_3$ characteristic ions have been subtracted from the spectrum.

$AlCl_3$/N-(1-butyl) pyridinium chloride (BPC) and $AlCl_3$/1-ethyl-3-methyl imidazolium chloride (EMIC) melts were used since some PAH's are soluble in these melts. As mentioned earlier, spontaneous oxidation of some polycyclic aromatic hydrocarbons has been reported in the 2:1 $AlCl_3$/BPC melt (92). A partial LSIMS spectrum obtained from a 2:1 $AlCl_3$/BPC melt is shown in Figure 40. The intense peaks observed at m/z 80 and 136 correspond to the pyridinium and butyl pyridinium cations, respectively. Ions arising from the non-specific fragmentation of the organic salt and its clusters result in the appearance of peaks of low relative abundance at every mass. The LSIMS spectrum of a 1.9:1 $AlCl_3$/EMIC melt is shown in Figure 41. The base peak in the spectrum observed at m/z 111 corresponds to the methyl-ethylimidazolium cation.

LSIMS spectra of solutions ca. 20 mole % naphthalene and pyrene in 2:1 $AlCl_3$/BPC melts are shown in Figures 42 and 43, respectively. Despite the high concentration of the PAH's, the molecular ions of naphthalene (observed at m/z 128, Figure 42) and pyrene (observed at m/z 202, Figure 43) constitute less than 20% of the total secondary ion current in their respective spectra. Naphthalene and pyrene are sparingly soluble in $AlCl_3$/EMIC melts. No ions characteristic of naphthalene or pyrene were observed from $AlCl_3$/EMIC solutions saturated with the respective PAH.

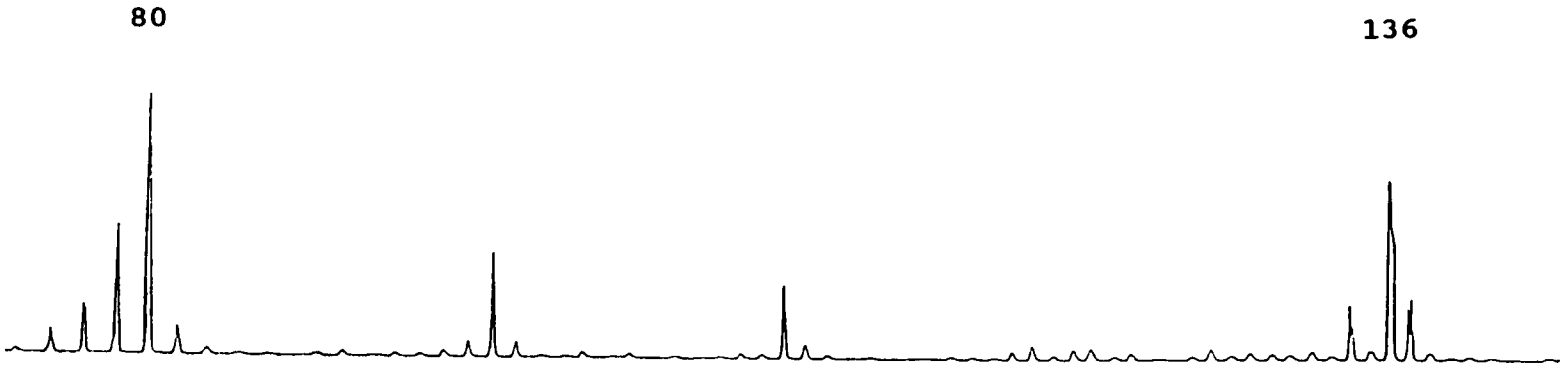


Figure 40. Partial SIMS spectrum of a 2:1 (mole ratio) $AlCl_3$/BPC melt in the region of m/z 76 - 141.

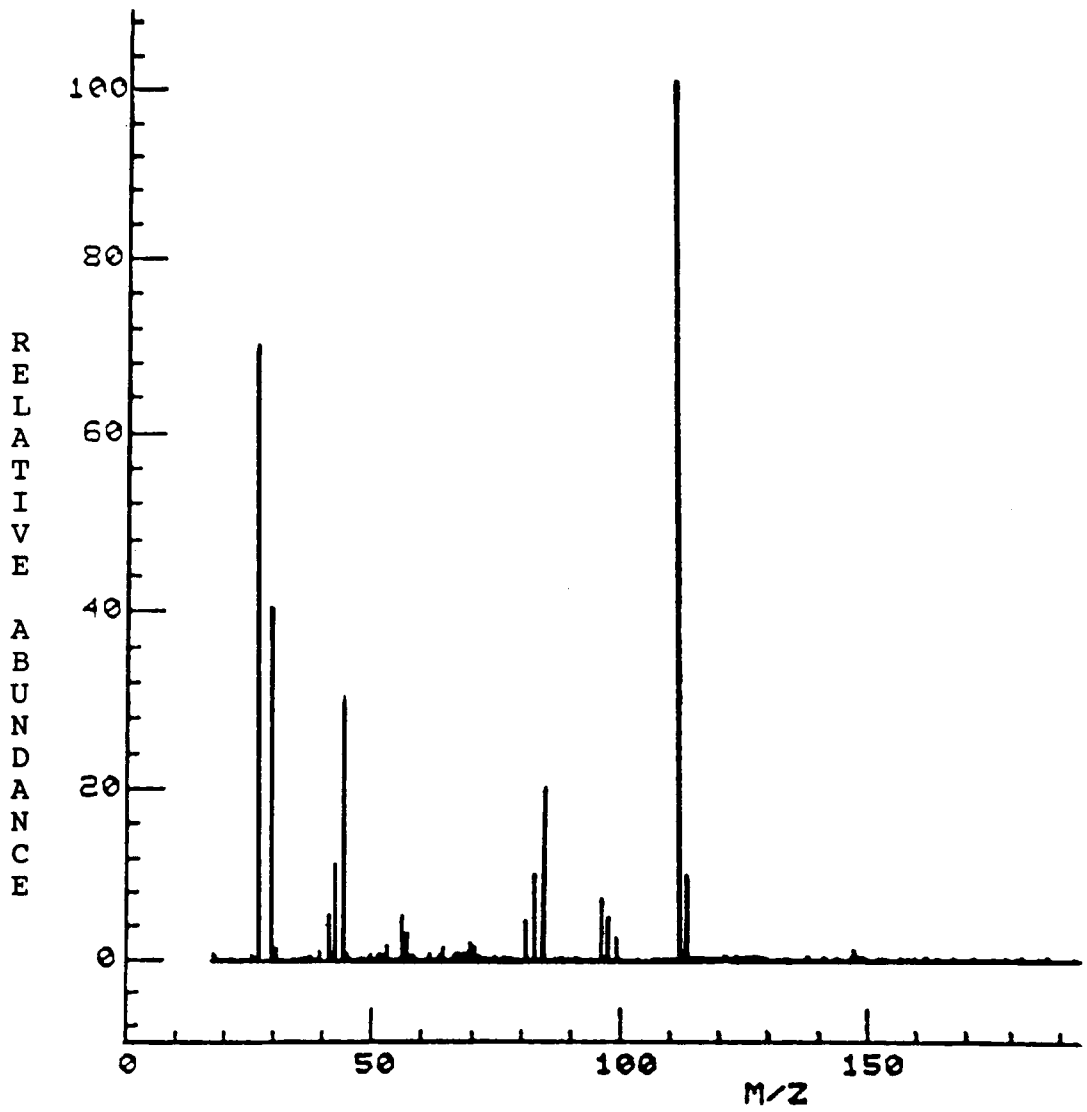


Figure 41. Positive SIMS spectrum of a 1.9/1 (mole ratio) $AlCl_3$/EMIC melt.

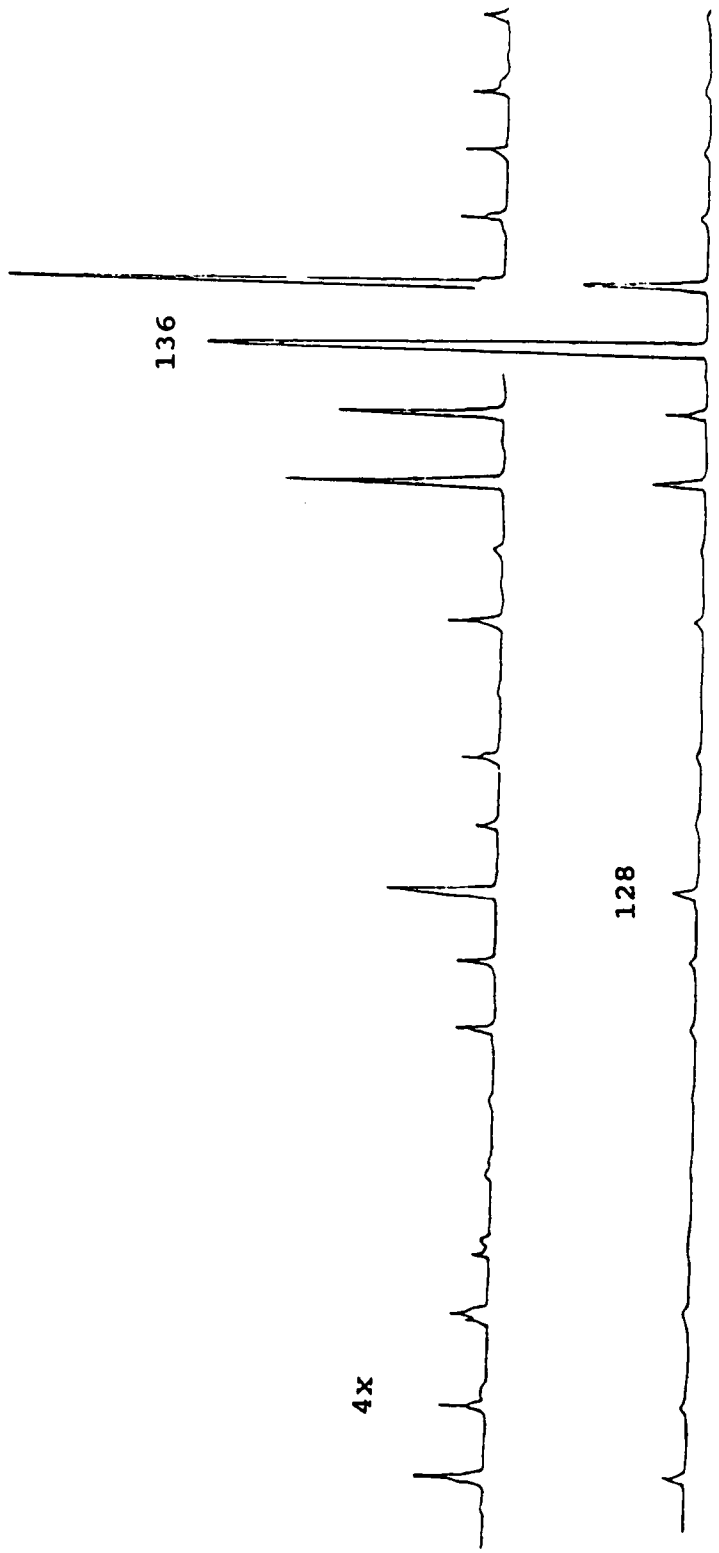


Figure 42. Partial SIMS spectrum of naphthalene//2:1 $AlCl_3$/BPC melt (ca. 20 mole % naphthalene) in the region of m/z 120 - 141.



Figure 43. Partial SIMS spectrum of pyrene//2:1 $AlCl_3$/BPC melt (ca. 20 mole % pyrene) in the region of m/z 130 - 207.

Several non-volatile liquids, listed in Table 6, were investigated as possible LSIMS matrices for PAH's. Stable SIMS spectra can be obtained from these neat liquids. Enhanced emission was not observed from PAH's dissolved in these solvents. The fraction of the total secondary ion current associated with the PAH's was approximately equal to the mole fraction of PAH in the sample. A variety of additives were used in an attempt to enhance the aromatic secondary ion yield. Addition of the additives, listed in Table 6, to each of the solvents listed in Table 6, failed to increase the fraction of the total secondary ion current associated with dissolved aromatics. The metal chlorides were either insoluble or reacted with the solvents.

Table 6.

Low Vapor Pressure Solvents and Additives Used

Solvent	Additive
2-Nitrophenyloctylether	$AlCl_3$
Dimethyl sulfoxide	$ZnCl_2$
Polyvinyl ether	$SbCl_3$
Polyphenyl ether (diffusion pump oil)	$SnCl_2$
	Benzoyl peroxide
Borate polyglycol ester (hydraulic fluid)	Tetracyanoquinodimethane
Glycerol	Trinitrophenol
1-Iodonaphthalene	I_2

CHAPTER IV

SUMMARY AND CONCLUSIONS

Secondary ion mass spectra of singly substituted aromatic/concentrated sulfuric acid solutions showed intense secondary ions characteristic of the dissolved aromatic compound. Sulfuric acid is a novel matrix which significantly enhances the emission of a number of aromatic compound classes. Enhanced secondary ion emission was observed for compound classes previously inaccessible to study by LSIMS. Substituents for which abundant secondary ion emission was observed include: ketones, aldehydes, carboxylic acids, nitriles, hydrocarbons, ethers, and nitrogen heterocycles. Many substituted aromatic compounds are soluble in concentrated sulfuric acid and these solutions are stable.

Abundant molecular ions and protonated molecules are observed simultaneously in LSIMS spectra of substituted aromatic/sulfuric acid solutions. The simultaneous abundance of secondary protonated aromatic molecules and aromatic molecular ions is a useful feature of LSIMS spectra of substituted aromatic/sulfuric acid solutions.
For most of the substituted aromatics investigated, the molecular ion to protonated molecule intensity ratio was characteristic of the analyte. Fragment ions reflected in LSIMS spectra of substituted aromatic/sulfuric acid

solutions could be related sensibly to gas phase fragmentations.

Spectra obtained from 1 to 2 μL samples were relatively free from chemical noise and the absolute and relative abundances of secondary ions were invariant for up to 30 minutes. Since secondary ion emission is intense and persistent, such solutions make it possible to obtain MS/MS spectra of selected species. Detection limits for some substituted aromatic compounds were estimated to be 10^{-12} moles.

The utility of sulfuric acid as a matrix for involatile, multifunctional aromatic compounds was demonstrated. LSIMS spectra of pterins were obtained from their sulfuric acid solutions. Pterins are involatile and virtually insoluble in common organic solvents. Enhanced secondary ion emission for substituted aromatics dissolved in H_2SO_4 appears to be general. LSIMS using sulfuric acid as a liquid matrix should be applicable to analysis of substituted aromatic compounds possessing substituents for which enhanced emission was observed.

The enhanced emission of both molecular ions and protonated molecules characteristic of dissolved analytes is consistent with the fact that the gas-phase-proton affinities of the conjugate bases of both ionic species are greater than the gas phase proton affinity of sulfuric acid. The intensities of molecular ion and the protonated molecule

observed in LSIMS spectra of substituted aromatic/sulfuric acid solutions are consistent with known condensed phase behavior. The $[M^{+\cdot}]/[(M+H)^+]$ intensity ratios which are observed appear to reflect the competition between substituent protonation and σ-complex formation. This behavior suggests that the precursors to molecular ions are the σ-complexes in solution whereas the precursors to the detected protonated secondary aromatic molecules were protonated on the substituent in solution.

Despite the fact that both sulfuric acid and acidic metal chlorides form σ-complexes with aromatic compounds, metal chlorides do not significantly enhance aromatic secondary molecular ion emission.

LIST OF REFERENCES

LIST OF REFERENCES

1. A. Benninghoven, F. G. Rudenauer, and H. W. Werner, in "Secondary Ion Mass Spectrometry: Basic Concepts, Instrumental Aspects, Application and Trends", John Wiley & Sons, New York, 1987.

2. M. Barber, R. S. Bordoli, G. J. Elliott, R. D. Sedgewick, and A. N. Tyler, Anal. Chem., 54, 645A (1982).

3. A. Aberth, in "Chemistry and Biology of Pteridines", W. Pfleiderer, Ed., Walter de Gruter, Berlin, 1975, p. 1.

4. M. R. Guerin and E. Baum, in "Polycyclic Hydrocarbons and Cancer", H. V. Gelboin, P. O. P. Ts'O, Eds., Academic Press, New York, 1978.

5. J. McCann, E. Choi, E. Yamaski, and B. N. Ames, Proc. Nat'l Acad. Sci. U. S. A. 1975, 72, 5135-5139.

6. M. L. Lee, M. V. Novotny, and K. D. Bartle, "Analytical Chemistry of Polycyclic Aromatic Hydrocarbons", Academic Press, New York, 1981.

7. M. A. Fox and S. Olive, Science, 205, 582 (1979).

8. B. Muel and S. Saguem, Int. J. Environ. Anal. Chem., 23, 135 (1985).

9. F. Valerio and A. Lazzarotto, Int. J. Environ. Anal. Chem., 23, 135 (1985).

10. T. L. Gibson, V. B. Smart, and L. L. Smith, Mutat. Res., 49, 153 (1978).

11. T. L. Gibson, P. E. Korsog, and G. T. Wolff, Atmos. Environ., 20, 1575 (1986).

12. T. Ramdahl, Environ. Sci. Technol., 17, 666 (1983).

13. N. Takeda, K. Teranishi, and K. Hamada, Bull. Environ. Contam. Toxicol., 33,410 (1984).

14. J. C. Nixon, in "Folates and Pterins", R. L. Blakely and S. J. Benkovic, Eds.; John Wiley & Sons, New York, (1985) pp. 1-42.

15. F. W. McLafferty, (Ed.) "Tandem Mass Spectrometry", Wiley Interscience, New York, 1983.

16. R. D. Macfarlane and D. F. Torgerson, Science, 191, 920 (1976).

17. M. A. Posthumus, P. G. Kistemaker, H. L. C. Muezelaar, and M. C. T. N. de Brauw, Anal. Chem., 50, 985 (1978).

18. R. J. Colton, D. A. Kidwell, G. O. Ramseyer, and M. M. Ross, in "Desorption Mass Specrtrometry. Are SIMS and FAB the Same?", P. A. Lyon, Ed., American Chemical Society, Washington, DC, 1985.

19. P. J. Todd, G. L. Glish, and W. H. Christie, Int. J. Mass Spectrom. Ion Processes, 61, 215 (1984).

20. M. Barber, R. S. Bordoli, R. D. Sedgwick, and A. N. Tyler, Nature, 293, 270 (1981).

21. A. Benninghoven, Z. Physik, 230, 403 (1970).

22. K. Wittmaack, J. Maul, and F. Schulz, Int. J. Mass Spectrom. Ion Phys., 11, 23 (1973).

23. C. W. Magee, W. L. Harrington, and R. E. Honig, Rev. Sci. Instr., 49, 477 (1978).

24. C. Fenselau, in "Ion Formation from Organic Solids", A. Benninghoven, Ed., Springer-Verlag, Berlin, (1983) p. 90.

25. E. Depauw, Mass Spectrom. Rev., 5, 191 (1986).

26. S. A. Carr, V. N. Reinhold, B. N. Green, and J. R. Hass, Biomed. Mass Spectrom., 12, 288 (1985).

27. M. Barber, R. S. Bordoli, G. J. Elliott, A. N. Tyler, J. Bill, and A. N. Green, Biomed. Mass Spectrom., 11, 182 (1984).

28. W. Aberth, K. M. Straub, A. L. Burlingame, Anal. Chem., 54, 2029 (1982).

29. C. Fenselau and R. J. Cotter, Chem. Rev., 87, 501 (1987).

30. J. L. Gower, Biomed. Mass Spectrom., 12, 191 (1985).

31. M. E. Rose, C. Longstaff, and P. D. G. Dean, Biomed. Mass Spectrom., 10, 512 (1983).

32. G. S. Groenewold and P. J. Todd, Anal. Chem., 57, 886 (1985).

33. A. Benninghoven, Int. J. Mass Spectrom. Ion Phys., 459 (1983).

34. K. Harada, M. Suzuki, and H. Kimbara, Org. Mass Spectrom., 17, 386 (1982).

35. J. A. Sunner, R. Kulatunga, and P. Kebarle, Anal. Chem., 58, 1312 (1986).

36. J. A. Sunner, R. Kulatunga, and P. Kebarle, Anal. Chem., 58, 2009 (1986).

37. A. Benninghoven, Int. J. Mass Spec. Ion Phys., 53, 85 (1983).

38. S. A. Martin, C. E. Costello, and K. Biemann, Anal. Chem., 54, 2362 (1982).

39. B. D. Musselman, J. T. Watson, and C. K. Chang, Org. Mass Spectrom., 21, 215 (1986).

40. T. Keough, Anal. Chem., 57, 2027 (1985).

41. B. D. Musselman, J. Allison, and J. T. Watson, Anal. Chem., 57, 2425 (1985).

42. K. L. Busch, S. E. Unger, A. Vincze, R. G. Cooks, and T. Keough, J. Am. Chem. Soc., 104, 1507 (1982).

43. E. Depauw, Anal. Chem., 55, 2195 (1983).

44. G. S. Groenewold, P. J. Todd and M. V. Buchanan, Anal. Chem., 56, 2251 (1984).

45. G. C. Didonato and K. L. Busch, Anal. Chim. Acta, 56, 2251 (1985).

46. J. Meili and J. Siebl, Org. Mass Spectrom., 19, 581 (1984).

47. W. Vetter and W. Meister, Org. Mass Spectrom., 20, 267 (1985).

48. R. Walder and J. L. Franklin, Int. J. Mass Spectrom. Ion Phys., 36, 82 (1980).

49. R. G. Cooks and K. L. Busch, Int. J. Mass Spectrom. Ion Processes, 53, 111 (1983).

50. K. L. Busch and R. G. Cooks, Science, 218, 247 (1982).

51. Q.-W. Huang, G.-L. Wu, and H.-T. Tang, Int. J. Mass Spectrom. Ion Processes, 70, 145 (1986).

52. G. Bojesen and J. Moller, Int. J. Mass Spectrom. Ion Processes, 68, 239 (1986).

53. A. M. Fallick, F. C. Walls, and R. A. Laine, Anal. Biochem., 159, 132 (1986).

54. R. D. Grigsby, S. E. Scheppele, Q. G. Grindstaff, G. P. Sturm, Jr., L. C. E. Taylor, H. Tudge, C. Wakefield, and S. Evans, Anal. Chem., 54, 1108 (1982).

55. G. Dube, Org. Mass Spectrom., 19, 242 (1984).

56. F. H. Field, J. Phys. Chem., 86, 5115 (1982).

57. M. A. Rudat and C. N. McEwen, Int. J. Mass Spectrom. Ion Phys., 46, 351 (1983).

58. D. E. Smith and B. J. Munson, J. Am. Chem. Soc., 100, 497 (1978).

59. R. Walder and J. L. Franklin, Int. J. Mass Spectrom. Ion Phys., 36, 85 (1980).

60. R. J. Gillespie, E. D. Hughes, and C. K. Ingold, J. Chem. Soc., 2473 (1950).

61. M. S. Newman and N. C. Deno, J. Am. Chem. Soc., 73, 3651 (1951).

62. M. Liler, "Reaction Mechanisms in Sulfuric Acid and Other Strong Acid Solutions", Academic Press, London, 1967.

63. W. H. Lee, in "The Chemistry of Non-Aqueous Solvents Volume II", J. J. Lagowski, Ed., Academic Press, New York, 1967, pp. 129-138.

64. W. J. Roedel, J. Aerosol Sci., 10, 375 (1979).

65. H. K. Cammenga, F. W. Schultze, W. Thuerl, J. Chem. Eng. Data, 22, 131 (1977).

66. O. T. Fasullo, "Sulfuric Acid", McGraw-Hill, New York, 1965, pp. 51-68.

67. R. J. Gillespie and R. F. M. White, Trans. Faraday Soc., 54, 1846 (1958).

68. W. J. Moore, "Physical Chemistry", Prentice-Hall, Englewood Cliffs, N. J., 1962, pp. 332-333.

69. J. C. D. Brand, A. W. P. Jarvie, and W. C. J. Horning, J.Chem. Soc., 3844 (1959).

70. M. M. Ross and R. J. Colton, Anal. Chem., 55, 150 (1983).

71. M. M. Ross and R. J. Colton, Anal. Chem., 55, 1170 (1983).

72. R. J. Day, S. E. Unger, and R. G. Cooks, Anal. Chem., 52, 557A (1980).

73. H. Grade and R. G. Cooks, J. Am. Chem. Soc., 100, 5615 (1978).

74. R. B. Freas and J. E. Campana, Inorg. Chem., 23, 4654 (1984).

75. R. J. Gillespie and J. V. Oubridge, J. Chem. Soc ., 2804 (1959).

76. V. Gold and J. Tye, J. Chem. Soc., 2173 (1952).

77. H. Kon and M. S. Blois, Jr., J. Chem. Phys., 23, 743 (1958).

78. W. I. Aalbersberg, G. J. Hoijtink, E. L. Mackor, and W. P. Weijland, J. Chem. Soc., 3049 (1959).

79. C. T. Davis and T. A. Geissman, J. Amer. Chem. Soc., 76, 3507 (1954).

80. H. Cerfontain, H. J. A. Lambrechts, Z. R. H. Schaasberg-Nienhuis, H. Coombes, P. Hadjigeorgiou, and G. P. Tucker, J. Chem. Soc. Perkin Trans. 2, 659 (1985).

81. C. Ris and H. Cerfontain, J. Chem. Soc. Perkin Trans. 2, 1438 (1975).

82. H. J. A. Lambrechts, J. Mul, and H. Cerfontain, J. Chem. Soc. Perkin Trans. 2, 677 (1985).

83. S. I. Weissman, E. DeBoer, and J. J. Conradi, J. Chem. Phys., 26, 963 (1956).

84. A. Carrington, F. Dravieko, and M. C. R. Symons, J. Chem. Soc., 947 (1959).

85. P. D. Sullivan, I. J. Ocasio, X. Chen, and F. Bannoura, J. Am. Chem. Soc., 108, 257 (1986).

86. R. Stewart and K. Yates, J. Am. Chem. Soc., 82, 4059 (1960).

87. R. Stewart, "The Proton: Application to Organic Chemistry", Academic Press, Orlando, Fl., 1985.

88. R. J. Gillespie and J. A. Leisten, Quart. Rev. Chem. Soc., 8, 40 (1954).

89. H. Cerfontain, "Mechanistic Aspects of Aromatic Sulfonation and Sulfation", Wiley Interscience, New York (1968).

90. G.W. Wheland, J. Am. Chem. Soc., 64, 900 (1942).

91. H. Bock and W. Kain, Acc. Chem. Res., 15, 9 (1982).

92. J. Robinson and R. A. Osteryoung, J. Am. Chem. Soc., 101, 323 (1979).

93. J. S. Wilkes, J. A. Levisky, R. A. Wilson, and C. L. Hussey, Inorg. Chem., 21, 1263 (1982).

94. C. L. Hussey, In "Advances in Molten Salt Chemistry, vol. 5", G. Mamantov, Ed., Elsevier Science Publishing Co., Amsterdam, 1983, pp. 185-230.

95. B. L. Ackerman, A. Tsarbopoulos, and J. Allison, Anal. Chem., 57, 1766 (1985).

96. T. Kuster and A. Niederwieser, J. Chromatogr., 278, 245 (1983).

97. P. Haug, Anal. Biochem., 37, 285 (1970).

98. P. Haug and T. Urushibara, Org. Mass Spec., 3, 1365 (1969).

99. S. Mazumdar, C. Redmond, W. Sollectio, and N. Sussman, J. Air Pollut.Control Assoc., 25, 382 (1975).

100. R. J. Sexton, Arch. Environ. Health, 1, 208 (1960).

101. D. F. S. Natusch, Environ. Health Perspect., 22, 78 (1978).

102. L. DeMaio and M. Corn, J. Air Pollut. Control Assoc., 16, 67 (1966).

103. R. C. Pierce and M. Katz, Environ. Sci. Technol., 9, 347 (1975).

104. E. Esmen and M. Corn, Atmos. Environ., 5, 571 (1971).

105. D. A. Lane and M. Katz, in "Fate of Pollutants in the Air and Water Environments", I. H. Suffet, Ed., Wiley Interscience, New York, Part 2, 1977, p. 137.

106. D. A. Saucy, G. E. Cabaniss, and R. W. Linton, Anal. Chem., 57, 876 (1985).

107. J. M. Benson, A. L. Brooks, Y. S. Cheng, T. R. Henderson, and J. E. White, Atmos. Environ., 19, 1169 (1985).

108. J. F. Thomas, M. Mukai, and B. D. Tebbens, Environ. Sci. Technol., 2, 33 (1968).

109. R. A. Yokley, A. A. Garrison, E. L. Wehry, and G. Mamantov, Environ. Sci. Technol., 20, 86 (1986).

110. K. Nikolaou, P. Masclet, and G. Mouvier, Sci. Total Environ., 32, 103 (1984).

111. G. A. Eiceman and W. J. Vandiver, Atmos. Environ., 17, 461 (1983).

112. E. Denoyer, T. Mauney, D. F. S. Natusch, and F. Adams, in "Microbeam Analysis", K. F. J. Heinrich, Ed., San Francisco Press: San Francisco, 1982, p. 191.

113. M. Menzinger and L. Wahlin, Rev. Sci. Instrum., 40, 102 (1969).

114. W. H. Christie, D. H. Smith, H. S. McKown, and G. R. Hertel, Int. J. Mass Spectrom. Ion Phys., 8, 311 (1972).

115. P. J. Todd and G. S. Groenewald, Anal. Chem., 58, 895 (1986).

116. R. J. Gillespie, T. E. Peel, and E. A. Robinson, J. Am. Chem. Soc., 93, 5083 (1971).

117. R. Flowers, R. J. Gillespie, and J. V. Oubridge, J. Chem. Soc., 80, 1925 (1956).

118. R. A. Yokley, Ph. D. Dissertation, University of Tennessee, Knoxville (1985).

119. R. A. Carpio, L. A. King, R. E. Lindstrom, J. C. Nardi and C. L. Hussey, J. Electrochem. Soc., 101, 3776 (1979).

120. H. E. Darling, J. Chem. Eng. Data, 9, 421 (1964).

121. F. McLafferty, "Interpretation of Mass Spectra," University Science Books, Mill Valley, Ca., (1980).

122. A. C. Buchanan, A. S. Dworkin, and G. P. Smith, J. Org. Chem., 46, 471 (1981).

123. H. Cerfontain, A. W. Kaandorp, and F. L. J. Sixma, Rec. Trav. Chem., 82, 565 (1963).

124. M. Liler and D. Kosanovic, J. Chem. Soc., 2542 (1950).

125. R. J. Gillespie, J. Chem. Soc., 2542 (1950).

126. J. C. D. Brand, W. C. Horning, M. B. Thornley, J. Chem. Soc., 1374 (1952).

127. W. Ligon and S. B. Dorn, Int. J. Mass Spectrom. Ion Proc., 57, 74 (1984).

128. A. Streitwieser, Jr., "Molecular Orbital Theory for Organic Chemists", Wiley Interscience, New York (1961).

129. P. J. Todd; Surface Concentration in Liquid SIMS; Presented at the 35th ASMS Conference on Mass Spectrometry and Allied Topics, Denver, Colorado, May 24-29, 1987.

130. D. H. Aue and M. T. Bowers, in "Gas Phase Ion Chemistry, Vol. 2", Academic Press, Orlando,Fl., 1979.

131. H. M. Rosenstock, K. Draxl, B. W. Steiner, and J. T. Herron, J. Chem. Phys. Ref. Data, 6, Suppl. No. 1. (1977).

132. D. R. Stull and H. Prophet, (Eds.), JANAF Thermochem. Tables, Nat. Stand. Ref. Data Ser. National Bureau of Standards NSR DS-NBS 37, U. S. Govt. Print. Off., Washington, DC. (1971).

133. M. Karni and A. Mandelbaum, Org. Mass Spectrom., 15, 53 (1980).

134. N. J. Turro, "Modern Molecular Photochemistry", Benjamin/Cummings, New York (1978).

135. L. P. Hammett and A. J. Deyrup, J. Amer. Chem. Soc., 54, 2721 (1932).

136. H. J. Chen, L. E. Hakka, R. L. Hinman, A. J. Kresge and E. B. Whipple, J. Amer. Chem Soc., 93, 5102 (1971).

137. M. T. Reagan, J. Amer. Chem. Soc., 91, 5506 (1969).

138. R. Foster, "Organic Charge-Transfer Complexes", Academic Press, London (1969).

139. A. C. Buchanan, III, R. Livingston, A. S. Dworkin, and G. P. Smith, J. Phys. Chem., 84, 423 (1980).

140. W. I. Aalbersberg, G. J. Hoijtink, E. L. Mackor, and W. P. Weijland, J. Chem. Soc., 3055 (1959).

141. R. C. Weast, (Ed.), "Handbook of Chemistry and Physics, 64th Edition", CRC press: Boca Raton, Florida, p. D162 (195).

APPENDICES

APPENDIX A

REAGENTS AND REFERENCE COMPOUNDS

Reagent	Purity	Supplier[a]
Sulfuric Acid	98 wt. %	Mallinckrodt
Oleum (30% SO_3)	AR[b]	Fisher Scientific
Boric Acid	AR	Aldrich
Glycerol	99.5%	Aldrich
2-Nitrophenyl octyl ether	>99%	Fluka
Dimethyl sulfoxide	AR	Eastman Kodak
Polyvinyl ether	AR	Aldrich
Polyphenyl ether (diffusion pump oil)	-	Monsanto
Borate polyglycol ester (hydraulic fluid)	-	Olin Chemicals
1-Iodonaphthalene	AR	Aldrich
$ZnCl_2$	99.99%	Aldrich
$SnCl_2$	99.99%	Aldrich
$BiCl_3$	99.99%	Aldrich
$HgCl_2$	AR	Fisher Scientific
$ZnCl_2$	AR	Fisher Scientific
$TeCl_4$	99.99%	Aldrich
$InCl_3$	99.99%	Aldrich
$PbCl_3$	99.99%	Aldrich
$SbCl_5$	AR	Aldrich
$SnCl_2$	99.99%	Aldrich
$SnCl_4$	99.99%	Aldrich

APPENDIX A (continued.)

Reagent	Purity	Supplier
Benzoyl peroxide	AR	EM Science
I_2	AR	Mallinckrodt
Tetracyanoquinodimethane	98%	Aldrich
2,4,6-trinitrophenol	AR	Aldrich
NaI	AR	Mallinkcrodt
NH_4HSO_4	AR	Fischer Scientific

Reference Compound	Purity	Supplier
phenazine	98%	Fluka
dibenz(a,j)acridine	98%	Sigma
benzo(a)pyrene-6-ol	-	Alfred Bader
benzoic acid	99%	Aldrich
2-acetonaphthone	99%	Aldrich
2-naphthalenecarboxaldehyde	98%	Aldrich
9-anthracenecarboxaldehyde	97%	Aldrich
1-pyrenecarboxaldehyde	98%	Aldrich
2-naphthoic acid	99%	Aldrich
9-anthracenecarboxylic acid	98%	Aldrich
1-naphthol	99%	Aldrich
2-methoxynaphthalene	99%	Aldrich
dihydroanthracene	97%	Aldrich
9-methylanthracene	95%	Aldrich
2-t-butylanthracene	98%	Aldrich
9-phenylanthracene	98%	Aldrich

APPENDIX A (continued.)

Reference Compound	Purity	Supplier
9-anthracenecarbonitrile	97%	Aldrich
9-phenanthrenecarbonitrile	97%	Aldrich
3-methylindole	98%	Aldrich
carbazole	99%	Aldrich
benzo(c)cinnoline	99%	Aldrich
1-aminoanthracene	90%	Aldrich
9-aminophenanthrene	96%	Aldrich
9-phenanthrol	Technical	Aldrich
9-oxodihydroanthracene	AR	Aldrich
1,9-benzanth-7-one	Technical	Aldrich
9-phenanthrenecarboxaldehyde	Technical	Aldrich
6-benzo(a)pyrenecarboxaldehyde	-	Alfred Bader
acridine	AR	Aldrich
1-naphthalenecarbonitrile	Technical	Aldrich
2-nitronaphthalene	99%	Aldrich
1-chloroanthracene	99%	Aldrich
benzene	AR	Aldrich
aniline	99%	Fisher
anisole	99%	Fisher
pyrene	99%	Aldrich
naphthalene	98%	Aldrich
anthracene	98%	Aldrich
perylene	99%	Aldrich
anthraquinone	97%	Aldrich

APPENDIX A (continued.)

All the pterins used in this investigation were obtained from Bruce Jacobson (Oak Ridge National Laboratory).

a Supplier Addresses

Aldrich Chemical Co.
Milwaukee, Wisconsin

Eastman Kodak Chemical Co.
Rochester, New York

EM Science
Gibbstown, New Jersey

Fisher Scientific
Fair Lawn, New Jersey

Fluka Chemical Co.
Hauppage, New York

Mallinckrodt, Inc.
Paris, Kentucky

Olin Corporation
Stamford, Connecticut

b AR - Analytical Reagent Grade

APPENDIX B.

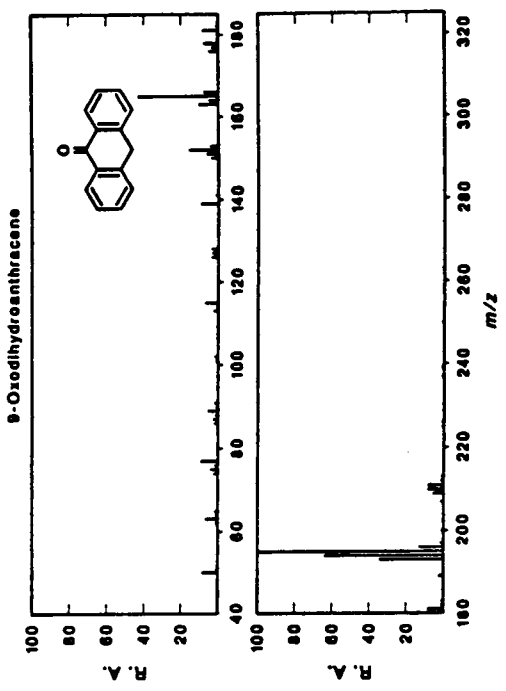
Compound Nominal Mass, $[M^{+\cdot}]/[(M+H)^+]$, and LSIMS Spectra of the Substituted Aromatic Hydrocarbons Investigated.

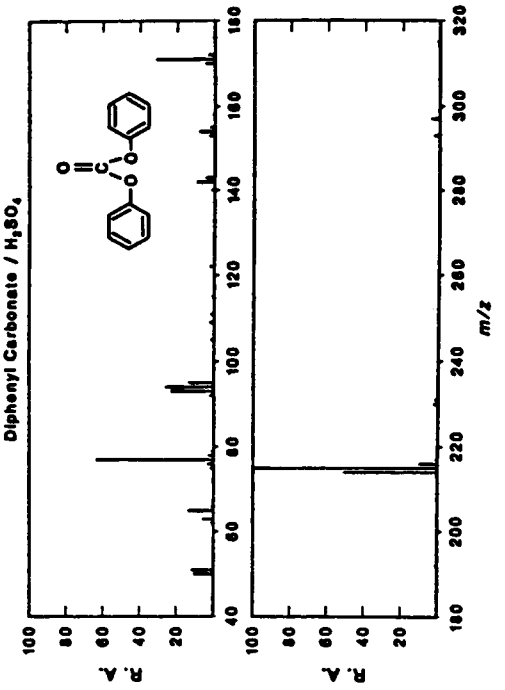
Compound	Nominal Mass	$[M^{+\cdot}]/[M+H^+]$[a], %
2-acetonaphthone	170	41
9-oxodihydroanthracene	194	59
1,9-benzanthr-7-one	230	26
diphenyl carbonate	214	54
2-naphthalenecarboxaldehyde	156	49
9-phenanthrenecarboxaldehyde	206	55
9-anthracenecarboxaldehyde	206	61
1-pyrenecarboxaldehyde	230	97
6-benzo(a)pyrene-carboxaldehyde	280	100
benzoic acid	122	26
2-naphthoic acid	172	140
9-anthracene carboxylic acid	222	395
1-naphthol	144	22
9-phenanthrol	194	62
benzo(a)pyrene-6-ol	268	483
2-methoxynaphthalene	158	68
dihydroanthracene	180	-
9-methylanthracene	192	100
2-t-butylanthracene	234	64
9-phenylanthracene	254	71
1-naphthalenecarbonitrile	153	125
9-phenanthrenecarbonitrile	203	192
9-anthracenecarbonitrile	203	429

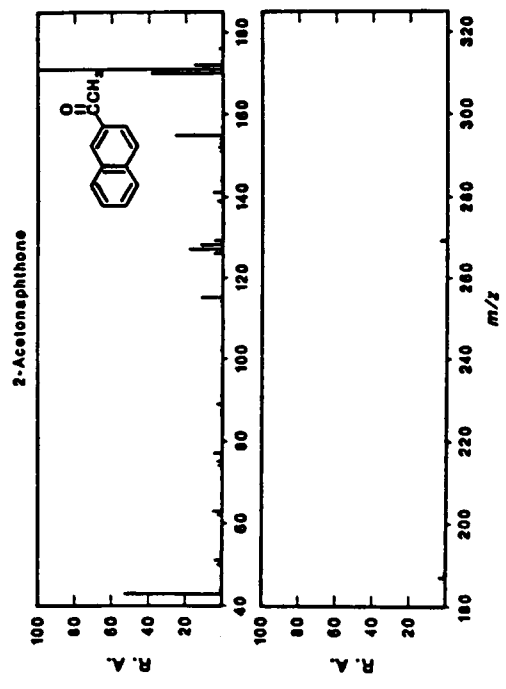
Appendix B (continued).

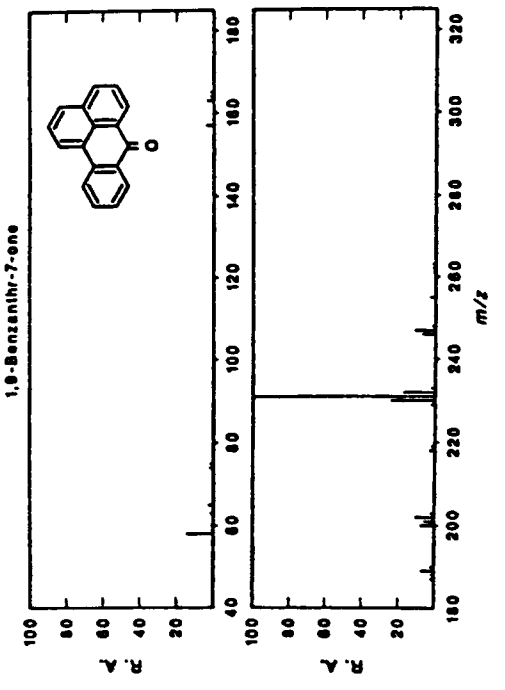
Compound	Nominal Mass	$[M^{+\cdot}]/[M+H^+]$[a], %
3-methylindole	131	20
carbazole	167	157
acridine	179	35
phenazine	180	14
benzo(c)cinnoline	180	10
dibenz(a,j)acridine	279	35
1-aminoanthracene	193	b
9-aminophenanthrene	193	b
1-aminopyrene	217	b
1-nitronaphthalene	173	99
1-nitroanthracene	223	15
3-nitropyrene	247	20
3-nitroperylene	297	66
1-chloroanthracene	212	1700[c]

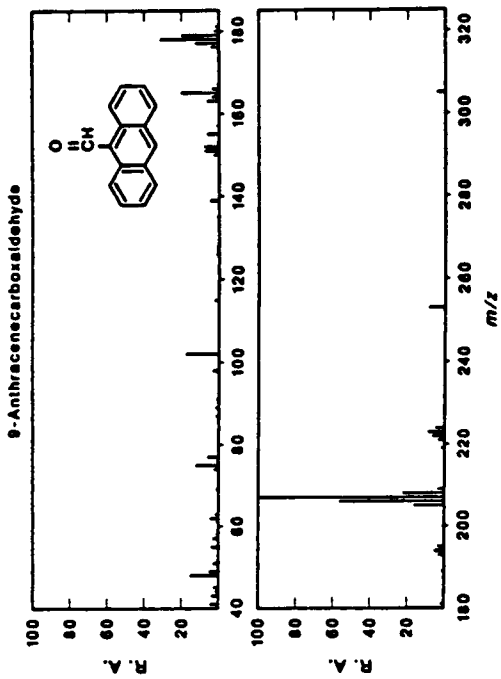
a Corrected for ^{13}C contribution from $M^{+\cdot}$.
b Intensity is time-dependent
c Intensities from ions containing ^{35}Cl and ^{37}Cl are summed.

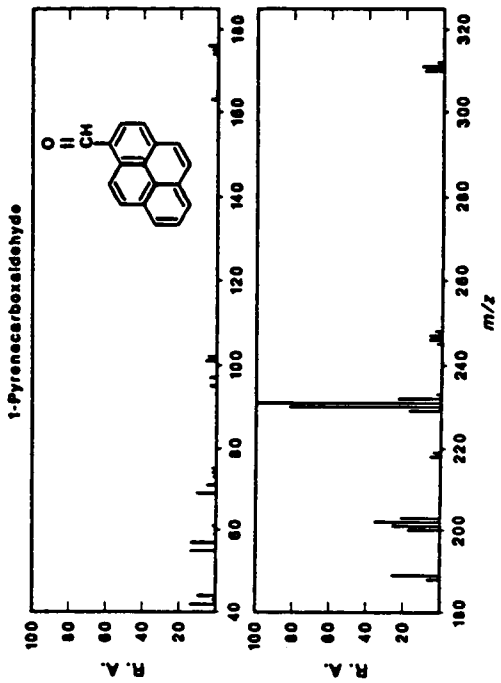

9-Oxodihydroanthracene
R. A.
m/z

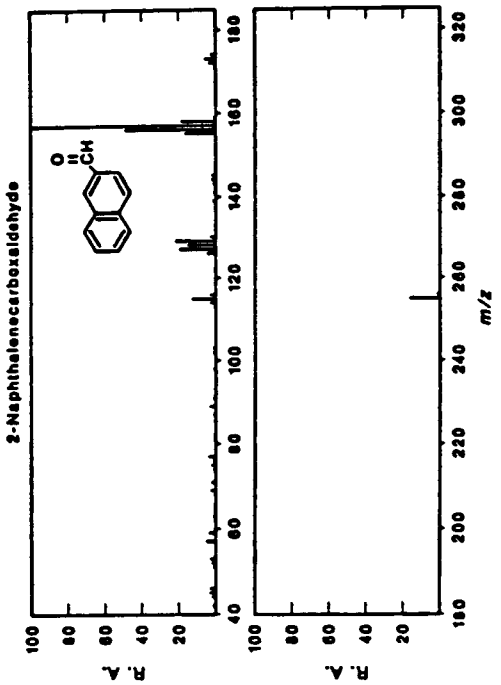

Diphenyl Carbonate / H_2SO_4
R. A.
m/z

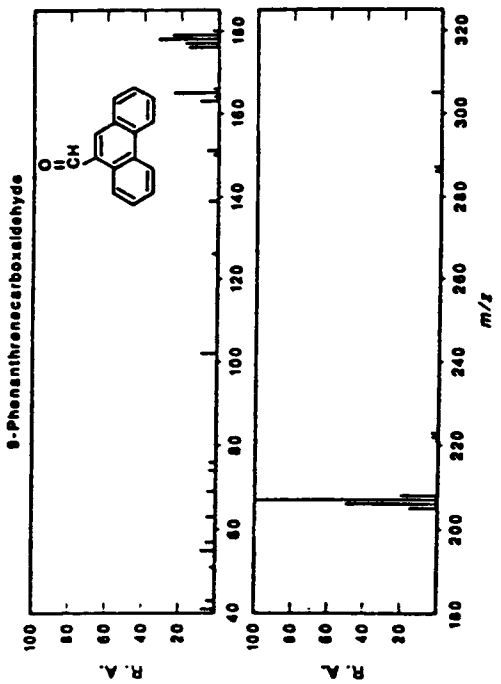

2-Acetonaphthone
R. A.
m/z

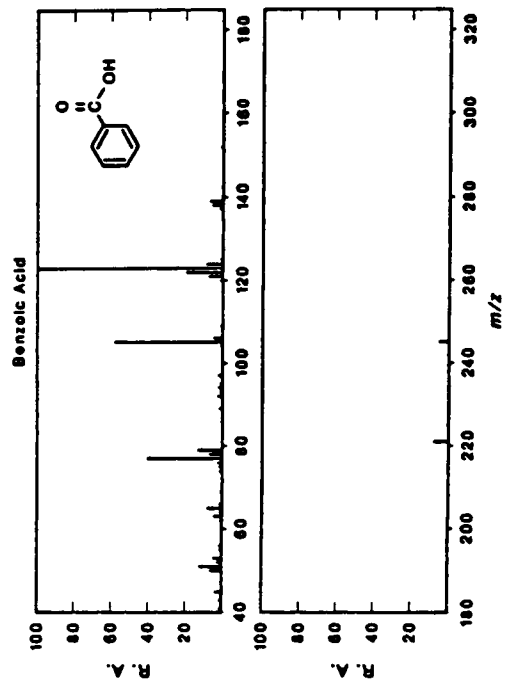

1,9-Benzanthr-7-one
R. A.
m/z

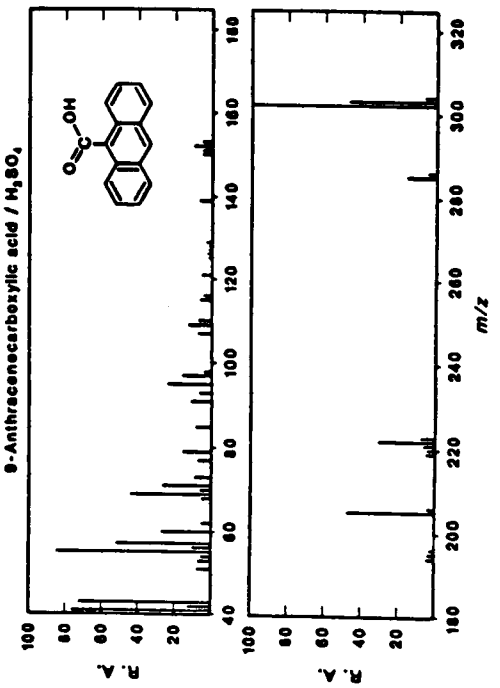

9-Anthracenecarboxaldehyde
R. A.
m/z

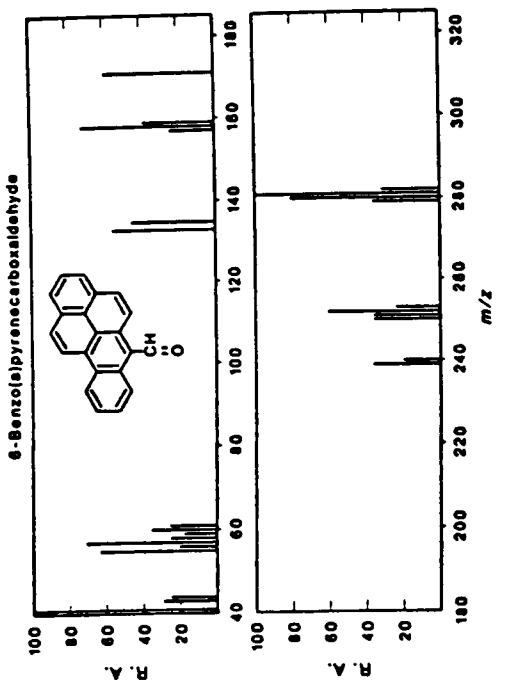

1-Pyrenecarboxaldehyde
R. A.
m/z

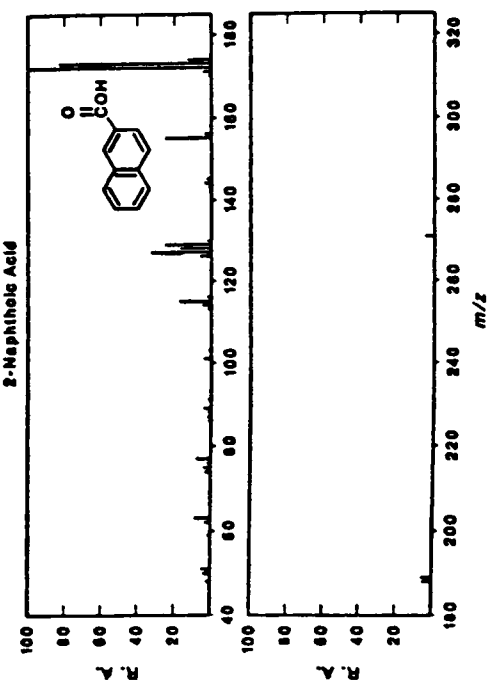

2-Naphthalenecarboxaldehyde
R. A.
m/z

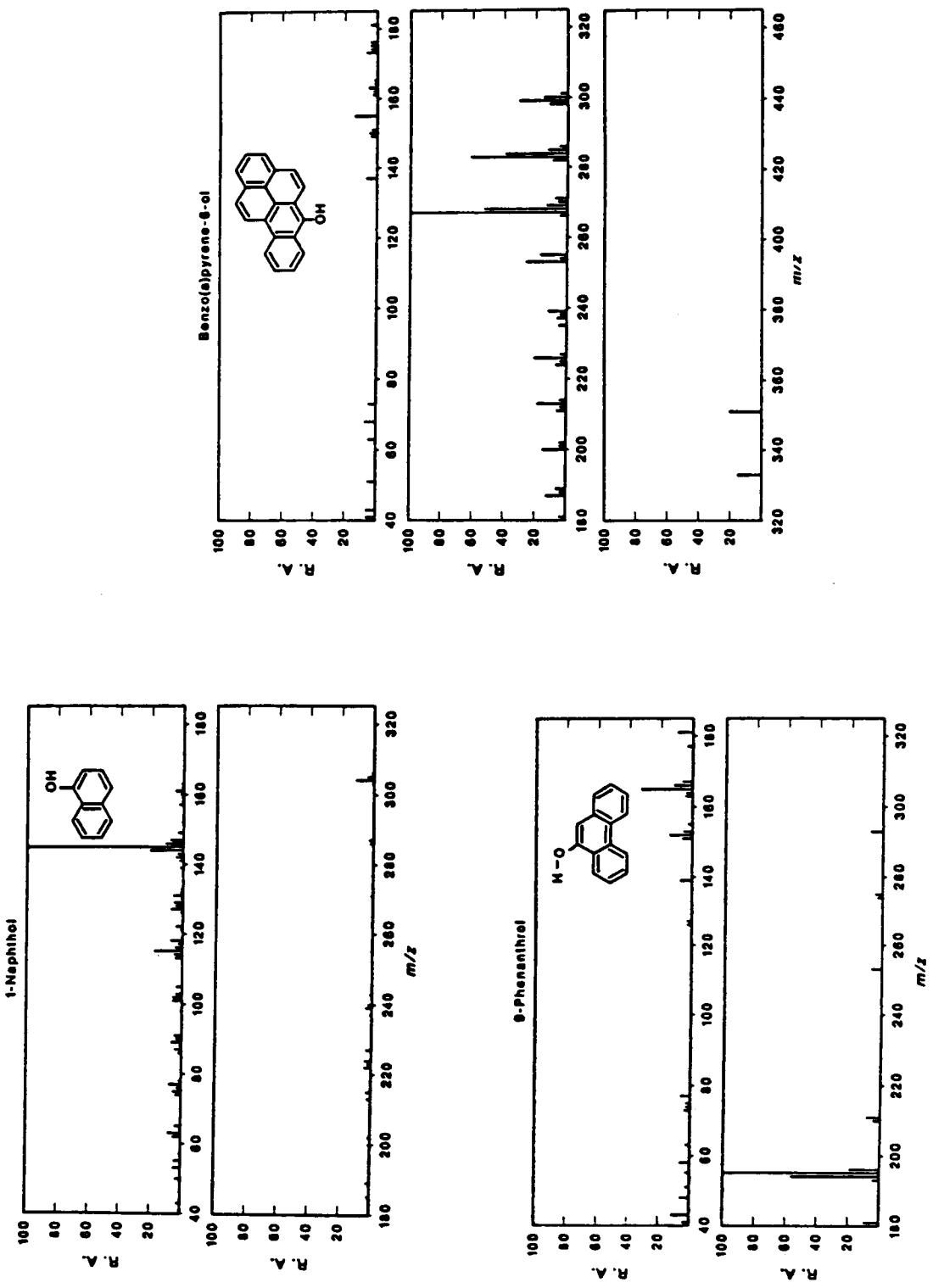

9-Phenanthrenecarboxaldehyde
R. A.
m/z

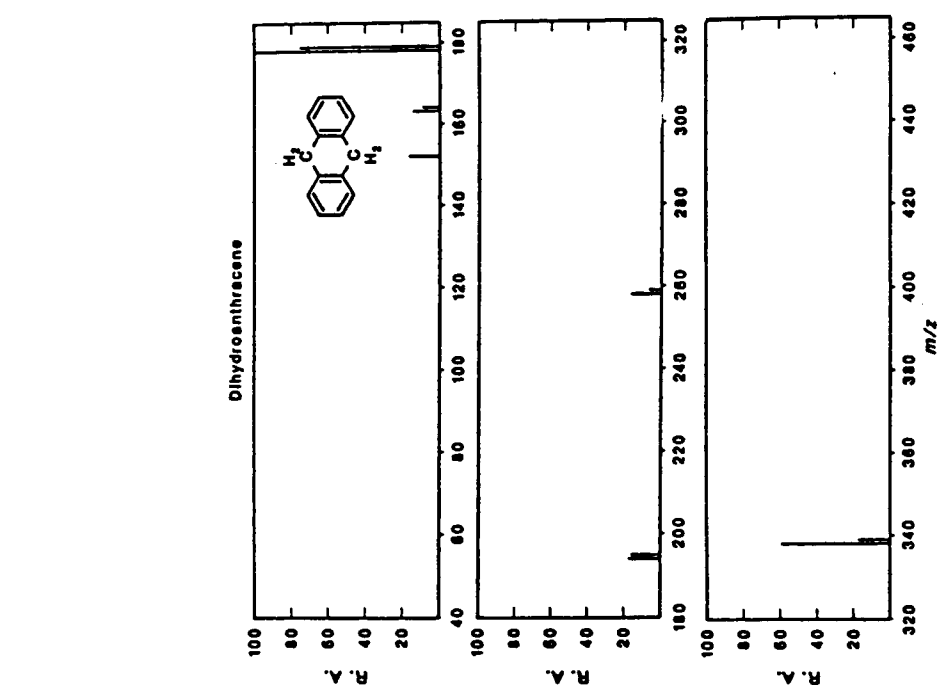

Benzoic Acid
R. A.
m/z

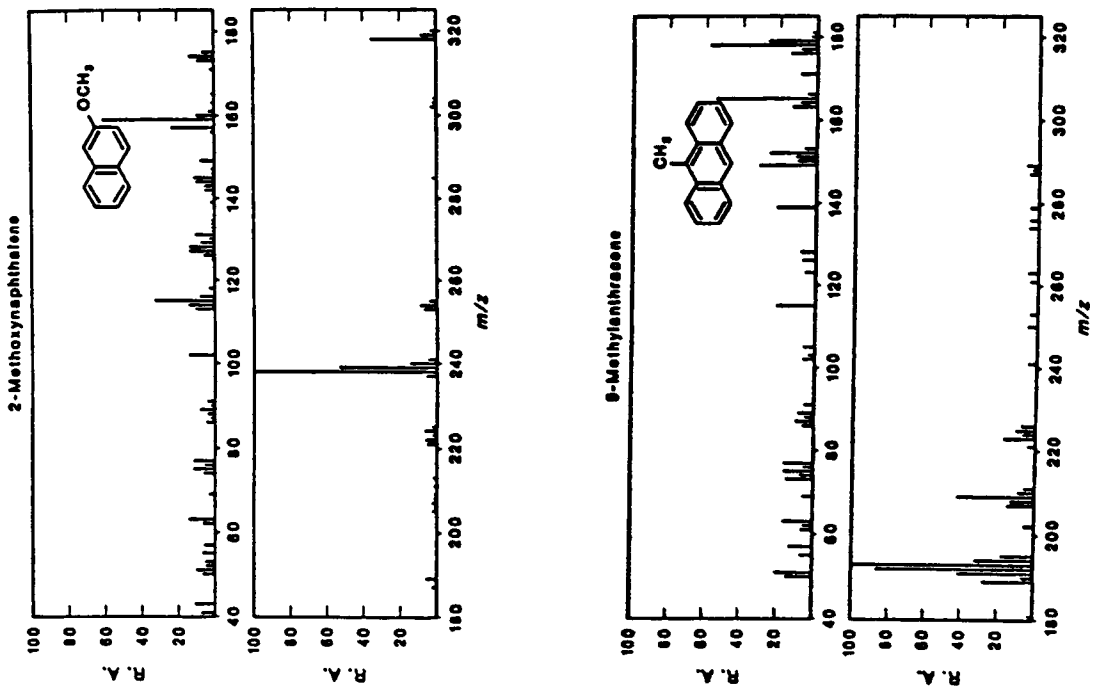

9-Anthracenecarboxylic acid / H_2SO_4
R. A.
m/z

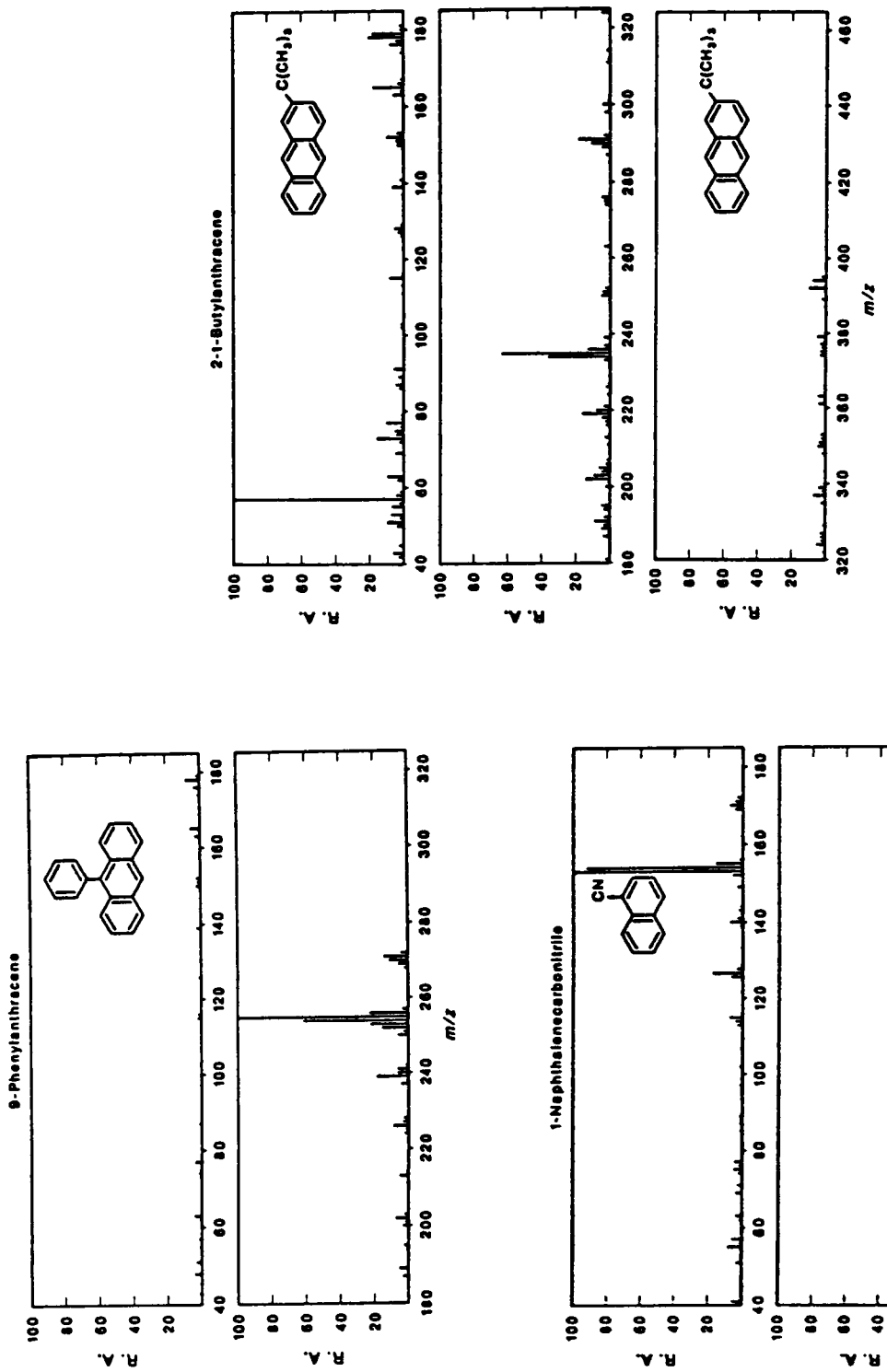

6-Benzo(a)pyrenecarboxaldehyde
R. A.
m/z

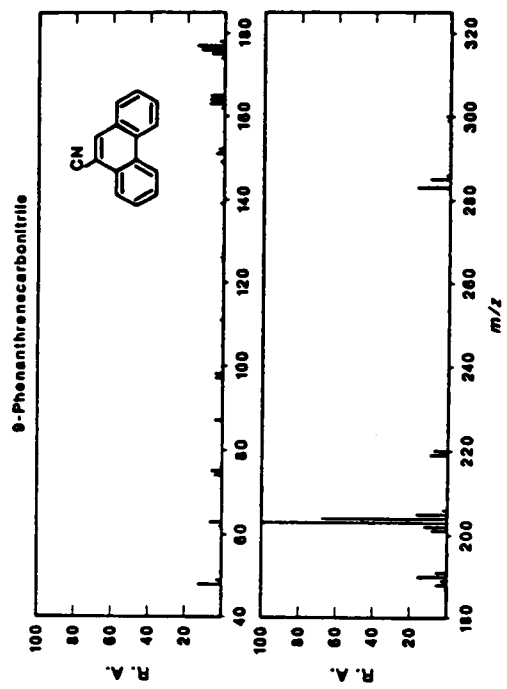

2-Naphthoic Acid
R. A.
m/z

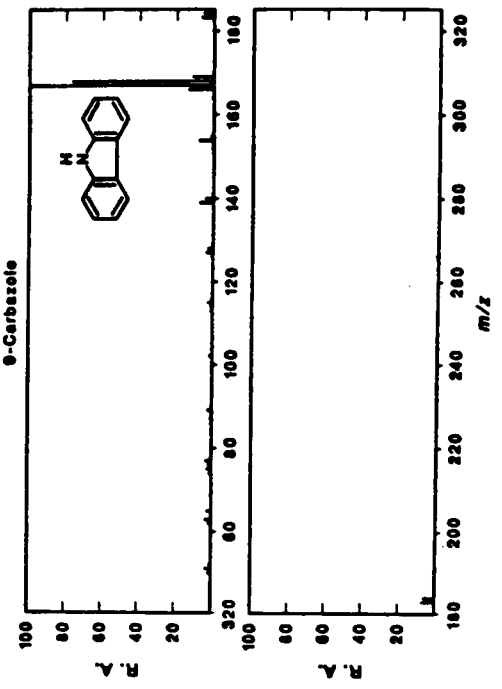

Benzo(a)pyrene-6-ol
1-Naphthol
9-Phenanthrol
R. A.
m/z

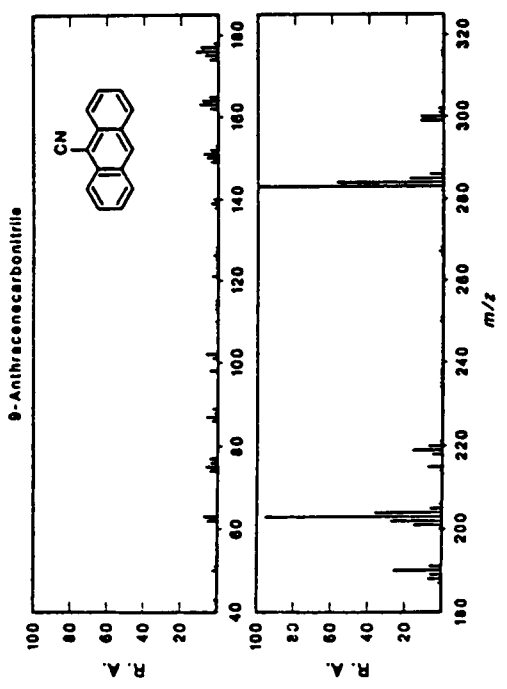

Dihydroanthracene
R. A.
m/z

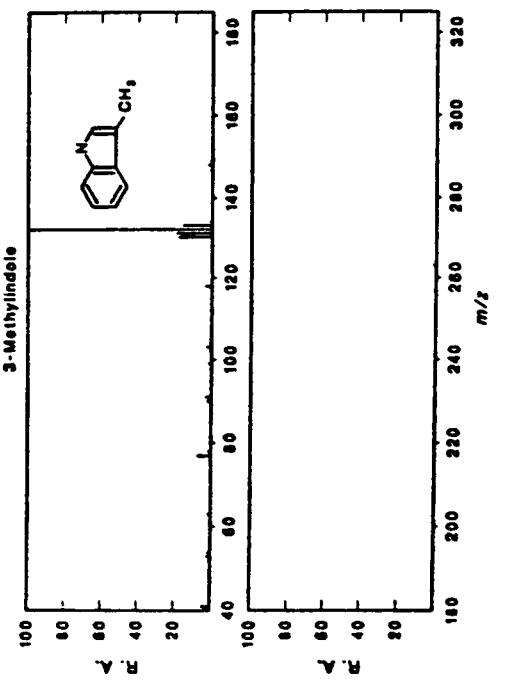

2-Methoxynaphthalene
9-Methylanthracene
R. A.
m/z

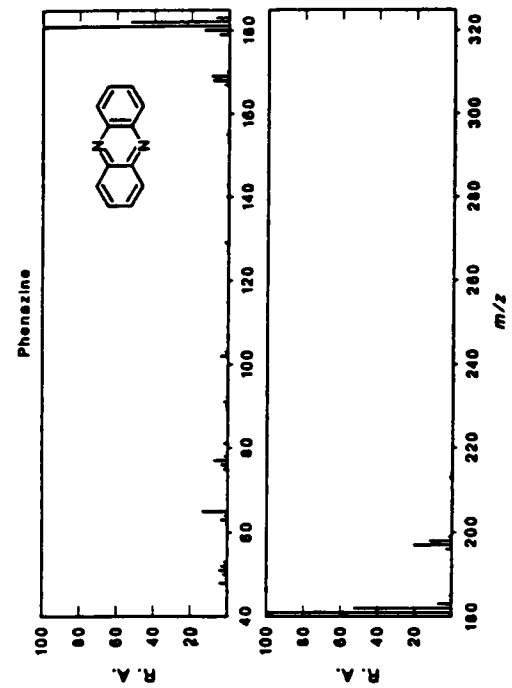

9-Phenylanthracene
2-t-Butylanthracene
1-Naphthalenecarbonitrile
R. A.
m/z

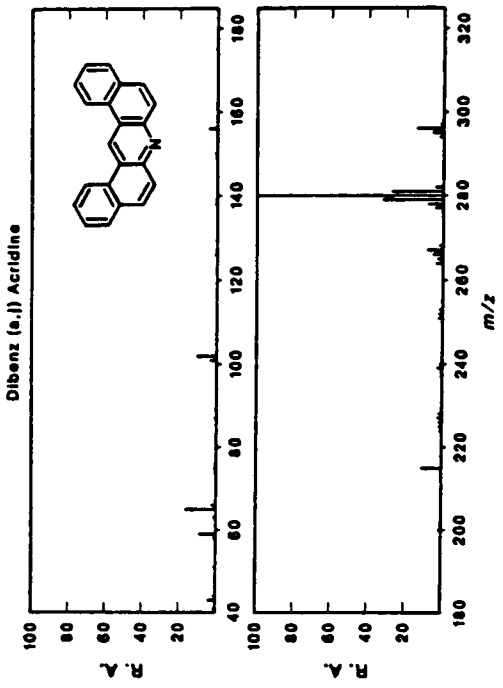

9-Phenanthrenecarbonitrile
CN
R. A.
m/z

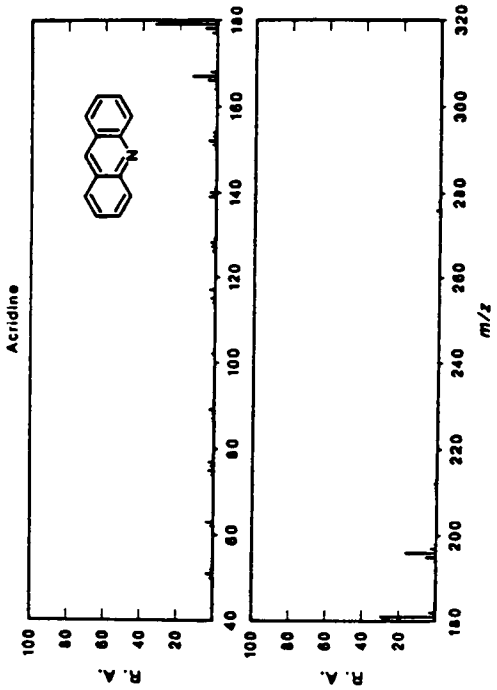

9-Carbazole
H
N
R. A.
m/z

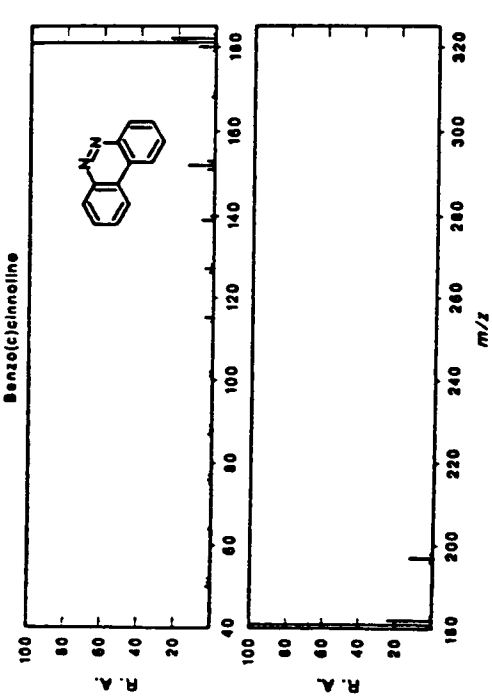

9-Anthracenecarbonitrile
CN
R. A.
m/z

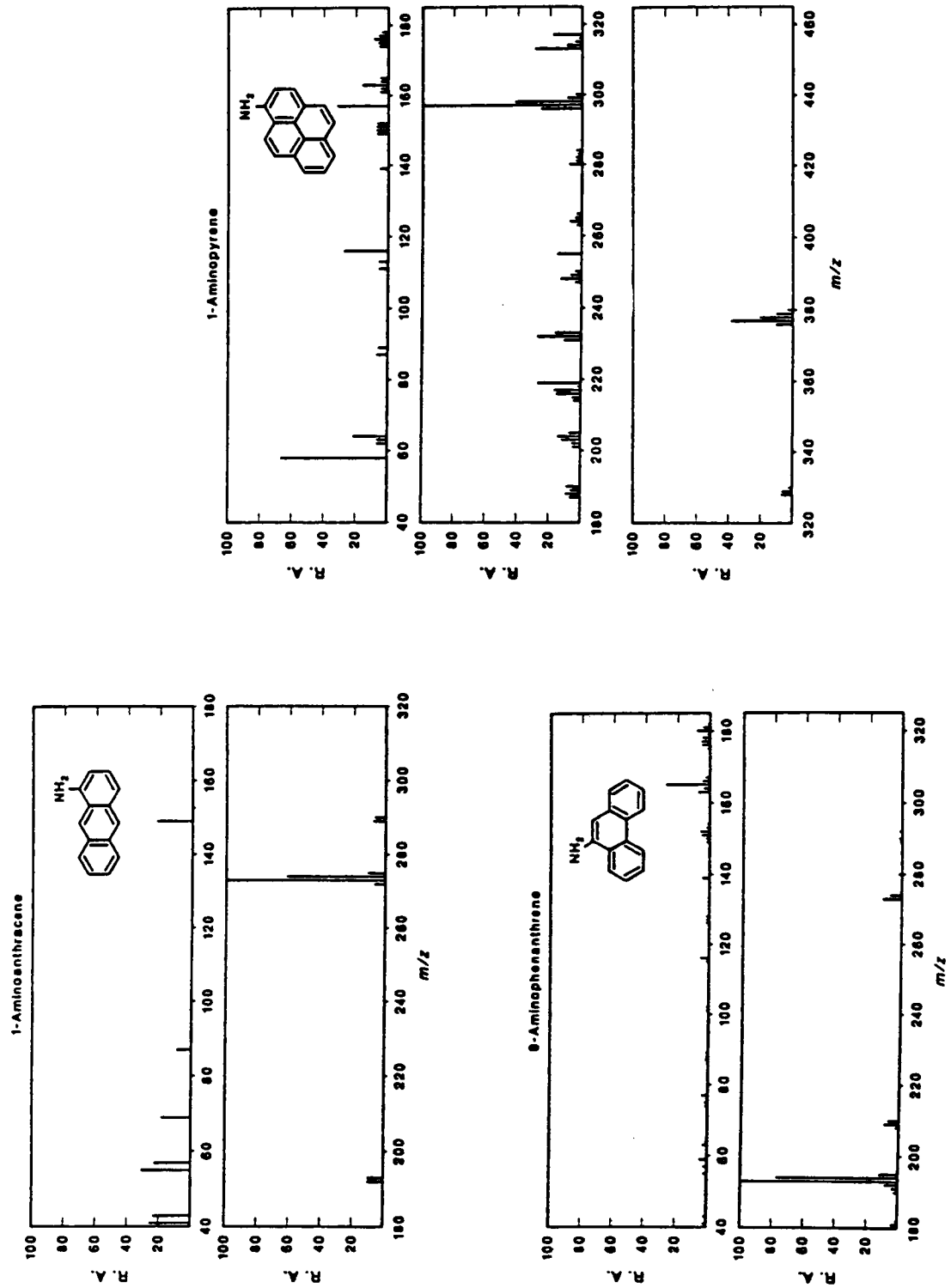

3-Methylindole
CH3
N
R. A.
m/z

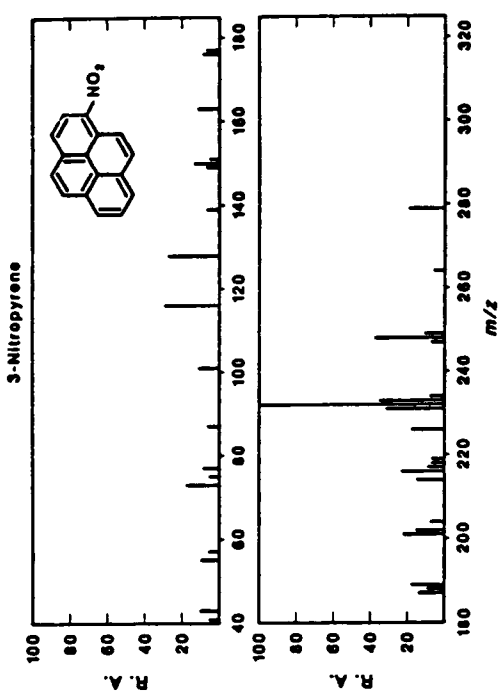

Phenazine
R. A.
m/z

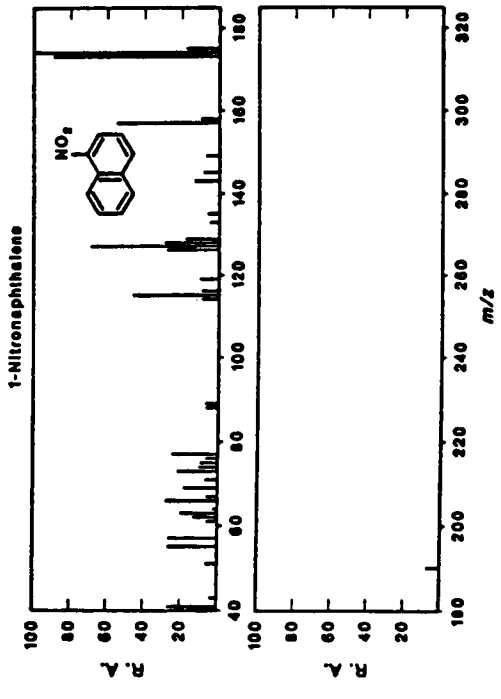

Dibenz (a,j) Acridine
R. A.
m/z

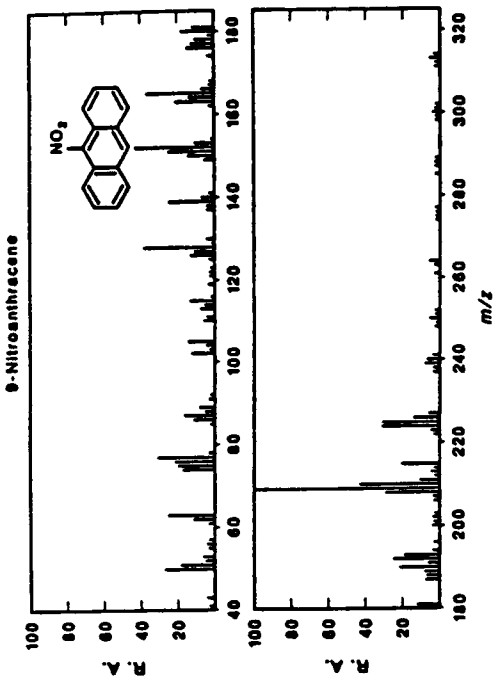

Acridine
R. A.
m/z

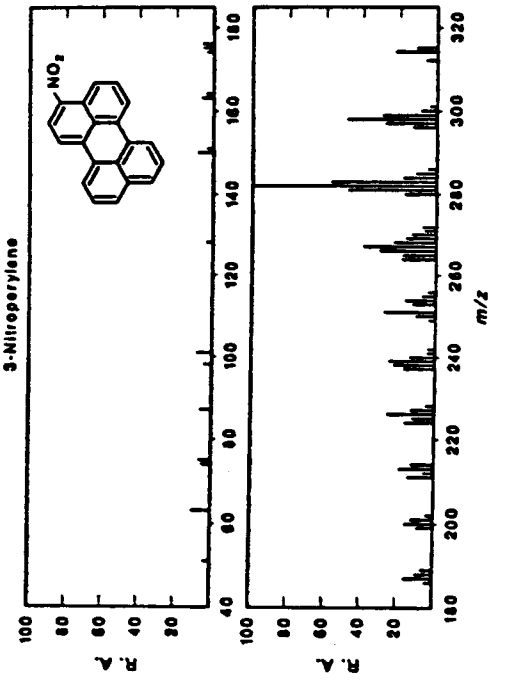

Benzo(c)cinnoline
R. A.
m/z

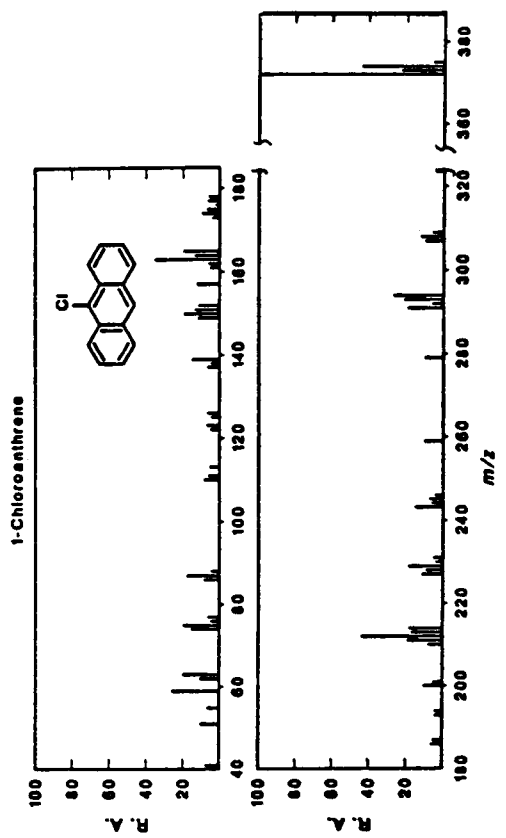

1-Aminoanthracene
9-Aminophenanthrene
1-Aminopyrene
R. A.
m/z


3-Nitropyrene
NO2
R. A.
m/z


1-Nitronaphthalene
NO2
R. A.
m/z


9-Nitroanthracene
NO2
R. A.
m/z


3-Nitroperylene
NO2
R. A.
m/z


1-Chloroanthrene
Cl
R. A.
m/z

VITA

Christopher Patrick Leibman was born in Verdun, France on February 20, 1958. He and his family moved to Kingsport, Tennessee in 1961, where he graduated from Dobyns-Bennett High School in 1976. He entered the University of Tennessee, Knoxville, and received a Bachelor of Science in Chemistry in June of 1981. The following September he entered the graduate school of the University of Tennessee. While in graduate school, he received a graduate teaching assistantship, a graduate research assistantship, and an Oak Ridge Associated Universities Fellowship. In June of 1983 he married Kimber Leigh Thornton of Asheville, North Carolina.

The author is a member of the American Chemical Society and the American Society for Mass Spectrometry. The author has accepted a post-doctoral position at Los Alamos National Laboratory.